

Effects of Cold Physical Plasma on Human Leukocytes

I n a u g u r a l d i s s e r t a t i o n

zur

Erlangung des akademischen Grades

Doktors der Naturwissenschaften (Dr. rer. nat.)

der

Mathematisch-Naturwissenschaftlichen Fakultät

der

Ernst-Moritz-Arndt Universität Greifswald

vorgelegt von

Sander Bekeschus

geboren am 18.06.1985

in Berlin

Greifswald, den 27.11.2014

Dekan: Prof. Dr. rer. nat. Klaus Fesser

1. Gutachter: Prof. Dr. med. Barbara M. Bröker

2. Gutachter: Prof. Dr. Mark Hampton

Tag der Promotion: 10. Juni 2015

Contents

Abbreviations

VII

<i>Chapter 1. Introduction</i>	<i>1</i>
1. Plasma	1
2. Plasma medicine	2
2.1. Plasma decontamination	2
2.2. The application of cold plasma to eukaryotic cells and tissues	3
2.3. The atmospheric pressure argon plasma jet <i>kinpen</i>	4
3. The immune system	7
3.1. Mononuclear cells (PBMCs)	9
3.2. Polymorpho-nuclear cell (PMNs)	12
3.3. Neutrophils extracellular traps (NETs)	14
3.4. Neutrophils in pathological conditions	15
4. The wound	15
4.1. Healing phases	16
4.2. Non-healing wounds	18
5. Molecular events in cell biology	19
5.1. Signal transduction	19
5.2. Respiration and proliferation	20
5.3. Oxidative stress	20
5.4. Cell death	22

Chapter 2.	<i>Materials</i>	24
1.	Laboratory equipment and instruments	24
2.	Consumables	26
3.	Chemicals and solutions	27
4.	Media and buffers	28
5.	Kits	29
6.	Software and online databases	29
Chapter 3.	<i>Methods</i>	31
1.	Plasma and liquid characterization	31
1.1.	Plasma treatment of liquids and cell suspension	31
1.2.	Optical emission spectroscopy	32
1.3.	Quantification of reactive species in liquids	33
1.4.	Characterization of cell culture supernatants	34
2.	Cell isolation and flow cytometry	36
2.1.	The principle of flow cytometry	36
2.2.	Flow cytometry and cell sorting	37
2.3.	Isolation of PBMCs	38
2.4.	Isolation of PBMCs subpopulations	38
2.5.	Isolation of PMNs	39
3.	Characterization of plasma-treated PBMCs	40
3.1.	Cell viability	40
3.2.	Cellular oxidation	42
3.3.	Detection of cell proliferation	43
3.4.	Intracellular cytokine measurement	44
3.5.	Measurement of intracellular thiol content	45
3.6.	Cell surface marker expression on T lymphocytes	45
3.7.	Measurement of mitochondrial membrane potential	46
3.8.	Intracellular measurement of protein-phosphorylation	46

4.	Characterization of plasma-treated neutrophils	47
4.1.	Viability	47
4.2.	Oxidation	47
4.3.	Oxidative burst	47
4.4.	Phagocytosis and killing	48
4.5.	NET quantification using a plate reader	49
4.6.	Assessment of extracellular and active MPO	49
4.7.	NET quantification using fluorescence image analysis	50
4.8.	NET confirmation using confocal laser scanning microscopy	50
5.	Statistics	52
Chapter 4.	<i>Aim of this work</i>	53
Chapter 5.	<i>Results</i>	54
1.	Characterization of cold plasma and plasma-treated liquids	54
1.1.	Molecular reactive species in the plasma gas phase	54
1.2.	Plasma-treated buffered solutions	56
1.1.	Summary of results	58
2.	Effect of plasma on oxidation and viability of human PBMCs	59
2.1.	Oxidation and cellular damage were a consequence of exposure to plasma	59
2.2.	Cell death was a consequence of apoptosis but not necrosis	63
2.3.	Plasma selectively inactivated effector/memory T _H cell subset	66
2.4.	Summary of results	68
3.	Plasma treatment alters lymphocyte function and phenotype	69
3.1.	Proliferation was reduced but not halted in viable T lymphocytes	69

3.2.	Cytokine expression was significantly altered in T lymphocytes	72
3.3.	Summary of results	75
4.	What are the mechanisms of the effects of plasma on immune cells?	76
4.1.	Cytotoxicity effects were dependent on plasma treatment conditions	76
4.2.	Hydrogen peroxide was central in plasma-mediated cytotoxicity	78
4.3.	H ₂ O ₂ was the main but not the only oxidizing agent in cells	81
4.4.	Summary of results	83
5.	Plasma treatment of human neutrophils	84
5.1.	Plasma oxidized neutrophils but only partially induced apoptosis	84
5.2.	Cellular oxidative burst remained functional after plasma treatment	87
5.3.	Plasma treatment induced neutrophil extracellular trap formation	90
5.4.	Neutrophil cytokine and MPO release was also modulated after exposure to plasma	93
5.5.	Summary of results	95
Chapter 6.	Discussion	96
1.	Generation of reactive species by plasma, and their interplay	96
2.	Behavior of monocytes and lymphocytes in response to plasma treatment	97
2.1.	The redox modulation after plasma treatment	98
2.2.	Plasma treatment and apoptosis	99
2.3.	Differences in apoptotic responses between PBMCs subpopulations after plasma treatment	100
2.4.	The effect of plasma on cytokine and chemokine production	102
2.5.	The role of H ₂ O ₂ in plasma-mediated oxidative stress and cell death	103

3.	The Neutrophil response after exposure to plasma	105
3.1.	The effect of plasma on neutrophil function and cytokine release	105
3.2.	Neutrophil viability and extracellular trap formation after plasma treatment	106
4.	Leukocyte responses after cold plasma treatment: implications and potential significance in chronic wounds	107
 <i>Chapter 7. Summary</i>		<i>109</i>
 <i>Chapter 8. References</i>		<i>111</i>
 Acknowledgements		125
Appendix		127

Abbreviations

' , min	minute
μl	microliter
μm	micrometer
μM	micromolar
ANOVA	analysis of variances
APC	allophycocyanine / antigen-presenting cell
ar	argon gas control (plasma off)
AVBB	Annexin V binding buffer
CD	cluster of differentiation
Cy	cyanine
DAPI	4',6-Diamidin-2-phenylindol
ddH ₂ O	double distilled H ₂ O
DNA	deoxyribonucleic acid
e.g.	<i>exempli grati</i> (for example)
ELISA	enzyme-linked immunosorbent assay
FACS	fluorescent-activated cell sorting
FCS	fetal calf serum (fetal bovine serum)
Fig.	figure
FITC	fluorescein isothiocyanate
g	g-force (9.81 m/s ²)
GSH	glutathione (reduced state)
h	hour
Hank's	Hank's buffered saline solution (HBSS)
i.e.	<i>id est</i> (that is)
IFN	interferon
IL	interleukin
LPS	lipopolysaccharide
MFI	mean fluorescence intensity
MHC	major histocompatibility complex
NET	neutrophil extracellular traps
nm	nanometer

O/N	over night
PBMCs	peripheral blood mononuclear cells
PBS	phosphate buffered saline
PE	phycoerythrin
PHA	phytohemagglutinin
PMA	phorbol-12-myristat-13-acetat
PMNs	polymorpho-nuclear cells
R10F	RPMI1640 supplemented with 10 % FCS
redox	reduction-oxidation reaction
RNS	reactive nitrogen species
ROS	reactive oxygen species
RPMI	Roswell Park Memorial Institute (medium)
RT	room temperature
s	second
SD	standard deviation
SE	standard error
slm	standard liter per minute
tab.	table
TCR	T-cell receptor
TGF	transforming growth factor
T _H	T helper cell
TNF	tumor necrosis factor
UV	ultra violet

Chapter 1. Introduction

1. Plasma

The term “plasma” is Greek and means “something molded”. “Plasma” is commonly associated with blood plasma but the term homonymously also means physical plasma. It was used first in 1879 describing “radiating matter” (1). In 1928, Langmuir investigated the flow of physical plasma which reminded him of blood plasma flowing through veins (2). In physics, plasma is described as the fourth state of matter (3). It is assumed that a majority of visible matter in the universe is in plasma-state. On earth, plasma appears in form of, e.g., lightening, *aurora borealis*, or fire. Plasmas are also generated artificially for technical applications for example in welding, neon lights, modern head light systems in cars, energy saving light bulbs, or modern televisions.

Plasma is generated by energizing gas up to a critical point at which electrons dissociate from atoms. The resulting ionized gas contains charged particles, while the overall charge remains electrically neutral. Typical particles being generated include ions, electrons, or reactive oxygen and nitrogen species (ROS/RNS). Electric and magnetic fields, light (visible, infrared, UV), and neutral particles are also generated (4). In this work, a plasma jet was used that is operated at atmospheric pressure. The plasma is generated by applying a high-frequency alternating voltage to a gas. The electron flux displays a high velocity and is hot. These fast electrons then ionize molecules of a feed gas, e.g., argon. Argon molecules on the other hand are bigger than electrons and hence slower in the electric field, preventing their acceleration. Also, fast electrons inefficiently transfer their energy (heat) to ions which consequently remain cold. As the ion temperature of a gas determines its overall temperature, the plasma contains highly energized particles on the one hand without displaying the significant temperature increase that would usually come with them (non-equilibrium plasma) on the other. Additional cooling of plasma can be achieved using high feed gas fluxes, e.g., of argon. The feed gas flux also drives the plasma and its charged (argon) particles to the outside to create the plasma-effluent. Once outside, charged particles further react with molecules of

ambient air to create non-radical (hydrogen peroxide, ozone) or radical species (hydroxyl radical, nitrogen monoxide) (4,5). Details about various types of plasma generation can be found elsewhere (6,7). In the past years, cold plasma applications have gained interest in the biomedical field.

2. Plasma medicine

The first “biological” application of plasma was carried out by the German company *Siemens*. Using plasma, ozone was generated to decontaminate water of waterworks (8). Detailed investigations of the mechanisms, however, raised the interest of scientists only three decades ago when principles of microbial decontamination with plasma were investigated (9,10). The antimicrobial efficiency of cold plasmas started to increasingly become appreciated in the late-1990s and the term “plasma medicine” was subsequently coined (11). Until today, plasma-mediated decontamination is the largest field of research and application within this young discipline.

2.1. Plasma decontamination

Cold plasma inactivates various non-pathogenic and pathogenic biological entities. Planktonic or biofilm-building bacteria such as *Streptococcus mutans* (12), *Staphylococcus aureus* (also MRSA) (13), *Pseudomonas aeruginosa* (14), or *Escherichia coli* (15) can be destroyed. Similar effects were observed in eukaryotic parasites (16), yeast (17), viruses or nucleic acids (18,19) as well as infectious proteins (20). Development of bacterial resistance was not observed so far (21). Owing to its low temperatures, plasma decontamination has also been successfully applied to food (22), heat sensitive clinical consumables (23,24), or room air (25). In life science, plasma is frequently used to render tissue culture plastics more adhesive to adherent cells. Plasma sources are adjusted to each application; for example, large area plasma beams are used for food decontamination. Yet, the antimicrobial mechanisms of plasma are not completely understood. It is known that phagocytes generate reactive species to kill bacteria entrapped in their phagolysosome. Plasma also generates various reactive

species and, in *in vitro* experimentations, deposits them in liquids where the species exhibit antibacterial effects (26). In non-buffered solutions, the pH decreases significantly following plasma treatment which helps to kill bacteria (27). Ozone and UV-radiation generated by plasma also exhibit antimicrobial properties (28-30). It is likely that a combination of those stressors exert the desired plasma effects on microorganisms (31). Further, it was observed that gram-positive bacteria are more prone towards plasma decontamination than gram-negative bacteria (32,33). The antimicrobial action of plasma is not restricted to agar cultures or bacterial suspensions but is also effective on live or dead skin (34,35). It appears plausible that in chronic wounds, decreasing the bacterial burden with plasma treatment may foster wound healing, provided that there is a dose window between the antimicrobial activity and tissue damage caused by cold plasma. Accordingly, the effects of plasma on eukaryotic cells, such as epithelia, were increasingly investigated in the last years.

2.2. The application of cold plasma to eukaryotic cells and tissues

Different types of eukaryotic cells have been studied after plasma treatment so far. Two clinical applications are in focus in plasma medicine: enhancing the wound-healing response in dermatology, and killing of tumors in oncology. Prolonged plasma treatment can induce apoptosis in many cell types including keratinocytes (36), fibroblasts (37), and different tumor cell lines (38-40). In plasma-treated endothelial cells, toxic but also stimulating effects were observed (41). In fibroblasts, enhanced proliferation after plasma treatment was shown to be due to an elevated release of fibroblast-growth-factors (42). Generally, (apoptotic) signaling events involving ERK, JNK, p53, and/or p38 MAP-kinase were found in plasma-treated cells (43-45).

In vivo and *ex vivo* animal studies showed no histological skin damage following plasma treatment, while at the same time wound healing was improved (46-51). Experimentations were conducted in pigs, rats, mice, dogs, and cats. The treated wounds were either of experimental origin or naturally occurring chronic injuries in pets failing standard wound therapy. A study of burn wounds in mice showed that plasma treatment enhanced angiogenesis (52). Full-thickness cutaneous wound healing was found to be accelerated after

exposure to plasma as well (53). Using other mouse models, U87 gliomas and cutaneous melanoma were also successfully treated (54,55). To assure safety of plasma applications, the amount of energy introduced by plasma into the skin was determined, and no UV or heat-induced damage was found (56-58). Further, no DNA-damage was present in cells of *ex vivo* treated human skin (59). An *in vivo* study showed that for decontamination of intact skin, plasma was similarly effective compared to an antiseptic agent (60). In another study, plasma was superior to antiseptics in decontaminating bacteria in hair follicles due to the plasma's increased penetration depth (61). In humans, small-scale clinical studies using cold plasmas have been carried out in the past years. Two studies demonstrated reduction of bacteria in chronic wounds of 24 and 36 patients, respectively. Neither pain nor skin irritation were observed (62,63). Regarding non-healing wounds, plasma significantly improved healing in 40 patients with skin transplantation (64). Plasma was ineffective in the treatment of pruritus, however (65). Exposure to plasma increases the skin absorption of low molecular compounds, which could be useful to enhance availability of pharmacological agents (66). Other emerging fields of applications are odontology and implantology. Plasma improved cellular adhesion on implants while simultaneously mediating antimicrobial effects (67-69). Dental implants frequently become infected and the resulting chronic inflammation disturbs integration of implants into tissue. Plasma has been shown to effectively reduce biofilms present on implants, providing a promising tool for the reduction of peri-implantitis.

Regardless of specific applications, it is of crucial importance to ensure that plasma treatment is safe. *In vitro* studies, conducted under OECD guidelines for mutagenicity, showed no cancerous potential of two plasma sources which are officially accredited for biomedical applications (70,71). In a clinical study (five individuals), laser-induced wounds were plasma-treated with the kinpen and no precancerous skin features occurred up to 12 months after treatment (72).

2.3. The atmospheric pressure argon plasma jet *kinpen*

The kinpen is a commercially available atmospheric pressure argon plasma jet. Its concentric, light-weighted, and pen-like design was developed for biomedical applications and allows

precise and arbitrary 3D movements (73). The hand-held unit is operated using a power supply and a gas supply unit. In this work, the kinpen 09 was used. It is certified and complies with EU standards (certificate nr. 609.003.1). Its successor, the kinpen med, is the first plasma source accredited as a medical product. The kinpen 09 and kinpen med are similar in construction. In their metal housing, a central, rod-like electrode (radius 5 mm) is mounted and shielded by a dielectric ceramic capillary connected to a grounded ring electrode. The inner and outer diameter is 15 mm and 25 mm, respectively. The plasma is generated by applying a sinusoidal voltage (2-6 kV_{pp}) with a frequency of 1.0-1.1 MHz to the central electrode. Depending on the parameters used, the plasma effluent displays a length of 7 mm to 15 mm, with 1 mm in diameter. Argon is used as feed gas, but small amounts of other molecular gases can be admixed. The plasma itself is discontinuous, exhibiting temperatures of 37-62 °C. High spatial and temporal optical resolution of the plasma revealed that it propagates in a bullet-like manner (74). If applied as recommended, temperature or UV-radiation are not harmful to humans (75,73). Recently, a gas curtain was introduced, shielding the plasma from ambient air (76). This allows for detailed control of the environmental conditions surrounding the plasma, which strongly influence its chemistry (77,78).

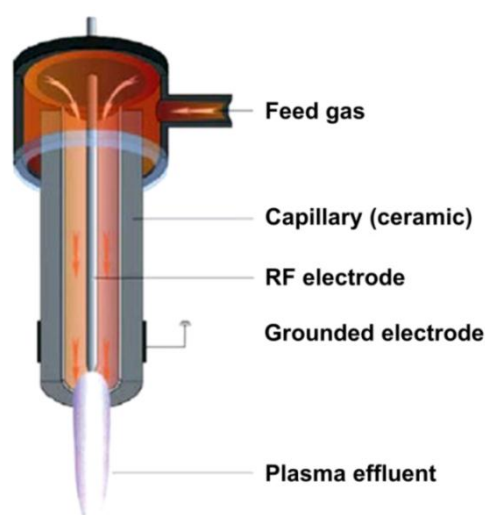


Fig. 1*: Schematic of the kinpen.

Feed gas (noble gas) is driven through the capillary. Applying a radiofrequency voltage, the plasma is ignited at the electrode. The gas flux propagates the generated plasma to the outside where it becomes visible as the effluent.

**reproduced from (73) with permission from Wiley Materials*

The physical and chemical aspects of the plasma generated by the kinpen have been investigated previously. The jet generates reactive species of many kinds. It is estimated that hundreds of different reactions take place in the plasma gas phase (79). Physical methods, e.g., optical emission spectroscopy or Fourier-transformed infrared (FTIR) absorption spectroscopy, help to quantitate emission lines which can be attributed to specific reactive molecules (74). The kinpen does not produce significant amounts of nitric monoxide (NO) but admixture of synthetic air into the effluent increases NO production (80). The jet also generates significant amounts of ozone. Furthermore, high concentrations of $\cdot\text{HO}$ are released which is thought to form hydrogen peroxide (81) in non-oxygenated areas in the plasma gas phase (82). Upon contact, the reactive species of the plasma gas phase react with liquids and cells. The underlying chemistry is highly complex and far from understood. Most species display a short half-life and are highly reactive, which makes their detection challenging (83).

Tab. 1: Properties of the kinpen 09. Parameters were summarized according to (73).

parameter	value
length	170 mm
diameter	20 mm
weight	170 g
input power	30 W
output power	0.5-1.0 W
gas flux	multiple standard liters per minute
feed gas	noble gases, <1 % admixture of molecular gases possible
effluent length	10-15 mm
effluent temperature	0 mm: 49-60 °C
(at distance from the nozzle)	5 mm: 48-61 °C
	10 mm: 41-51 °C
	15 mm: 37-40 °C
radial temperature	25-28 °C at ± 2 mm from the effluent axis
ozone concentration	0.1 ppm
nitrogen dioxide concentration	not detected
UV-radiation	UV-A and UV-B, no /few UV-C (84,85)

Numerous studies investigated effects of plasma generated by the kinpen on prokaryotic or eukaryotic cells. Antimicrobial effects are well documented (86) including the *Bacillus subtilis* redox proteome and -transcriptome after plasma exposure (87). Using the kinpen, biofilms were edged from implant surfaces, increasing cyto-adhesive properties for eukaryotic cells at same time (67,69). Cytotoxic properties of the plasma were investigated in HaCaT keratinocytes: single- but not double strand DNA-breaks, and a cell cycle arrest in G2 phase were observed (88,89). Transcriptomic analysis showed numerous, redox-based changes including the appearance of wound healing-relevant oxidoreductase transcripts (90). At the protein level, proteomic profiles were defined (91). Irritating or inflammatory effects of this plasma were investigated using the *Hen's Egg Test Chorio-Allantoic-Membrane* (HET-CAM) assay and found to be acceptable for medical treatment (92,93). Using this assay, tumors grown on the CAM were eliminated following exposure to plasma (94). Studies investigating effects of kinpen-generated plasma in humans have been described in the previous section (95,60,96,61,72,97). Many of these studies were carried out to elucidate beneficial effects of plasma in wound healing. They were mainly focused on investigations of skin cells. At the starting point of this thesis in 2011, cells of the immune system have received very little attention so far in plasma medicine. This only includes a study of enhanced plasma-assisted intracellular killing of leishmania in human macrophages (79), and dubious results about lymphocytes exposed to a dielectric barrier discharge (98). Yet and in wound healing, immune cells are central in the orchestration of molecular events important for the successful resealing of the tissue.

3. The immune system

“Immunity” is derived from *immunitas* which is Latin and refers to the protection from legal prosecution. In biology, immunity means protection from disease. Components that are part of this protection are referred to as immune system. In the field of immunology, immune responses take place at the molecular, cellular, and organismic levels (99).

Multicellular organisms have a (more or less complex) immune system to defend the organism against invading pathogens. The human immune system consists of a humoral and a

cellular part which can be subdivided into an innate and adaptive portion. Close interaction is required to elicit optimal and fast responses. The innate immune system recognizes evolutionary conserved structures on microorganisms which are often essential for their physiology. These structures are called *microbe-associated molecular patterns* (MAMPs) and they are detected by *pattern recognition receptors* (PRR) on cells. The latter are highly expressed on neutrophils, macrophages, dendritic cells, and mast cells. However, innate immunity is sometimes not sufficient to fight invading microorganisms. The adaptive immune system is able to generate a multitude of T cell receptors and antibodies, adding selectivity and speed to the eradication of the invading microorganisms. T and B lymphocytes constitute the cellular part of the adaptive immune responses, whereas B lymphocyte-derived plasma-cells secrete powerful proteins of the humoral adaptive immune responses: antibodies. Adaptive immune responses are not immediate but, once established, immune memory can be maintained throughout the whole life if re-infection occurs on a frequent basis. The immune system is present in each tissue and compartment of the body. Its cells originate from the bone marrow and often mature in the periphery. They travel through the body with the blood or lymphatic fluid to quickly reach any site of infection. In immunological research, blood is the primary source of human immune cells for investigation. (100,101)

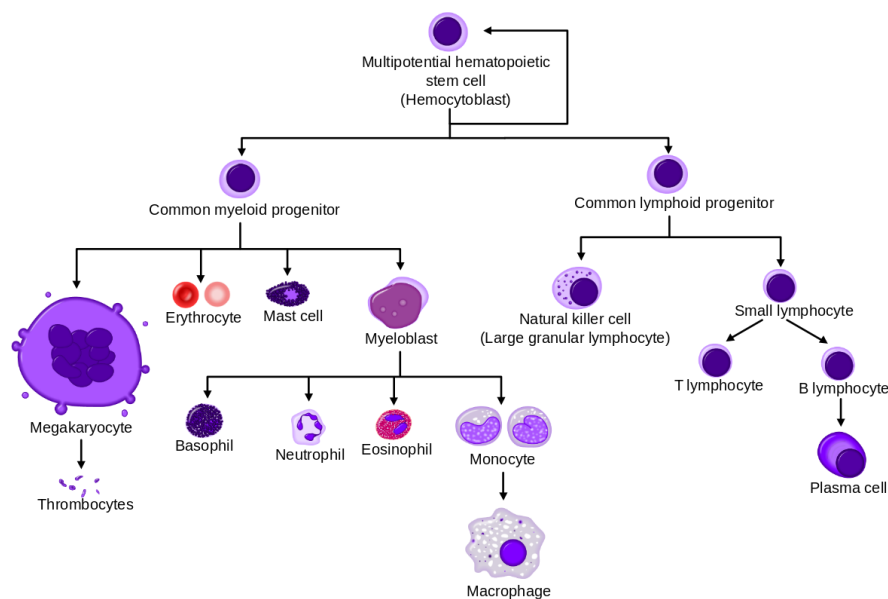


Fig. 2*: Hematopoiesis of human blood cells.

All blood cells descend from common multi-potent stem cells residing in the bone marrow. These differentiate into either common myeloid or lymphoid progenitor cells, which give rise to the many other cell types.

**reproduced from "hematopoiesis simple" by Mikael Häggström*

Human blood cells descend from one of two different common progenitor cells. The myeloid progenitor-derived cells belong to the innate immune systems and also give rise to erythrocytes. The lymphoid progenitor-derived cells are evolutionary younger and, with the exception of NK cells, belong to the adaptive immune system. Two major populations can be obtained by centrifugation techniques of peripheral blood: peripheral blood mononuclear cells (PBMCs) and polymorpho-nuclear cells (PMNs).

3.1. Mononuclear cells (PBMCs)

Peripheral blood mononuclear cells (PBMCs) are a fraction of the white blood cells. PBMCs contain many different cell types and subsets including monocytes and lymphocytes (102). The main populations are introduced here. Immune cell subtypes can be distinguished by their expression profiles of distinct cell surface markers, so-called *cluster determinants* (CD). (100,101)

Monocytes

Monocytes constitute about 20 % of PBMCs and belong to the innate immune system. They are generated within hematopoietic tissues from a common myeloid progenitor. After differentiation and maturation they enter the blood stream. Monocytes are precursors of macrophages and dendritic cells in the tissues. They have a large non-segmented nucleus and leave the blood to differentiate into macrophages. These cells are omnipresent throughout the body and are thus the first to encounter invading pathogens. They can detect and engulf microorganisms in a PRR-dependent manner. The pathogen is ingested and trapped in the phagosome. Upon macrophage activation, a hostile environment and a low pH are generated in the phagosome, effectively killing microorganisms. Moreover, macrophages are professional antigen-presenting cells (APCs), decorating major histocompatibility class II (MHC II) receptors with peptides from digested bacteria. If presented to the T Helper (T_H) cell with T-cell receptor (TCR) specific for those peptides, an adaptive immune response can be mounted against an antigen. Antigens are foreign (or in case of autoimmune diseases

bodily molecules) that can result in generation of antigen-specific antibodies.

Macrophages communicate bacterial invasion (or detection of their products, e.g., LPS) to other immune cells via immune hormones, so called cytokines. Dependent on the specific type, these proteins prime, activate, and/or attract specific immune cells to migrate to the site of infection. Macrophages also release pro or anti-coagulative factors, and tissue-digesting enzymes (103). They are thought to be the key regulatory cells in wound healing, and chronic wounds have been attributed to macrophage malfunctioning (104). Human blood monocytes highly express CD14, enabling their identification by flow cytometry (105). Upon tissue injury, they are second only to neutrophils to be recruited from the blood stream (106).

T lymphocytes

T lymphocytes are part of the adaptive immune system and characterized by presence of their TCR. T lymphocyte progenitor cells descend from lymphoid progenitors in the bone marrow and mature in the thymus. The majority of TCRs on T cells consist of $\alpha\beta$ -chains, a minority of $\gamma\delta$ -chains. $\gamma\delta$ T cells constitute a distinct T cell subset (they do not display CD4, CD8, or CD28) which is enriched in mucosal surfaces and the skin (107). $\gamma\delta$ T cells scan surface molecules of other cells, including keratinocytes, for the presentation of phospholipids on CD1, and secrete cytokines upon antigen recognition. In healthy tissues, their shape resembles dendritic cells but they quickly round up after wounding. $\alpha\beta$ T cells (from here on simply called “T cells”) can be classified by expression of CD8 (cytotoxic T cells, CTLs) or CD4 (T helper cells, T_H). $CD8^+$ T cells bind MHC I, which is displayed on all nucleated cells of the body. Peptide fragments of non-endosomal proteins are constantly loaded onto MHC I molecules and thus reflect the intracellular protein content. If a cell is infected by a virus or is otherwise stressed or cancerous, $CD8^+$ cells specific for that pathogenic or pathological peptide sequences can lyse the targets. In contrast, $CD4^+$ T cells scan MHC II on APCs. There are many T_H subsets including T_H0 , T_H1 , T_H2 , T_H9 , T_H17 , T_H22 , and T_{reg} , and detailed information about their specific functions can be found elsewhere (108).

Activation of T cells via the TCR triggers signaling pathways involving the phosphorylation of NF κ B and ERK1/2. The activation state of the peripheral blood T cells can further be distinguished via expression of different surface molecules. Naïve T cells, which have not yet

encountered their specific antigen, are positive for CD62L. Its ligand CD34 is expressed on specialized endothelial cells lining the high endothelial venules in secondary lymphatic organs, such as lymph nodes or the spleen. This enables the naïve T cells to enter these organs where they “scan” MHC molecules on professional APC for the peptide specific to their TCR. Naïve T cells are characterized by their expression of CD45RA but not CD45R0 (109). In contrast, effector/memory T cells express CD45R0 but not CD45RA. T cell activation can be achieved experimentally in an antigen-dependent or independent manner. It can be triggered either by using anti-CD3 and anti-CD28 monoclonal antibodies or by pulsing cells with a mitogen such as phytohemagglutinin (PHA), a potent protein kinase C activator (110). Upon stimulation, cell proliferation takes places which can be followed by flow cytometry (111).

B lymphocytes

About 10 % of PBMCs are B lymphocytes. Similar to T cells, they derive from lymphoid progenitor cells. They mature in the bone marrow to become mature naïve B cells, which enter the circulation. Once in the blood, they also home into secondary lymphoid tissues. B cells display B-cell receptors (BCR) on their cell surface. If a cognate antigen is recognized by the BCR, the receptor is internalized and antigen-derived peptides are presented on MHC II. T cell recognition of this peptide results in co-stimulation the B cell via ligation of CD40 on B cells and cytokine secretion of T cells (112). This interaction is the major component of the adaptive immune response, ultimately resulting in B cell proliferation and differentiation, and the production of antigen-specific antibodies by the resulting plasma cells. Antibodies facilitate immune defense against infectious agents but, if misdirected, they can also induce immune reactions to bodily antigens thereby causing autoimmune diseases. The B cell - T cell interaction is therefore subject to sophisticated control mechanisms (100). Human B cells uniquely express the B cell co-receptor CD19 which allows for their discrimination by flow cytometry.

NK cells

Natural killer (NK) cells constitute about 2-18 % of the PBMCs. They are recognized as a separate lymphocyte type (113) but belong to the innate immune system. NK cells are characterized by cytotoxicity and cytokine-mediated effector functions. They patrol the tissues and scan cells for “distress” or “alarm” molecules presented on the cell surface. Such stressed or malignant cells are killed. Human NK cells lack the TCR (CD3) but display the neural cell adhesion molecules (CD56) that allows for their discrimination by flow cytometry.

3.2. Polymorpho-nuclear cell (PMNs)

Polymorpho-nuclear cells were named after their lobed nucleus. PMNs consist of three populations (neutrophils, eosinophils, basophils) with neutrophils being the most prevalent (>95 % of PMNs and 40-75 % of leukocytes in peripheral blood). Eosinophils mediate effector responses towards multicellular parasites, while there is yet no clearly defined role of basophil biology. Neutrophils are the major phagocytic cell type and are the first to arrive from the blood at the site of injury. Neutrophil half-life in blood is thought to be 6-10 h (114). After phagocytosis of pathogens they become apoptotic and are cleared by macrophages. Recently, also a regulatory role in cell-cell communication was attributed to them. Neutrophils recruit macrophages via release of MIP-1 α and MIP-1 β , and are capable of secreting IL-1 β , IL-8, TNF α , and IP-10 (115). If stimulated by IL-12, neutrophils activate macrophages via IFN γ production. Vice versa, macrophage-derived TNF α , IL-1 β , and GM-CSF increase neutrophil survival (116). Neutrophils sensitively sense chemokine and cytokine gradients, and the mediator's concentration already determines neutrophil functions. For example, at low IL-8 concentrations neutrophils shed L-selectin (CD62L), with increasing concentrations inducing their oxidative burst. At the highest concentrations, cells degranulate (117).

Neutrophils have a plethora of biological weapons, all stored in granules of different types. Primary, peroxide-positive (azurophilic) granules are large (0.3 μ m), and contain myeloperoxidase, defensins, lysozymes, and numerous serine proteases (neutrophil elastase,

proteinase 3, cathepsin G), all displaying antimicrobial action (118-120). Secondary granules (0.1 μm) primarily contain lactoferrin and lysozyme. Tertiary granules are storage for different metalloproteases (gelatinase, leucolysin) important in tissue remodeling. A fourth set of vesicles buds not from the Golgi apparatus, but instead from the membrane, and contains endocytosed and membrane bound proteins. The antimicrobial proteins of granules can be classified into cationic peptides (α -defensins, LL-37, BPI, histones), enzymes (lysozyme, proteinase 3, neutrophil elastase, cathepsin G, azurocidin), and metal chelators (lactoferrin, calprotectin) (121).

Equally efficient to pathogen control by granules, neutrophils can quickly produce large quantities of reactive oxygen species (ROS) in a process called oxidative or respiratory burst. In principle, ROS modify or damage biological entities as they alter lipid and protein structures. ROS production is achieved by the superoxide-producing NADPH-oxidase (Nox2) on the phagosomal and plasma membrane, which quickly assembles upon neutrophil activation. Superoxide itself is not a strong oxidant, and many downstream reactions can occur (122). It rapidly dismutates to form hydrogen peroxide (H_2O_2), and can react with nitric oxide (NO^\cdot) to form the strong oxidant peroxynitrite. The second key enzyme in the neutrophil's biology is myeloperoxidase (MPO) (123). In the presence of H_2O_2 and halides it forms hypohalous acids. However, the high reactivity of hypochlorous acid means that much of it reacts directly with granule proteins in the phagosome, rather than bacteria. It is therefore assumed that antimicrobial chloramines are formed with host proteins (124). The high relevance of neutrophil-formed ROS is seen in patients lacking components of the NADPH oxidase complex (chronic granulomatosis patients) who frequently suffer strong infections (125). It is now accepted that neutrophils also act as inducers of adaptive immunity. The first to arrive at the wound, they create the setting for the inflammatory response via *de novo* cytokine secretion (126). Neutrophils produce IL-12 with the potential to induce $\text{T}_\text{H}1$ cell responses (127). In turn, $\text{T}_\text{H}1$ cells secrete $\text{IFN}\gamma$ that prolongs neutrophil life span and increases their phagocytic capacity (128). If cultured with $\text{IFN}\gamma$ and GM-CSF, neutrophils display high numbers of MHC II, CD80, and CD86, which are molecules suitable for neutrophils to serve as professional antigen presenting cells (129). Indeed, CD8^+ T cell differentiation following neutrophil antigen presentation has been observed in mice (130).

3.3. Neutrophils extracellular traps (NETs)

In 2004, Brinkmann and colleagues have made a fascinating finding, showing that neutrophils use DNA as antibacterial agent (131) and calling these structures neutrophil extracellular traps (NETs). NET-release is thought to be a new form of cell death: NETosis, different from apoptosis and necrosis. NETosis is believed to be an active form of cell death and neutrophils die in the moment NETs are released. However, there are also reports on viable neutrophils releasing NETs using mitochondrial DNA (132). First, nuclear membranes disintegrate, followed by chromatin relaxation, mixing of cytoplasmic and nuclear components, and finally extrusion of DNA. The DNA is decorated with histones and antimicrobial cytoplasmic and granular proteins (133). Oxidases (Nox2, MPO) and ROS are essential for NET formation upon bacterial stimuli (134,135). MPO is thought to have an indirect role in chromatin condensation before NET-release as neutrophil elastase translocated to the nucleus early, while MPO did so later (136). However, recent evidence suggests that there is also an oxidase-independent trigger mechanism responsible for NET-production (137). *In vivo* relevance of NETs is implied by the finding that microorganisms positive for the DNA-degrading enzyme deoxyribonuclease (DNase) showed enhanced dissemination in the host (138).

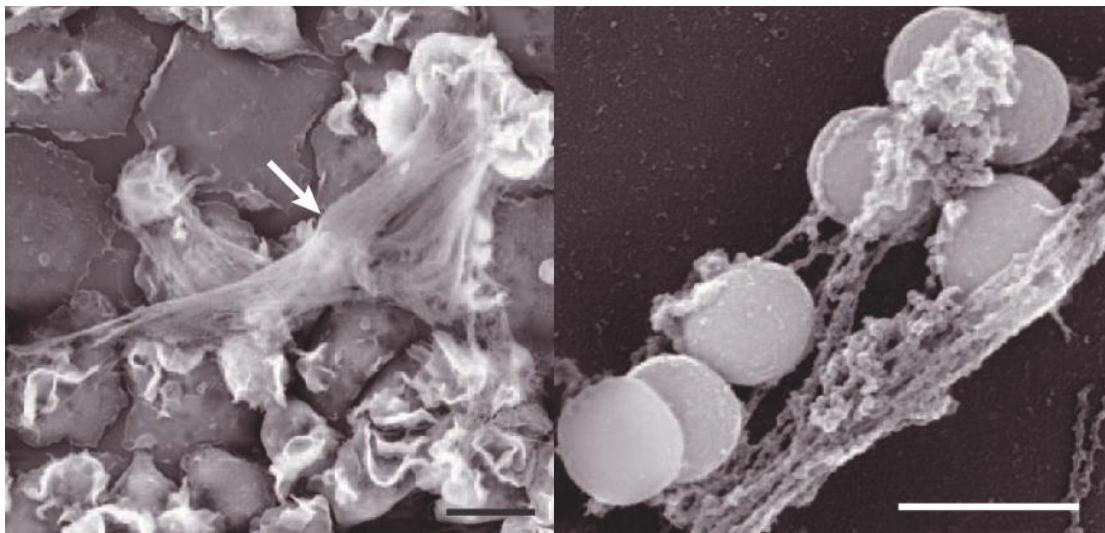


Fig. 3*: Neutrophil extracellular traps (NETs).

Neutrophils form large extracellular structures made of DNA (left). These structures entangle bacteria (here, *Staphylococcus aureus*) leading to their death or mediating growth inhibition (right).

**reproduced from (139) with permission from Nature Publishing Group*

3.4. Neutrophils in pathological conditions

Neutrophils are assumed to be short-lived cells. It is their fate to either get cleared in the circulation / bone marrow, or to die at the site of infection. Neutrophils carry large amounts of molecules that are toxic to microorganisms and host tissue alike. Many chronic diseases are characterized by either a sustained neutrophil influx or a hampered clearance of apoptotic neutrophils by macrophages. Reduced neutrophil apoptosis was observed in presence of inflammatory mediators such as GM-CSF and LPS, or in hypoxic conditions (140). Failure to control presence of neutrophils is implicated in cystic fibrosis, chronic obstructive pulmonary disease, rheumatoid arthritis, and chronic wounds, where sustained neutrophil infiltration promotes tissue damage. This is mainly mediated by a failure of dampening inflammation, which results in attraction of more neutrophils. In these pathological conditions, complex networks of cytokines, chemokines, and lipid mediators often act in concert.

Neutrophil activity is also associated with autoimmune disease. In neutrophil-infiltrated tissues, both destruction and inflammation are present. This increases the likelihood of mounting an immune response against self-antigens. Anti-neutrophil cytoplasmic antibodies (ANCA), specific against MPO or PR3, are consistently associated with Wegener's granulomatosis (121). ANCA or antibodies against chromatin are present in systemic lupus erythematosus (SLE), and a link between NETs, hampered DNA removal, and SLE has been suggested. NETs have also been shown to bind inside the vasculature, and by this serve as a potential scaffold stimulus to induce thrombosis (141).

4. The wound

In life, tissue injury is inevitable. Here, microorganisms invade compromised tissues and cause infection. For this, tissues display a high plasticity and the ability to seal a gap, while bacteria are being removed by immune cells: to heal.

4.1. Healing phases

The process of wound healing is characterized by four continuous, overlapping, and precisely programmed phases: hemostasis, inflammation, proliferation, and remodeling (142). Hemostasis is characterized by vascular constriction and platelet aggregation, degranulation, and fibrin formation (thrombus). In the inflammatory phase, neutrophils infiltrate the wound site, followed by monocytes and lymphocytes. During the proliferation phase, re-epithelialization occurs, while new blood vessels are formed (angiogenesis) and collagen is synthesized for new extracellular matrix formation. Finally, collagen and the vasculature are remodeled. Many different cell types are involved in the healing process. For wound closure, fibroblasts (and keratinocytes) are essential for extracellular matrix deposition, and tissue remodeling. Sequential immigration of neutrophils, macrophages, and lymphocytes helps to eradicate infectious agents, and to orchestrate the wound healing phases and cell immigration.

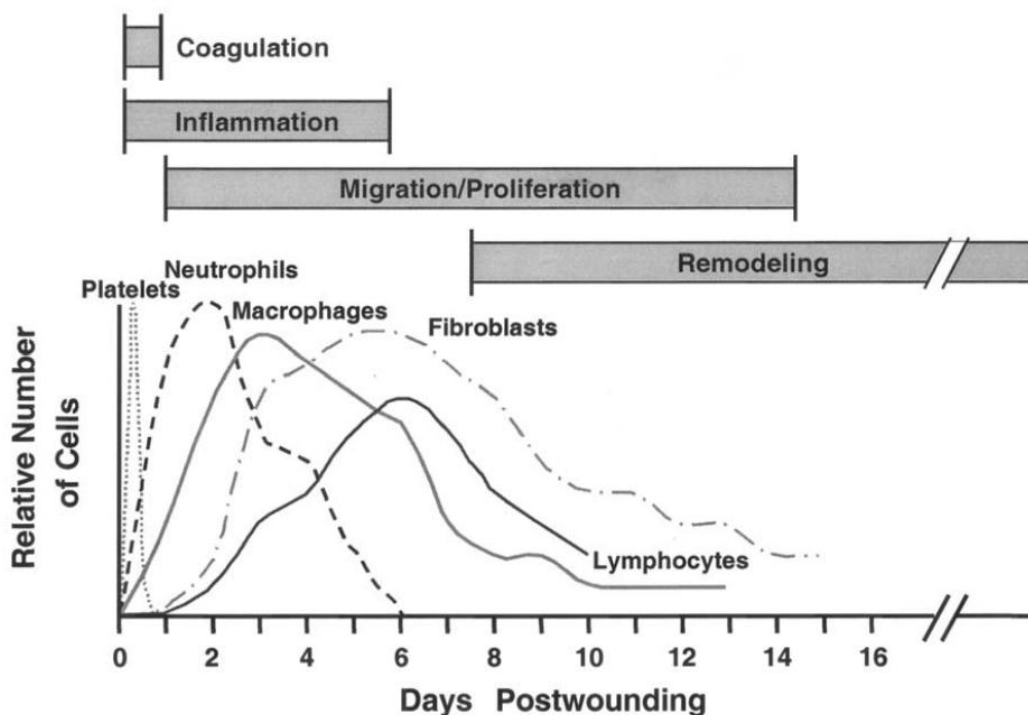


Fig. 4*: Chronological resolution of the influx of different cell types after wounding.

**reproduced from (143) with permission from Elsevier*

Neutrophils are attracted by GM-CSF and IL-8 (144). Further, platelets release α -granules containing EGF, PDGF, and TGF β . PDGF aids in attracting neutrophils, while TGF β converts immigrating monocytes to macrophages. Macrophages initiate the formation of granulation tissue and release IL-1, IL-6, and growth factors that act in a paracrine and autocrine fashion (145). The phagocytes take up and kill large amounts bacteria. Neutrophils are thought to die after phagocytosis or killing. Macrophages reside at the wound site to pave the way for its resolution by phagocytosing dead cells, and by coordinating the healing response via release of cytokines and growth factors. Macrophages promote the proliferative phase, and stimulate fibroblast and keratinocyte growth, as well as VEGF-mediated angiogenesis (146). The role of lymphocytes in wound healing is not completely understood but some studies point to a beneficial role of T_H cells, while excessive numbers of CD8⁺ T cells are detrimental (147,148). Skin-resident $\gamma\delta$ T cells have positive effects in wound healing (149).

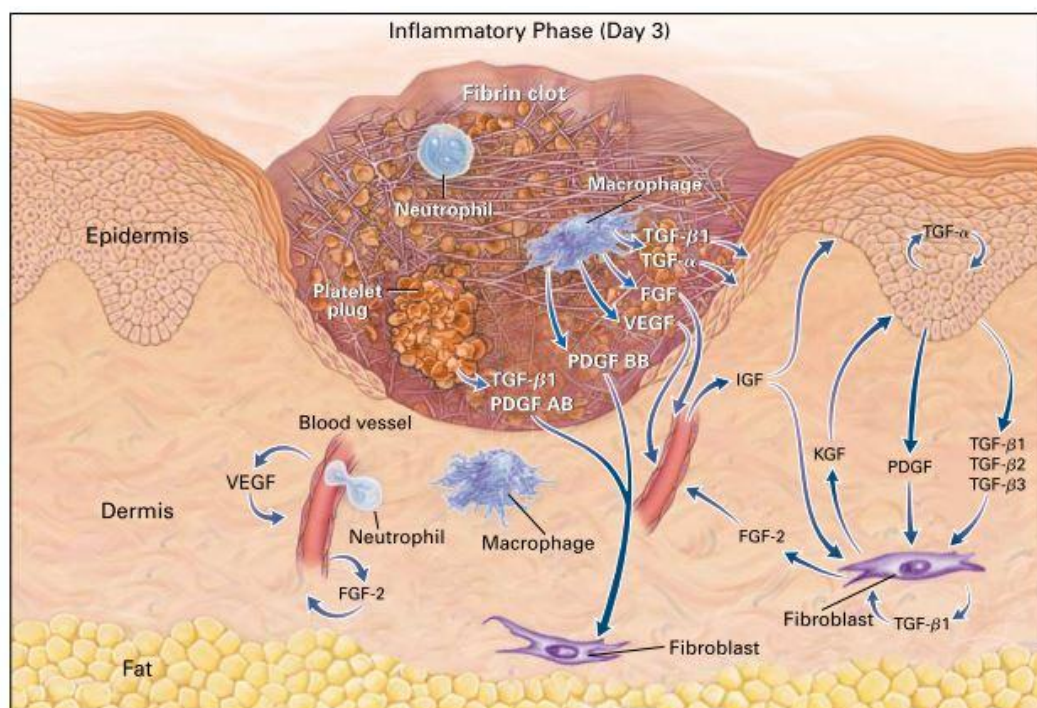


Fig. 5*: Cutaneous wound healing.

Depicted are relevant cell types and their soluble mediators engaged in wound healing.

**reproduced with permission from (150), Copyright Massachusetts Medical Society*

4.2. Non-healing wounds

Non-healing wounds are a major health issue in the western world, causing an estimated \$3 billion per year in the US (151,152). By definition, non-healing or chronic wounds “failed to progress through the normal stages of healing and therefore enter a state of pathologic inflammation” (153). It is possible that different parts of a wound may be stuck in different healing phases, having lost the ideal synchrony of events (154). Consequently, healing is delayed and incomplete, resulting in poor anatomical and functional outcome. Chronic wound etiology is heterogeneous but most ulcers are caused by ischemia, secondary to diabetes mellitus, venous stasis, and pressure. Additionally, wound healing can be compromised by infection with microorganisms (155). In healing wounds, inflammatory processes effectively eradicate microbial invasion whereas in deteriorated tissues (ischemia, hypoxia, devitalized tissue, and chronic inflammation) this process may be impeded. Consequently, inflammation, e.g., mediated by neutrophils, cannot be resolved. In normal healing, neutrophil presence is self-limited to 72-96 h after wounding (151); in non-healing wounds they are present throughout the healing process (156). The continuous presence of neutrophils leads to an imbalance in proteinase and cytokine concentrations. Proteinases degrade tissue, and this proteolytic environment disallows creation of sufficient extracellular matrix, thus inhibiting cell migration and collagen deposition. These conditions seem to be an indirect result of an amplified cytokine secretion. This includes $\text{TNF}\alpha$, CCL2 (MCP-1), IL-1 β , and IL-8. These factors are predominantly secreted by neutrophils, macrophages, and T cells (157-159). By contrast, anti-inflammatory cytokines are not elevated, further spurring the inflammatory bias. Nevertheless, TGF β has failed clinical trials for treatment of chronic wounds (160), whereas VEGF has shown promising results in diabetic foot ulcers (161). Unfortunately, to date there is no generally accepted chronic wound animal model available (162), rendering animal experiments difficult to interpret. This applies, for example, to studies addressing the role of bacteria in improper wound healing. While presence of bacteria is a well-recognized factor in chronic wounds (163) their eradication is not necessarily associated with improved healing response (164). There are reports about pets with non-healing wounds that failed several (antimicrobial) wound therapies, but could ultimately be cured by plasma treatment (50). This

corroborates findings in initial clinical trials, where cold ionized gas displayed promising results (165,65,64,62,166,96).

5. Molecular events in cell biology

The objective of this work is to explore the reactions of immune cells to cold plasma at the cellular and molecular level. Therefore, the molecular mechanisms underlying the cellular behavior are briefly reviewed.

5.1. Signal transduction

Cells specifically respond to their environment. They integrate external stimuli via cell surface molecules (receptor proteins) that are often linked to membrane bound intracellular proteins. The latter transduce the signal to the nucleus where gene transcription is initiated or altered (outside-in signaling). Thus, signal transduction, or simply “signaling”, is required for adjusting cellular activity to environmental changes (167). External stimuli can be of physical-chemical (e.g., temperature, pH, oxidative stress) or biological nature (e.g., cytokines). The latter are usually too large and hydrophobic to penetrate membranes. Therefore, they are usually bound by receptors, allowing the cell to fine tune its biological functions including cell proliferation, a process important in wound healing.

Cytokine signaling is of special importance in the immune response as it mediates directed responses to stimulus. Although many cytokines responses involve similar signal transduction pathways, the JAK/STAT pathway, the response is largely dependent on the cell’s history, explaining the pleiotropic and/or specific action of cytokines (168). Likewise, growth factors including PDGF, FGF, or EGF regulate cell proliferation, differentiation, survival, and metabolism. These molecules bind to receptor tyrosine kinases that have an intrinsic kinase as part of their cytosolic domain. Receptor activation results in downstream signaling of the MAP-kinase pathway. This leads to activation of transcription factors, ultimately facilitating the generation of new proteins (167).

5.2. Respiration and proliferation

Cells grow and divide; both processes that require energy. Cell division, or *proliferation*, is the asexual form of replication. Essentially, parent cells replicate their genomic DNA by a process called mitosis and eventually split into two daughter cells. Proliferation is highly regulated and provides for, e.g., tissue regeneration by fibroblasts and keratinocytes and adaptive immune responses. It can be initiated by binding of specific growth factors or other appropriate cell receptor signaling.

The energy required for such cellular processes can be stored for a short term in form of molecular bonds (ATP), concentration gradients (protons in lysosomes), and electric potential (electrons in mitochondria). Cells can transfer energy from one type into another, e.g., fat cells use chemical energy stored in long chain fatty acids to generate heat in peroxisomes, thus protecting the body from cold. Adenosine triphosphate (ATP), the central molecule for capturing, storing, and transferring energy, is generated in a process called aerobic cellular respiration. Glucose oxidation generates NADH reduction equivalents and their measurement, e.g., via resazurin, provides valuable information about the cellular state. There are various reactive intermediates being generated during respiration, e.g., the superoxide anion (O_2^-) radical comprising 1-2 % of all oxygen being metabolized (169). This species is unstable in solution, leading to the creation of H_2O_2 or $\cdot\text{HO}$ which in turn results in toxic modifications of proteins, DNA, and unsaturated fatty acyl groups in membrane lipids. Thus, during homeostasis, excessive amounts of reactive species, referred to as cellular *oxidative stress*, must be prevented to limit damage to cells and tissues (167).

5.3. Oxidative stress

Oxidative stress is a disturbance in the pro-oxidant/antioxidant system in favor of the former (170). Reactive oxygen and/or nitrogen species (ROS/RNS) are key components in oxidative stress. ROS/RNS are regulators required for wound healing (171,172), signaling, and angiogenesis (173). However, excessive amounts can be deleterious, effectively overwhelming cellular antioxidant defense systems. Reactive species are produced as a

byproduct of cellular metabolism in the respiratory chain. The major sources of ROS responsible for oxidative stress are the mitochondria. To maintain molecular homeostasis, cells have evolved several antioxidative defense mechanisms to cope with this stress. As a general rule, the more ATP a cell requires, the more oxygen is metabolized, and the more reactive oxygen intermediates are accidentally formed. The first “line of defense” against reactive species is superoxide dismutase, dismutating $\text{O}_2^{\cdot -}$ to H_2O_2 . The latter is then converted to H_2O by glutathione peroxidase that also detoxifies lipid hydroperoxide products. Peroxisomes and mitochondria of strongly metabolizing cell types, e.g., cardiac cells, have catalase in addition that helps breaking down H_2O_2 . Hydrogen peroxide itself is not a radical but is central in oxidative stress (174). This molecule can react to highly reactive HO^{\cdot} in presence of traces of metals such as iron or copper (Fenton reaction). Other enzymes that are scavenging reactive species are proteins of the thioredoxin and peroxiredoxin family (175), and the GSH/GSSG redox couple (176). Additionally, antioxidants such as α -lipoic acid, vitamin E, or intracellular ascorbate help to protect mitochondria and cells from extensive oxidative stress (167).

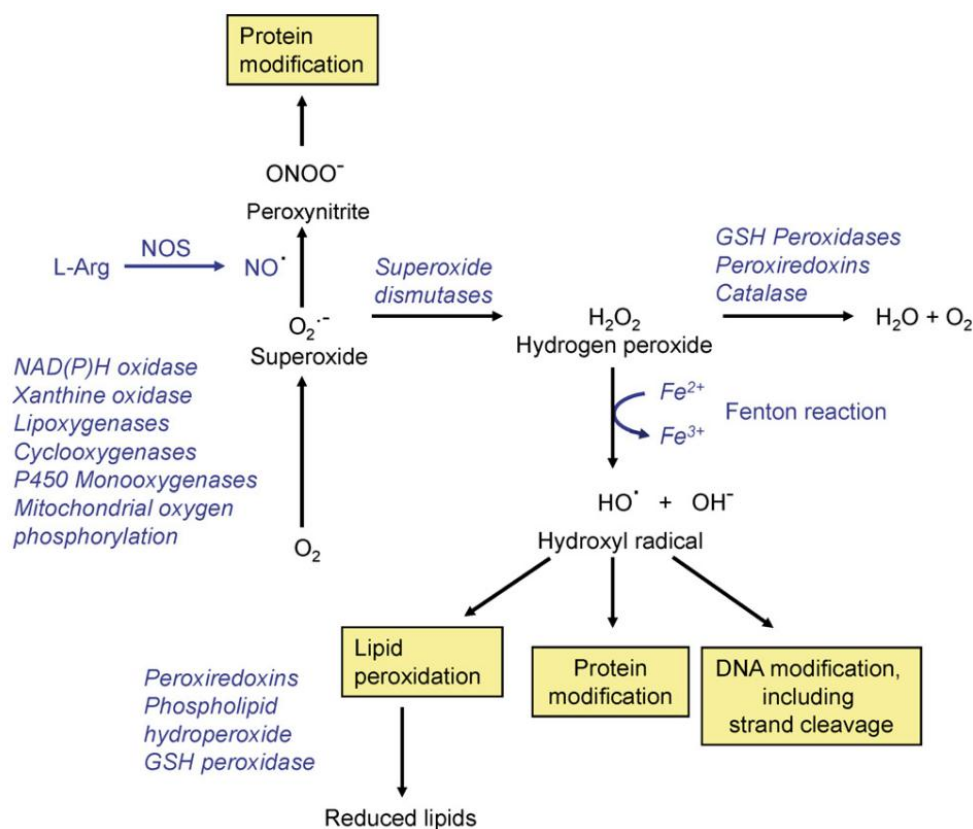


Fig. 6*: Origin and fate of biologically-relevant oxidants and reactive species.

*reproduced from (177) with permission from Elsevier

Oxidative stress is implicated in many diseases such as rheumatoid arthritis, diabetes, cancer, or cardiovascular disease, and is thought to be mediated by activated phagocytes. Hydrogen peroxide and superoxide are both products of the neutrophil oxidative burst, and readily lead to oxidative stress and lipid peroxidation. The latter results in formation of malondialdehyde (MDA), and increased MDA levels were found in slow-healing wounds of rats. This links oxidative stress to wound healing (178).

In rats, physiological concentrations of oxidants such as H_2O_2 a few days after wounding were found to be 100-250 μM but are very likely to be species and wound size dependent (179). Interestingly, these concentrations were modulated during different healing phases which again suggest a physiological role of oxidants in wound healing.

5.4. Cell death

Cell death can result from aggravated assault or in a programmed and “suicidal” fashion. The first type of death is called *necrosis*, the second *apoptosis*. Necrosis is primarily provoked by physical stimuli such as heat or tissue injury. In necrotic cell death, intracellular content can freely diffuse into the extracellular space. While some released molecules are toxic to neighboring cells, others (e.g., ATP) are sensed as “alarm” signals, so called *alarmins* or danger-associated molecular patterns (DAMPs). Tissue destruction by necrosis is followed by compromised barrier integrity which allows bacteria to enter. Alarmins serve as a warning signal and prepare the injured tissue to fight infection by inducing a strong inflammatory response.

However, under physiological conditions, most cells die by apoptosis. Apoptosis is a sequence of molecular events leading to the controlled breakdown of the cell (180). It is a vital process in many biological processes, including ontogenesis and organ development, tumor control, and immune cell regulation. Apoptosis can be mediated by so called extrinsic or intrinsic pathways. The extrinsic pathway is triggered by death-signals such as $\text{TNF}\alpha$, FAS-L, or TRAIL binding to so called death receptors such as TNFR1 , Fas, or TRAIL-R1 (Fig. 7). Upon ligand binding, adaptor molecules, e.g., TRADD or FADD are engaged to activate the regulator caspase 8. Sequential activation of cysteine-aspartic acid proteases

(caspases) plays a central role in apoptosis initiation. Activated caspase 8 activates the executioner caspase 3 that induces the mitochondrial release of apoptogenic factors (176).

Apoptosis can also be induced by oxidative stress. High ROS concentrations interfere with NF κ B activation which otherwise enhances production of anti-apoptotic proteins. Redox stress can be of intracellular or extracellular origin, and induces apoptosis via the intrinsic or mitochondrial pathway. As a result, the mitochondrial membrane potential is lost and mitochondrial pro-apoptotic proteins are released into the cytosol, triggering caspase-independent (AIF) or caspase-dependent (cytochrome C) initiation of apoptosis. AIF launches the nuclear DNA fragmentation and cytochrome C activates caspase 9; both processes are often present at the same time during ROS-mediated cell death. Besides necrosis and apoptosis, other types of cell death, e.g., NETosis (described above) or necroptosis exist, and further details about them can be found elsewhere (181,182).

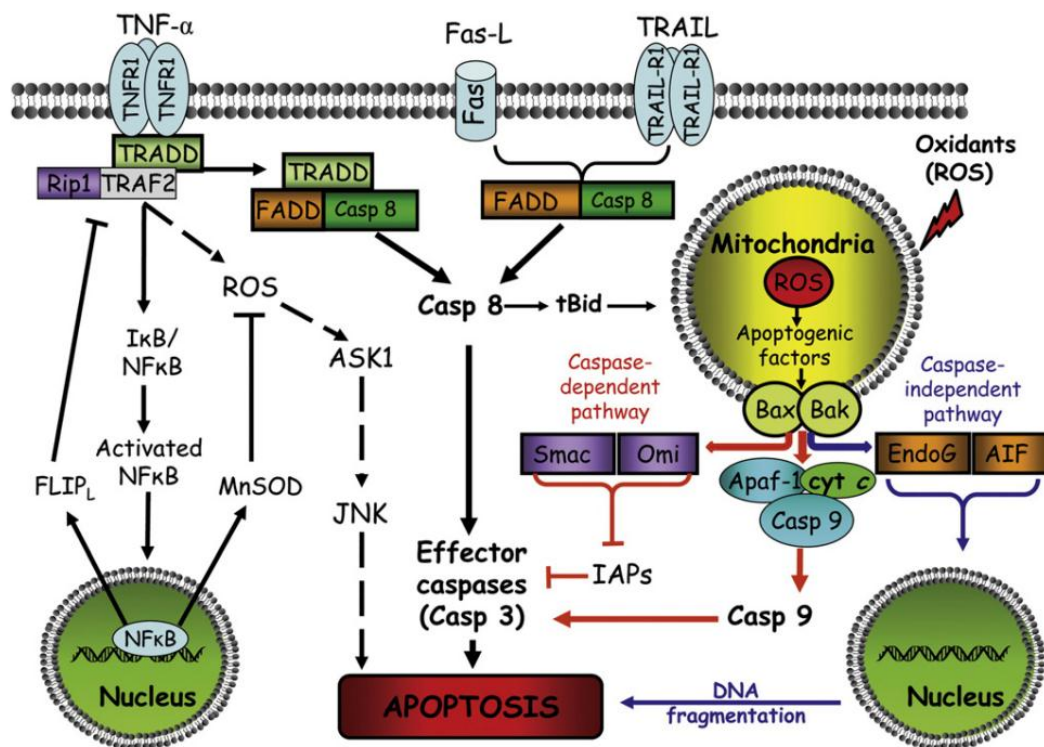


Fig. 7*: Intrinsic and extrinsic pathways of apoptosis.

**reproduced from (176) with permission from Elsevier*

Chapter 2. Materials

1. Laboratory equipment and instruments

argon plasma jet <i>kinpen 09</i>	neoplas, Germany
autoclave DX-100	Systec, Germany
AvaSpec-Dual USB2	Avantes, Netherlands
clean bench Safe2020	Thermo Scientific, USA
CO ₂ -incubator	
Inkubator 160	Mytron, Germany
CB210	Binder, Germany
colony counter SC6Plus	Stuart, UK
Flow cytometer and cell sorter	
<i>Avalon</i>	Propel labs, USA
<i>Attune</i>	Life Technologies, USA
FC500	Beckman-Coulter, USA
<i>Gallios</i>	Beckman-Coulter, USA
FACS Aria I, Aria II, Aria III	Becton-Dickinson, USA
<i>Luminex 100/200</i>	Invitrogen, USA
LSR II	Becton-Dickinson, USA
<i>MoFlo Astrios</i>	Beckman-Coulter, USA
<i>MoFlo XDP</i>	Beckman-Coulter, USA
freezer (-80 °C)	Thermo Scientific, USA
gas mixing machine	MKS Instruments, Germany
hot plate 062	Labotect, Germany
HPLC pump Dionex 3000	Thermo Scientific, USA
micro scale	Sartorius, Germany
microscopy	
AxioCam MP	Carl Zeiss, Germany
microscope Axiovert 40 CFL	
microscope Observer Z.1	
microscope Leica DMI6000B	Leica, Germany
microscope IX82 2	Olympus, Japan

multichannel pipette	Eppendorf, Germany
multipipette plus	Eppendorf, Germany
<i>NanoDrop</i> 2000c	Thermo Scientific, USA
pH-Meter <i>SevenEasy</i>	Mettler-Toledo, Switzerland
<i>pipetboy</i>	Integra, Germany
pipettes	Eppendorf, Germany
plate reader	
M200 pro, F200 pro	Tecan, Austria
<i>FluoStar</i> Optima	BMG Labtech, Germany
<i>VarioSkan</i> Flash	Thermo Scientific, USA
plate shaker Grant-Bio PHMP-4	Keison, UK
precision router Step-Control Zero2	CNC-Technik, Germany
rotator	
Bio RS-24	BioSan, Letvia
SB3	Stuart, UK
Sciex API 4000QTRAP	Applied Biosystems, USA
separation magnet Big Easy Sep	StemCell Technologies, Canada
spectrophotometer	
4500	Hitachi, Japan
Specord 210 Plus	Analytik Jena, Germany
Thermoblock TB2	Biometra, Germany
Thermo-Cycler	Biometra, Germany
Thermomixer comfort	Eppendorf, Germany
Vacutip, Vacusafe	Integra, Germany
Vortex Genie 2	Scientific Industries, USA
water bath	Memmert, Germany
water bath (ultrasonic)	VWR, Germany
water purification system Milli-Q	VWR, Germany
xyz-table	Nanotec, Germany
Centrifuges:	
5804R	Eppendorf, Germany
5810 and 5810R	
Concentrator Plus	
Mini-Spin	
Cytospin 4	Thermo Scientific, USA

2. Consumables

12 x 75 mm (FACS) tubes (PP, PS)	Sarstedt, Germany
beakers	VWR, Germany
butterfly needle	Becton-Dickinson, USA
cell strainer	
70 µM	Miltenyi Biotec, Germany
100 µM	Becton-Dickinson, USA
centrifuge tubes	Sarstedt, Germany; TPP, Switzerland
columbia blood agar plates	Becton-Dickinson, USA
cotton swap, sterile	Eurotubo, Peru
cover slips	Roth, Germany
cuvettes	VWR, Germany
Cytospin clips and funnels	Thermo Scientific, USA
dispenser tips, sterile	Brand; Eppendorf; Germany
Eppendorf tubes, sterile	Roth; Eppendorf, Germany
filters (0.2 and 0.45 µm)	VWR, Germany
gases (99,99 % purity)	
Ar, N ₂ , O ₂ , synthetic air	Air Liquide, France
gloves	Ansell, Australia; VWR, Germany
laboratory glass bottles, sterile	VWR, Germany
leukosep tubes	VWR, Germany
microscope slide	Roth, Germany
multiwell plates (6-, 12-, 24-, 96-well; flat or round bottom) , sterile	Corning, USA; NUNC, Denmark; Sarstedt Germany; TPP, Switzerland
parafilm	Pechiney Plastic Packaging, Chicago, USA
pasteur pipettes, sterile	Roth, Germany
PCR tubes, sterile	Corning, USA
petri dishes, sterile	60 mm; Sarstedt, Germany
pipette tips, sterile	Eppendorf, Germany
reservoir	Corning, USA
serological pipettes, sterile	Sarstedt, Germany
syringes, sterile	Terumo, Japan
vacutainer	Becton-Dickinson, USA

3. Chemicals and solutions

(4-(2-hydroxyethyl)-1-piperazineethanesulfonic acid) (HEPES)	Sigma, USA
3,3',5,5'-Tetramethylbenzidine (TMB)	Sigma, USA
³ H-methyl-thymidine	Amersham, UK
4-Aminobenzoic acid hydrazide (4-ABAH)	Sigma, USA
ammonium chloride	Sigma, USA
beads (flow cytometry)	
0.2, 1.0, 2.0, 6.0, 10.0 µm YG or YO	Polysciences, USA
Performance Tracking beads	Life Technologies, USA
FlowCheck, FlowSet	Beckman-Coulter, USA
Rainbow 1 peak, 6 peak, 8 peak	Spherotech, USA
bovine serum albumin (BSA)	Sigma, USA
brefeldin A (1000x)	BioLegend, USA
calcium chloride (CaCl ₂)	Sigma, USA
carboxyfluorescein succinimidyl ester	Molecular Probes, USA
catalase	Sigma, USA
<i>Cohn</i> II fraction	Sigma, USA
cytochrome C	Sigma, USA
density gradient separation medium (Ficoll)	PanBioTech, Germany
dextran (technical grade)	Serva, Germany
dH ₂ O, PCR grade	Roche, Switzerland
dimethylsulfoxide (DMSO)	Sigma, USA
<i>Dulbecco's</i> PBS (1x and 10x)	PanBioTech, Germany
ethanol, absolute	Roth, Germany
ethylenediaminetetraacetic acid (EDTA)	Sigma, USA
fetal calf serum (FCS)	Sigma, USA
focusing fluid (Attune)	Life Technologies, USA
glutamine	Biochrom, Germany
glutathione	Sigma, USA
Hank's buffered saline solution (HBSS)	PanBioTech, Germany
hydrogen peroxide (H ₂ O ₂), 30 %	Sigma, USA
ionomycin	Sigma, USA
<i>IsoFlow</i> sheath fluid	Beckman-Coulter, USA
isopropanol	Sigma, Germany

<i>IsoTone</i> (8x)	Beckman-Coulter, USA
JC-1	Enzo Life Science, USA
lipopolysaccharide (LPS)	Sigma, USA
MACS running buffer	Miltenyi, Germany
methanol, absolute	Sigma, USA
monensin (1000 x)	BioLegend, USA
paraformaldehyde (PFA)	Roth, Germany
Penicillin/streptomycin	Sigma, USA
phorbol-12-myristat-13-acetat (PMA)	Sigma, USA
phytohemagglutinin (PHA)	Remel, Großbritannien
resazurin	Life Technologies, USA
<i>Roswell-Park-Memorial-Institute</i> (RPMI) 1640 Medium	PanBioTech, Germany
shutdown solution (Attune)	Life Technologies, USA
sodium azide	Sigma, USA
sodium chloride (NaCl)	Sigma, USA
sodium hydroxide (NaOH)	Sigma, USA
<i>Staphylococcus aureus</i> superantigens (SAg)	institute of immunology, Greifswald, Germany
superoxide dismutase (SOD)	Sigma, USA
taurine	Sigma, USA
<i>thioltracker violet</i>	Molecular Probes, USA
trypan blue	Biochrom, Germany
Tween20	Sigma, USA
tyrosine	Sigma, USA
uric acid	Sigma, USA

4. Media and buffers

Annexin V binding buffer	10 mM HEPES 140 mM NaCl 2.5 mM CaCl ₂
FACS buffer	PBS 2 % FCS 0.02 % sodium azide 2 mM EDTA

lysis buffer	10 mM potassium carbonate
	155 mM ammonium chloride
	0.1 mM EDTA
R10F	RPMI 1640 (without phenol red)
	10 % FCS
	200 mM glutamine
	0.1 mg L ⁻¹ penicillin / 100 U ml ⁻¹ streptomycin
wash buffer (ELISA)	PBS
	0.05 % Tween20

5. Kits

Amplex ultra red	Molecular Probes, USA
CD4 negative isolation	Stem Cell Technologies, France
cytokine human 10-plex panel (Luminex)	Life Technologies, USA
<i>MeasureIt</i> nitrite detection	Molecular Probes, USA
<i>Phagoburst</i>	Glycotope, Germany
<i>PicoGreen</i> dsDNA Assay	Life Technologies, USA

6. Software and online databases

Attune v2.1	Life Technologies, USA
AvaSoft 7.6	Avantes, Niederlande
AxioVision Rel. 4.8.2	Carl Zeiss, Germany
BioPlex Manager 5.0	BioRad, Hercules, , USA
MXP / CXP	Beckman-Coulter, USA
Endnote 5.0.1	Thomson Reuters, USA
FACSdiva 6.0, 8.0	BD, USA
FlowJo 7.6.5 und Vx	Treestar Inc, USA
i-Control 1.10	Tecan, Österreich
ImageJ	Wayne Rasband, NIH, USA
Kaluza 1.3 and Kaluza Acquisition 1.0	Beckman-Coulter, USA
Leica TCS SP5 application suite 2.72	Leica, Germany
Microsoft Office suite	Microsoft, USA
Scholar	Google, USA

Materials

Prism 6.05	Graph Pad Software, USA
SkatIt 2.5	Thermo Scientific, USA
Fluorescence spectra analyzer (online)	BioLegend (USA); Beckton-Dickinson (USA); Life Technologies (USA)
Summit 6.2.3	Beckman-Coulter, GmbH
ThermoIQ	Thermo Fischer, USA
UV Solutions 3.0	Hitachi, Japan
WinAspect Plus	Analytik Jena, Germany
WinPC-NC	Burkhard Lewetz, Germany

Chapter 3. Methods

1. Plasma and liquid characterization

1.1. Plasma treatment of liquids and cell suspension

One ml of liquid or cell suspension was plasma-treated in a cavity of a 24 well plate. The height of the cavity was 16.5 mm with a diameter of 15 mm and an area of 1.9 cm². Cells were concentrated at 10⁶ per ml if not stated otherwise. For treatment, a computer program was written that placed the ceramic nozzle of the jet exactly 5 mm above the center of each well using a computer-driven *xyz* table. During treatment, the plasma jet rested at this position and the treated liquid or suspension was mixed by the argon flux. When the programmed treatment time was finished, the jet was automatically hovered to the center of the next well. This procedure allowed a reproducible and sequential treatment of multiple samples.

Cells were treated directly with plasma if not stated otherwise. For indirect treatment, 1000 µl of medium was exposed to plasma twice as long as indicated and 500 µl were then added to 500 µl of cell suspension at 2 x 10⁶ cells per ml of medium. This resulted in a 1:2 dilution of both cell concentration and plasma-treated medium.

The feed gas flux (argon) was set to 3 standard liters per minute (slm) if not stated otherwise. Gas flow rates were calibrated and adjusted precisely (± 0.1 %) using a gas flow controller. This device also allowed the controlled admixture of molecular gases or experimentally humidified argon gas to the main argon feed gas stream. The system (including plasma jet, flow controller, and relevant tubing) was always flushed with argon gas alone for at least 30 min prior to treatment to eradicate residual humidity. For experimentally added humidity, argon gas was driven into H₂O (bubbler) and the gas was re-unified with the dry argon flux. Portion of wet gas was adjustable using a flow controller. In one experimental setting, exogenous O₂ or humidity were completely shielded from the plasma effluent using a gas curtain. Shielding gas flux in the gas shielding device was 2 slm of N₂, and feed gas flux of

the plasma jet was 1 slm of argon with admixture of 10 sccm N₂. Due to the feed gas flux, water evaporated from treated solutions. For treatment times exceeding 1 min, ddH₂O was added after exposure. This accounted for lost volume and was meant to keep the solution at isoosmotic conditions. At or below 1 min of treatment time, less than 4 % of total volume evaporated. Here, no ddH₂O was added to minimize additional errors by this procedure. Evaporation was independent of the plasma being ignited or off, as thermal contribution of plasma to water evaporation was negligible.

In all experiments, argon gas controls were conducted. As argon is a noble (inert) gas, no effect on cells was observed in all experiments (except where indicated in neutrophil experiments). Therefore, showing argon controls in each graph was omitted. Before and after treatment, cells were incubated in an incubator at 37 °C, 5 % CO₂, and near 100 % relative humidity. This condition allowed stabilizing the pH in carbonate-buffered solutions, e.g., medium. To control for effects of certain reactive species or oxidants, catalase (cat; 5-20 µg/ml, equivalent to 10.6 - 22.4 units; scavenges hydrogen peroxide), superoxide dismutase (SOD; 20 µg/ml; scavenges superoxide), or uric acid (UA; 100 µM; scavenges reactive nitrogen species and especially peroxynitrite) were added before or after treatment as indicated. As it was shown in this work that plasma generated H₂O₂, the peroxide alone was also experimentally added in some assays. For this, 30 % H₂O₂ with stabilizers was diluted two times 1:100 in PBS, yielding a solution of 1 mM H₂O₂. Final dilution was done in 1 ml of liquid or cell suspension.

1.2. Optical emission spectroscopy

The gas and plasma system was flushed with argon gas for 1 h to eradicate residual humidity. The jet was then centered in front of a UV/VIS/NIR compact fiber optic spectrometer (Avaspec-2048-USB-2, Avantes). It uses an entrance slit width of 25 µm which results in a spectral resolution of 0.7 nm. The size of the spectrometric quartz glass lens covered the whole length of the effluent, and emission intensities from 195-975 nm were recorded using a computer. The integration time of light collection was 110 ms, and intensity was recorded in ADC counts using a 2048 pixel CCD detector and AvaSpec software. Peak intensities were

calculated as an average of ten consecutive measurements and normalized to the highest peak where indicated. Addition of molecular gases was done using a mass flow controller. The plasma effluent immediately changed in size and color and emission spectra were compared to control using argon gas plasma alone.

1.3. Quantification of reactive species in liquids

Quantification of hydrogen peroxide and nitrite

Quantification of H_2O_2 or NO_2^- was done according to manufacturer's instructions using *Amplex ultra red* or *MeasureIt nitrite detection*, respectively. Using horseradish peroxidase to catalyze the reaction, Amplex red is a highly specific probe for hydrogen peroxide but not superoxide and it reacts with hypochlorous acid only at very high concentrations ($> 1\text{mM}$) (183). Samples were plasma-treated and added to wells (4 replicates per sample) of a black 96 well plates containing the detection mix for H_2O_2 or NO_2^- . Fluorescence was recorded using a microplate reader (Tecan F200) with suitable excitation and emission filters (*Amplex ultra red*: 535 / 590 nm, *MeasureIt nitrite detection*: 360/465). Final concentrations were calculated using a H_2O_2 and NO_2^- standard curve, respectively. H_2O_2 measurements were also carried out in supernatants of PBMCs. Here, cells were spun prior to supernatant collection and quantification of H_2O_2 .

Quantification of superoxide anion

The superoxide anion (O_2^-) can be specifically detected using cytochrome c (184). For quantification of O_2^- , cytochrome c (final concentration 120 $\mu\text{g/ml}$) and catalase (final concentration 20 $\mu\text{g/ml}$) were added to 1 ml of medium. Before treatment, absorbance of solution was blanked using a disposable cuvette in a spectrophotometer (HitachiSpec) at 550 nm. Solution was then transferred to wells of a 24 well plate and subsequently plasma-treated before being transferred back into the original cuvette. Quantification was done by calculating the absolute increase of absorption after plasma treatment and by using the molar extinction coefficient of cytochrome c ($\epsilon = 21.1 \times 10^3 \text{ M}^{-1}\text{cm}^{-1}$). Assay specificity

was verified by addition of superoxide dismutase (SOD) before plasma treatment (20 µg/ml).

Relative quantification of oxidized glutathione

Glutathione (GSH) was added to 1 ml of fully supplemented medium (R10F) at a final concentration of 50 µM. After plasma treatment, 900 µl per sample were added to cuvettes containing 100 µl of PBS and 200 µM 5,5'-dithiobis-2-nitrobenzoic acid (DTNB or Ellman's reagent) and measured spectrophotometrically at 412 nm due to reaction of GSH with DTNB. GSH, however, can become oxidized and forms GSSG. GSSG cannot react with DTNB to form a stable yellow product. The absorption of the liquid at 412 nm thus correlates with the availability of GSH.

Quantification of 3-nitrotyrosine and 3-chlorotyrosine

One ml of R10F or PBS was spiked with tyrosine (final concentration 1 mM) and plasma-treated for 60 s. Controls contained catalase (5 µg/ml), H₂O₂ (60 µM), or uric acid (100 µM). For indirect treatment, tyrosine was added to solution 30 s after plasma treatment. Quantification of 3-nitrotyrosine or 3-chlorotyrosine was done using a standard curve and *High-Performance-Liquid-Chromography* with consecutive mass spectrometric detection as described before (185). Detection limits were 1 nM for 3-nitrotyrosine and 0.8 nM for 3-chlorotyrosine. LC/MS experiments were done by Dr. Rufus Turner, Centre for Free Radical Research, Department of Pathology, University of Otago, Christchurch, New Zealand.

1.4. Characterization of cell culture supernatants

Plasma-treated cells were incubated at 37 °C and supernatants were collected by centrifugation (1000 x g for 10 min) after indicated time points. Eppendorf tubes (low protein-binding type) were stored at -80 °C until analysis. Target proteins were detected using sandwich enzyme-linked-immunosorbent-assay (ELISA). ELISA plates were bought pre-coated with primary antibody. Alternatively, 96 well plates with a high affinity for proteins were manually coated with primary antibodies in the plate O/N at 4 °C. Sample was

added, and plate-attached antibodies bound the target protein, e.g., an interleukin (IL). A second antibody was added which binds to another epitope of the target protein. This antibody was conjugated with horseradish peroxidase (HRP) that oxidizes a chromogenic substrate (TMB) under catalysis of H_2O_2 , forming a blue product. The reaction was stopped by addition of 2N sulfuric acid and yielded a yellow solution. Its absorbance at 450 nm (with 570 nm reference wavelength, measured using a Tecan M200 pro) correlates with target protein content in a near-linear fashion within pre-defined concentrations. Protein content can then be quantified using a standard curve. Using the same principles, semi-quantitative measurements were done using multi-analyte ELISA arrays that include only a negative and positive control for each of the twelve target proteins provided on each plate. These assays allowed finding an increase or decrease of the target protein concentration, and supernatants of three donors were pooled for these experiments. Additionally, ten cytokines were investigated using Luminex technology according to vendor's instructions. DNA concentrations in supernatants were quantified using PicoQuant (life technologies) reagent, calibrated with a standard curve of salmon-sperm DNA (life technologies), and measured using a plate reader (excitation 485, emission 535) according to instructions provided by the manufacturer.

target(s)	detection limit	vendor
GM-CSF	4 pg/ml	BioLegend
human chemokines	multiple	SA Bioscience
human elastase	2 pg/ml	eBioscience
human inflammatory cytokines	multiple	SA Bioscience
IL-1 β	1 pg/ml	BioLegend
IL-33	4 pg/ml	BioLegend
IL-6	8 pg/ml	BioLegend
IL-8	8 pg/ml	BioLegend
interferon gamma (IFN γ)	4 pg/ml	BioLegend
Lactate dehydrogenase B (LDHB)	8 ng/ml	AbCam
T _H 1 / T _H 2 / T _H 17 cytokine	multiple	SA Bioscience
thymic stromal lymphopoietin (TSLP)	2 pg/ml	BioLegend
tumor-necrosis-faktor alpha (TNF α)	2 pg/ml	BioLegend
vascular endothelial growth factor (VEGF)	8 pg/ml	eBioscience

2. Cell isolation and flow cytometry

2.1. The principle of flow cytometry

In flow cytometry, single particles or cells in suspension are investigated. Once inside the device, the liquid is focused in a way that the particles line up ideally one after the other in the sample stream. The sample stream then passes different lasers, which are mounted sequentially (usually about 125 μm apart) in modern cytometers. Particles passing a laser inevitably generate light scatter, which is historically used to characterize cell “size” (forward scatter) and “granularity” (side scatter), especially when measuring blood cells. Moreover, cells are often incubated with antibodies conjugated with fluorochromes and specific for an extracellular or intracellular epitopes of interest. Laser light-excited fluorochromes are brought into vibrational states, thereby losing energy before emitting light. Energy and wavelength are inversely correlated, and therefore the emitted light is predominantly of a higher wavelength (Stoke’s shift). Optical mirrors and filters allow for simultaneous detection of different wavelength bands specified by their coating, reflecting and transmitting light of interest. After light has passed the filters, emission intensities are recorded by photomultiplier tubes (PMTs) that amplify photon signals via quadratic electron dissipation. Analog-to-digital converters then allow signals to be displayed, analyzed, and compared by personal computers. Many different signals can be attributed to a single event, effectively allowing for multi-parametric characterization. As emission profiles are not always clearly separated between different fluorochromes, digital compensation aids in subtracting spill-over of light from one fluorochrome into any non-designated PMT. This was extensively used in multi-parametric panels using up to 10 colors simultaneously. A single event is only of poor statistical relevance and the advantage of flow cytometry is its ability to integrate hundreds of thousands of events into one single analysis. This allows separating *populations* by defining their boundaries of distribution using *gates*. These aspects make flow cytometry a powerful tool and the key method used in this work to characterize leukocytes following plasma treatment. (186)

2.2. Flow cytometry and cell sorting

In this work, different flow cytometers were utilized. At the *flow cytometry core facility* (Harvard Stem Cell Institute, Boston, USA), a 4-laser 11 color LSRII (Becton-Dickinson) was used. At this institute, lymphocytes were also sorted using a FACS ARIA I or II (Becton Dickinson), a *MoFlo XDP* or *Astrios* (Beckman-Coulter), and an *Avalon* (Propel Labs). During a research project at the *Centre for Free Radical Research* (University of Otago, Christchurch, New Zealand) samples were acquired using a Beckman-Coulter flow cytometer (FC500) with two lasers and 7 colors. In Greifswald at the centre of innovation competence (ZIK) *plasmatis*, flow cytometric measurements were conducted using a *Gallios* (3-laser, 10 colors). For sample acquisition out of 96 well plates, an *Attune* cytometer (2-laser, 6 color; life technologies) analyzed samples being acquired from an *Attune* auto sampler station. Cell sorting in Greifswald was done at ZIK HiKe using a FACS Aria III or at ZIK *plasmatis* using a 7-laser, 32 color *MoFlo Astrios*.

Cytometer performance was calibrated using fluorescent beads (Spherotech 8 peak rainbow calibration particles 3.1 μm) before each experiment. Day-to-day variation never exceeded $\pm 5\%$. Usually, 10.000-250.000 cells were acquired per sample. In regular flow cytometric experiments, LMD, FCS 2.0, or FCS 3.0 were analyzed with *Kaluza* software. Ninety-six well assay experiments were evaluated using *Attune* software. For large data analysis of cell sorting experiments (>1 Mio events), *Summit* software was used. CFSE proliferation modeling was analyzed using *FlowJo* software.

Emission filter values are given as wavelength \pm bandwidth in nm. The bandwidth value divided by two states the \pm bandpass from the center wavelength (e.g., 525/40 = 505-545 nm). All filters and dichroic mirrors used exhibited high transition steepness to minimize spillover. For compensation, single stained cells or compensation beads (eBioscience), or FMO controls were used, and automatic compensation was calculated using *Kaluza* software with unstained cells in the auto fluorescence gate. When necessary, isotype controls were included to determine exact gating positions.

2.3. Isolation of PBMCs

Upon blood donation at the blood bank (University Medicine of Greifswald, Germany), healthy blood donors gave written and informed consent about anonymous usage of blood for research purposes in the case that the donation is not suitable for clinical application. Human peripheral blood mononuclear cells (PBMCs) were isolated from buffy coats (erythrocyte-depleted blood bags). PBMCs can be obtained by centrifuging leukocytes over a sucrose gradient medium. Granulocytes contain many vesicles attributing a high density to these cells. Upon centrifugation, they (and remaining erythrocytes) pass through the density medium and the less-dense mononuclear cells stay on top of it (187). All steps were performed at room temperature. The cell suspension was diluted in PBS and layered over 10-15 ml of leukocyte separation medium (ficoll) in 50 ml tubes or leukosep-tubes. The cells were centrifuged with break off. The interphase cell layer, containing PBMCs, was harvested into a new tube using a sterile Pasteur pipette. If necessary, residual erythrocytes were lysed using ammonium chloride lysis buffer. After two wash steps with PBS, the cells were resuspended in full medium (R10F). For cell counting, a hemocytometer (Bürker chamber) was covered with a cover slip, the cell suspension (diluted 1:10 in trypan blue) was added, and the cell concentration quantified using phase contrast microscopy (AxioVert). Alternatively, cells were diluted 1:10 in PBS containing DAPI (500 nM) and counted using a syringe-pump driven flow cytometer for absolute count determination. Cell counting was always done in duplicates.

2.4. Isolation of PBMCs subpopulations

All steps were performed at room temperature. For magnetic separation, PBMCs were adjusted to 1×10^8 per ml in FACS buffer and incubated with an antibody-cocktail (Stem Cell Technologies). The latter either contained antibodies against the target cells (positive selection) or left the cells untouched by labeling all but the cells of interest (negative selection). Cells were then incubated with magnetic beads and subsequently magnetically separated (Big Easy, Stem Cell Technologies). Cells of interest were washed, resuspended in

R10F, and counted. For cell separation by cell sorting, PBMCs were adjusted to 10^8 per ml in FACS buffer and incubated with monoclonal antibodies coupled to different conjugates. After staining, cells were washed and adjusted to $1-5 \times 10^7$ per ml in FACS buffer. Using appropriate excitation and emission wavelengths, cells were sorted using a cell sorter.

2.5. Isolation of PMNs

Human neutrophils were isolated from venous blood of healthy controls, obtained with informed consent, and within the New Zealand Southern A Regional Ethics Committee approval for experiments at CFRR. All steps were performed at room temperature. Isolation of polymorpho-nuclear cells (PMNs) was done by adding dextran to blood and incubating the cells for 20-30 min. After this step, only few erythrocytes were present in the supernatant containing the leukocytes. Supernatant was taken off, carefully layered on top of Ficoll, and spun with the break off. Plasma, PBMCs, and ficoll were taken off. Residual PBMCs sticking to the tube walls were removed with sterile cotton swaps. Pellets were washed once in PBS before removing residual erythrocytes by hypotonic lysis. After washing, cells were resuspended in Hank's containing divalent cations, and counted.

3. Characterization of plasma-treated PBMCs

3.1. Cell viability

Cell viability was assessed by various means. Firstly, it was estimated by measuring the total cellular respiration. Here, PBMCs (10^6 per ml in R10F) were plasma-treated and subsequently aliquoted in 96 well plates (100 μ l/well). Resazurin (final concentration 200 μ M, Alfar Aesar, USA) was added, and plates were incubated for 48 h in an incubator. Resazurin can freely penetrate cell membranes. Metabolically active cells non-reversely reduce resazurin to its fluorescent product, resorufin. Fluorescence was detected using a plate reader and normalized to control fluorescence. Background fluorescence of wells containing medium with resazurin alone was subtracted from all samples.

Viability was also measured by flow cytometry as percentages of cells that neither display signs of apoptosis (phosphatidylserine exposure, caspase activation) nor of permanent cell membrane damage (late apoptosis or necrosis). Although apoptotic cells are not terminally dead no increase in percentages of non-apoptotic cells was observed. Thus and if not stated otherwise, percentage of cells negative for Annexin V and DAPI of PBMCs was assessed 24 hours after plasma treatment and incubation at 37 °C. Cells were harvested into FACS tubes, and stained with monoclonal antibodies directed against different cell surface markers to discriminate for subpopulations by flow cytometry. After washing with Annexin V binding buffer (AVBB), cells were stained in AVBB containing Annexin V conjugated to fluorescent probes. Annexin V binds to phosphatidylserine (PS), which is exposed on the outside of the cell membrane of early and late apoptotic cells (188). Cells were washed in AVBB and resuspended in AVBB containing a viability dye, which quickly enters cells with compromised membranes while diffusion into viable cells is very slow. Once inside the cell, dyes bind to nucleic acids and their fluorescence is enhanced (200-1000x), which is detectable by flow cytometry. In conjunction with Annexin V, dead cells can be discriminated for an early and late apoptotic phenotype. Proportion of early to late apoptotic cells is dependent on the incubation time after cytotoxic stimulus. Therefore, percentages of cells staining negative for Annexin V or DAPI (instead of percentages of early or late apoptotic cells) were shown.

Apoptotic cells also show DNA fragmentation which was measured by staining cells with Hoechst (10 μ M) 24 h after plasma treatment. In experiments measuring caspase 3/7 activity, cells were plasma-treated, incubated for various time points, harvested into FACS tubes, and CellEvent-reagent was added. It contains a peptide sequence that is preferentially cut by the caspase enzymes 3 and 7 but only in their active state. Upon cleavage, a peptide is released that displays high affinity for nucleic acids and strongly fluoresces upon binding. If the peptide is still attached to its original sequence, DNA-binding is not possible due to steric inhibition. Caspase-positive cells were quantified by flow cytometry. For fixed and permeabilized cells, fixable viability dyes (fvd) were used to discriminate live from dead cells. They do not stain nucleic acids but instead amine groups of proteins. These groups are highly present in the cytosol, which is accessible to fvd in dead cells. Intact cells only display few amine groups at the cell membrane. Staining was performed before permeabilization and excess dye was washed away. To investigate immediate cell death after plasma treatment (necrosis), 1 ml of PBMCs (10^6 per ml in R10F containing DAPI) were analyzed by flow cytometry. After recording a baseline (30 s) of DAPI positive cells naturally occurring in PBMCs isolations (usually 2-6 %), acquisition was halted, cells were directly plasma treatment and acquisition was continued immediately.

Monocytes, a subpopulation of PBMCs, contain myeloperoxidase (MPO). MPO converts H_2O_2 to $^{\cdot}OCl$ and can be inhibited using 4-ABAH (30 min prior to treatment, 100 μ M, Sigma). Viability of lymphocytes was compared between MPO-inhibited and control PBMCs (monocytes). The properties of viability dyes used in this work are summarized below.

dye	interacts with	emission filter used	vendor	final concentration
7-AAD	DNA	695 / 30 nm (bp)	BioLegend	1:100
Annexin V FITC	phosphatidylserine	525 / 40 nm (bp)	BioLegend, Enzo	1:250
Annexin V PE	phosphatidylserine	575 / 30 nm (bp)	BioLegend	1:250
Annexin V PE-Cy7	phosphatidylserine	>755 nm (lp)	eBioscience	1:250
CellEvent	active caspase 3/7	525 / 40 nm (bp)	Molecular Probes	1:100
DAPI	DNA	450 / 50 nm (bp)	Thermo Fischer	1 μ M
FVD eFluor 780	amine groups	>755 nm (lp)	eBioscience	1:10000
PI	DNA / RNA	620 / 30 nm (bp)	Sigma	1 μ g/ml
Zombie Yellow	amine groups	550 / 50 nm (bp)	BioLegend	1:100

Comparison of cell viability between different PBMCs subpopulations

PBMCs were seeded in 24 well plates and incubated O/N at 37 °C with or without PHA (500 ng/ml), or with or without staphylococcal superantigens (SAg). Superantigens were obtained from the Institute of Immunology and Transfusion Medicine, Department of Immunology, Greifswald, Germany. Equal amounts of five superantigens (SEB, SEI, TSST, SEO, SEQ) were used (final concentration: 1 µg/ml). Cells were then directly plasma-treated and incubated for another 24 h at 37 °C. PBMCs were harvested into FACS tubes, incubated with Cohn II fraction to saturate Fc-receptors, and stained with monoclonal antibodies directed against different surface markers. Using AVBB, cells were then washed and stained with Annexin V and DAPI as described above. Survival rates of six different populations were analyzed in two different panels measuring up to 8 colors simultaneously using flow cytometry. The following table summarizes the antibodies being used.

target	clone	isotype	conjugate	supplier	final concentration
CD3	UCHT1	m-IgG1	AF700	BioLegend	0.1 µg/ml
CD4	VIT4	m-IgG2a	APC	Miltenyi	0.2 µg/ml
CD4	RPA-T4	m-IgG1	PE-CF594	BD	0.2 µg/ml
CD8	BW135/80	m-IgG1	PerCP	Miltenyi	0.4 µg/ml
CD14	TÜK4	m-IgG2a	FITC	Miltenyi	0.1 µg/ml
CD19	HIB19	m-IgG1	PE	Miltenyi	0.5 µg/ml
CD56	HCD56	m-IgG1	APC-Cy7	BioLegend	0.2 µg/ml
CD161	HP-3G10	m-IgG1	APC	BioLegend	0.5 µg/ml
CD196	G034E3	m-IgG2b	PE	BioLegend	0.2 µg/ml
γδ-TCR	B1	m-IgG1	PE	Beckman-Coulter	1.0 µg/ml

3.2. Cellular oxidation

Staining of PBMCs was done according to protocols included in manufacturer's instructions. Briefly, cells were suspended in PBS and incubated with redox-sensitive probes at 37 °C. Monoclonal antibodies were present to later discriminate oxidation in different subpopulations using multicolor flow cytometry. Cells were then washed with FACS buffer or R10F and were suspended at 10⁶ per ml R10F in 24 well plates prior to plasma treatment.

After exposure, cells were harvested into FACS tubes, washed, and suspended in FACS buffer containing DAPI to discriminate live from dead cells. Median fluorescence intensity was acquired by flow cytometry, and modulation by plasma treatment was calculated by dividing MFI_{plasma} or $MFI_{\text{H}_2\text{O}_2}$ by MFI_{control} .

redox-sensitive probe	compartment	supposedly specific for	vendor	final concentration
APF	cytosol	ONOO ⁻ , ⁻ OCl, ⁻ HO	Mol. probes	10 μ M
C ₁₁ -Bodipy 581/591	membrane	lipid peroxidation	Mol. probes	1 μ M
CM-H ₂ DCF-DA	cytosol	ROS / RNS	Mol. probes	10 μ M
CM-H ₂ -TMRos	mitochondria	ROS / RNS	Mol. probes	5 μ M
DHR123	cytosol	ROS	VWR	20 μ M
HPF	cytosol	ONOO ⁻ , ⁻ HO	Mol. probes	10 μ M
Mitoxox ⁻ O ₂ sensor	mitochondria	⁻ O ₂	Mol. probes	5 μ M
<i>Mitotracker</i> orange	mitochondria	ROS	Mol. probes	10 μ M

The table summarizes the redox-sensitive probes used in this work. Specificity of probes to dedicated species is based on manufacturer's information. However, these often rely on results in cell-free, and simplified biological solutions as PBS and specificity may be altered in cellular environments (189,83,190).

3.3. Detection of cell proliferation

About 40 % of PBMCs are T cells, which proliferate upon activation. For functional analysis, 10⁶ cells per ml in R10F were incubated with the mitogen phytohemagglutinin (PHA; Remel, United Kingdom) that induces polyclonal activation of T cells. PBMCs were directly plasma-treated first, and then stimulated with PHA. After 72 h of stimulation, PBMCs were incubated for 17 h with ³H-methyl-thymidine with 0.5 mCi per well (Amersham, UK). Compared to a standard, proliferation can be measured in counts per minute (cpm). Triplicates of identically treated cells were used in all experiments.

For CFSE experimentations, isolated cells were suspended in PBS and stained with 2 μ M carboxyfluoresceinsuccinimidyl ester (CFSE) for 2.5 min at 37 °C. Cells were then washed in

FACS buffer, resuspended in R10F (10^6 per ml) and seeded in 24 well plates. PBMCs were either activated with PHA (500 ng/ml) or left unstimulated, and all cells were incubated for 48 h at 37 °C. Then, cells were directly plasma-treated without changing the cell culture medium, and incubated for another 120 h. Finally, cells were collected and CFSE-fluorescence was measured via flow cytometry, discriminating for CD4⁺ cells and excluding dead cells from analysis using DAPI (1 μ M).

3.4. Intracellular cytokine measurement

PBMCs (10^6 per ml in R10F) were seeded in 24 well plates. Cells were then pulsed with PHA (500 ng/ml) O/N or with LPS (10 ng/ml) for 1 h prior to addition of brefeldin A (1:1000) and plasma treatment. Cells were incubated for 18 h (for investigations of lymphocytes) or for 6 h (for investigations of monocytes) at 37 °C, and harvested into FACS-tubes. Staining with fluorochrome-conjugated monoclonal antibodies directed against cell surface antigens was carried out, followed by staining with fixable viability dyes in PBS. Cells were washed with FACS buffer, and fixed with paraformaldehyde at room temperature. Cells were washed and permeabilized using the Triton X-100. After staining for intracellular antibodies at RT, cells were washed and subsequently analyzed by flow cytometry.

target	isotype	clone	conjugate	supplier	final concentration
GM-CSF	rat IgG2a	BVD2-21C11	Pacific blue	BioLegend	0.1 μ g/ml
IFN γ	mouse IgG1	4S.B3	Alexa Fluor 700	BioLegend	0.1 μ g/ml
IL-1 α	mouse IgG1	364-3B3-14	PE	BioLegend	0.2 μ g/ml
IL-1 β	mouse IgG1	H1b-98	Pacific blue	BioLegend	0.1 μ g/ml
IL-6	mouse IgG1	MQ2-13A5	APC	BioLegend	0.1 μ g/ml
IL-8	mouse IgG1	E8N1	Alexa Fluor 488	BioLegend	0.1 μ g/ml
IL-10	mouse IgG1	JES3-9D7	Brilliant Violet 421	BioLegend	0.3 μ g/ml
IL-13	mouse IgG1	JES10-5A2	PerCP Cy5.5	BioLegend	0.3 μ g/ml
RANTES	mouse IgG2b	VL1	Alexa Fluor 647	BioLegend	0.2 μ g/ml
TGF β	mouse IgG1	1D11	Alexa Fluor 700	R&D systems	0.1 μ g/ml
TNF α	mouse IgG1	MaB11	PE-Cy7	BioLegend	0.1 μ g/ml

For the discrimination of T lymphocytes, monoclonal antibodies directed against CD3 were used. For gating of monocytes, PBMCs were incubated with CD14 (APC-Cy).

3.5. Measurement of intracellular thiol content

The intracellular redox state was investigated via measurement of free intracellular thiol content. PBMCs were plasma-treated and incubated for 2 h, 6 h, or 24 h at 37 °C. Cells were stained with *thioltracker probe* (10 µM), 7-AAD, and anti-CD4 APC antibodies in PBS containing divalent cations at 37 °C. After washing, *thioltracker violet* fluorescence was acquired by flow cytometry. The dye was excited at 405 nm and emission was recorded at 525/40 nm. Only DAPI-negative and CD4-positive events in the lymphocytes gate were considered for comparative analysis.

3.6. Cell surface marker expression on T lymphocytes

Similar to viability measurements, lymphocytes were investigated for cell surface marker expression 24 h after plasma treatment. PBMCs were harvested into FACS tubes, washed, stained with monoclonal antibodies conjugated to different fluorochromes, washed again, and measured by multicolor flow cytometry. In all experiments, T_H cells were investigated and discriminated against monocytes by using anti-CD4 and anti-CD14 antibodies. Dead cells were excluded using DAPI and Annexin V.

target	isotype	clone	conjugate	supplier	final concentration
CD4	VIT4	mouse IgG2a	APC	Miltenyi	0.1 µg/ml
CD14	M5E2	mouse IgG2a	PE-Cy7	BioLegend	0.1 µg/ml
CD45RA	T6D11	mouse IgG2b	PE	Miltenyi	0.2 µg/ml
CD45RO	UCHT1	mouse IgG2a	BV421	BioLegend	0.2 µg/ml
CD62L	145/15	mouse IgG1	FITC	Miltenyi	0.1 µg/ml

3.7. Measurement of mitochondrial membrane potential

PBMCs were plasma-treated and incubated for 2 h or 6 h prior to collection into FACS tubes. To determine the mitochondrial membrane potential of cells, they were washed and stained with JC-1 (final concentration 2 μ M), DAPI, and anti-CD4 APC antibodies at 37 °C. Only viable (DAPI) T_H cells were gated for JC-1 analysis. JC-1 exhibits green fluorescence when present as single molecule (monomer) in the cytosol. However, the probe is lipophilic and cationic, and rapidly aggregates in intact mitochondria (of viable cells) (191). Aggregation of JC-1 shifts its fluorescence emission towards orange-red.

3.8. Intracellular measurement of protein-phosphorylation

PBMCs (2.5×10^7 per ml in PBS) were stained with a fixable viability dye, washed with FACS buffer, and subsequently stained for cell surface markers. Cells were adjusted to 10^6 per ml in R10F, and 1 ml each was plasma-treated in 24 well plates. Immediately after treatment, medium alone or medium containing PMA (50 ng/ml) and Ionomycin (1 μ g/ml) was added to each well. Plates were incubated for 15 min at 37 °C. The cell suspension was subsequently harvested into FACS tubes. Cells were washed once and fixed with PFA at RT. Then, cells were washed and permeabilized with ice-cold (-20 °C) methanol for 30 min at 4 °C. Cells were then washed twice with FACS buffer and incubated with antibodies directed against phosphorylated epitopes of NF κ B and ERK1/2 for 60 min at RT. Again, cells were washed twice and resuspended in FACS-buffer prior to evaluation by multicolor flow cytometry. At least 100.000 events were recorded per sample.

target	isotype	clone	conjugate	supplier	final concentration
CD3	BW264/56	mouse IgG2a	FITC	BioLegend	0.1 μ g/ml
CD4	RPA-T4	mouse IgG1	APC	BioLegend	0.1 μ g/ml
pERK1/2	MILAN8R	mouse IgG1a	eFluor 710	eBioscience	0.6 μ g/ml
pNF κ B	B33B4WP	mouse IgG2a	PE	eBioscience	0.6 μ g/ml
Zombie Yellow	n.a.	n.a.	n.a.	BioLegend	1:500

4. Characterization of plasma-treated neutrophils

4.1. Viability

For flow cytometric evaluation of viability, neutrophils were plasma-treated in R10F at 10^6 cells per ml and incubated at 37 °C for 2 h, 6 h, or 24 h. PMNs were harvested into FACS tubes, stained with Annexin V and DAPI in AVBB, and evaluated by flow cytometry.

To investigate metabolic activity, cells were directly plasma-treated in 24 well plates, and aliquoted in 96 well plates. Resazurin reagent was added to each well and the plate was placed into a plate reader set to 37 °C. Resorufin fluorescence was recorded over 24 h (excitation wavelength 530 nm, emission wavelength 590 nm).

4.2. Oxidation

Measurement of cellular oxidation was similar to the methodology done for PBMCs. Briefly, PMNs were incubated with one of six different redox-sensitive probes before washing and diluting the cells at 10^6 per ml in R10F. One ml of PMNs was added to wells of a 24 well plates. After plasma treatment, cells were harvested into FACS tubes, washed, and fluorescence was acquired by flow cytometry. Mean fluorescence intensity was calculated using *Kaluza* software. In controls, catalase (5 µg/ml) was added prior to plasma treatment

4.3. Oxidative burst

Neutrophil oxidative burst was assessed by using the cytochrome c assay which measures superoxide production of stimulated cells. Here, Phorbol-12-myristat-13-acetat (PMA) is used to induce rapid activation of the granulocyte NADPH-Oxidase (Nox2) as described before (184). Briefly, 500 µl of PBS containing 48 mg/ml of cytochrome c and 40 mg/ml of catalase was added to cuvettes. PMNs (10^6 per ml in Hank's) were added to a 24 well plate and plasma-treated. Then, 500 µl of cell suspension was added to a cuvette and up to 6 cuvettes

were placed into a spectrophotometer at once to acquire absorbance kinetics in parallel. First, cuvettes were incubated for 10 min at 37 °C. Second, PMA was quickly added to all cuvettes (final concentration 100 nM) and absorption (path length = 10 mm) was measured every 20 s over 10 min at 550 nm. The absorption increased over time and the slope was calculated for a defined time frame set to be constant for all samples of the same run to assure comparability between samples. Absolute superoxide concentrations (μM per minute and 10^6 neutrophils) were calculated using the molar absorption coefficient of cytochrome c. All samples were normalized to control values set to 100 %. Also, SOD was added to PMNs to show the specificity of the assay.

Additionally, oxidative burst was evaluated using opsonized bacteria (*Escherichia coli*) and the probe DHR123, both provided in a commercial kit (phagoburst) and used according to the manufacturer's instructions (glycotype).

4.4. Phagocytosis and killing

For phagocytosis of live bacteria, autologous serum was collected for opsonization. Blood was clotted in a glass tube incubating for 1 h at 37 °C. The supernatant was collected and centrifuged. Again, the supernatant was taken off and centrifuged to dispose of RBC. Bacteria were cultured O/N in broth at 37 °C and kept at 4 °C prior to the start of the assay. The suspension was washed two times in PBS. For *Staphylococcus aureus*, another slow spin was done to discard cell clumps. The supernatant was resuspended in Hank's. The optical density of a 1:10 diluted cell suspension was measured at 550 nm, and related to a previously established standard curve of optical density vs. CFU. Bacteria were suspended in Hank's at a concentration of 2×10^8 per ml. In glass tubes covered with parafilm, they were then opsonized in Hank's containing 10 % autologous serum for 20 min at 37 °C (slow rotation at 6 rpm). Neutrophils were seeded at 10^7 per ml in Hank's containing 10 % autologous serum in wells of a 24 well plate. Cells were plasma-treated for 3 min. Addition of ddH₂O compensated for evaporated water. Immediately after treatment, 500 μl of bacterial cell suspension was added to each well, yielding a final cell number of 10^7 neutrophils and 10^8 bacteria (1:10). One well contained no neutrophils to establish a reference of colony

formation of non-phagocytosed bacteria. Two times 600 µl per well were aliquoted in two 1.7 ml Eppendorf tubes. Cells were incubated (6 rpm) for 30 min (*Staphylococcus aureus*) or 45 min (*Pseudomonas aeruginosa*) at 37 °C. Cells were then placed on ice and vortexed thoroughly. Neutrophils were lysed using pH11 H₂O. Suspension was further diluted two times to yield ~5000 CFU per ml. Twenty microliters of this suspension was spread on each of two halves of blood agar plates. Two agar plates (4 replicates) were used per sample. Plates were incubated O/N at 37 °C and CFU were counted on the following day.

4.5. NET quantification using a plate reader

The plate reader (Tecan M200 Pro) was warmed to 37 °C for at least 30 min prior to first readings. Twenty microliters of Triton-X 100 was added to several wells of a black 96 well plate. The detergent would lyse neutrophils to allow assessing the maximum DNA fluorescence of all cells of one well. All other sample wells received 20 µl of Hank's (100 µl to blank well). Additionally, a 10 µM working solution of Sytox Orange was prepared. Neutrophils (10⁶ per ml in Hank's) were added to wells of a 24 well plate immediately before plasma treatment. After exposure, aliquots were added to sample wells of the black 96 well plates. Two other aliquots were added to wells containing Triton-X 100 for measurement of total DNA fluorescence. After addition of the last sample, Sytox Orange was added to each well (final concentration: 2 µM). The plate was placed into the plate reader and fluorescence was read every two minutes over 4 h. The excitation wavelength was 530 nm and emission wavelength was 575 nm (± 4.5 nm).

4.6. Assessment of extracellular and active MPO

PMNs (10⁶ per ml in Hank's) were seeded into 24 well plates and were subsequently plasma-treated. Cells were incubated for 1 h at 37 °C. Cell suspension was harvested into Eppendorf tubes and centrifuged; supernatants were transferred into new Eppendorf tubes (low protein-binding type) and stored at -80 °C until use. For assessment of MPO-activity, supernatants were diluted 1:100 in PBS and 50 µl were added to black 96 well plates in

triplicates. Then, Amplex ultra red (final concentration 5 μM) and H_2O_2 (final concentration 40 μM) were added and fluorescence emission was acquired every minute over a 40-minute time period using a plate reader (excitation wavelength 535 nm, emission wavelength 590 nm). Fluorescence of controls containing Hank's, Amplex ultra red, and H_2O_2 alone without cells served as background and was subtracted from sample fluorescence.

4.7. NET quantification using fluorescence image analysis

Before starting experiments, the microscope (Carl Zeiss Observer Z.1 with motorized stage) stage was warmed to 37 °C for 30 min, calibrated, and positions of each well of a 24 well plate were adjusted to the center position. Additionally, the correct focus (z-plane) was set on irrelevant particles. Immediately before treatment, neutrophils (10^6 per ml in Hank's) were added to a 24 well plate. For each treatment, duplicates were set up. After the last treatment had finished, Sytox Orange (final concentration 200 nM) was added and the plate was inserted into the pre-warmed microscope stage. The plastic lid of the multiwell plate was taken off and a heatable (37 °C) glass-lid was applied to seal the stage, effectively maintaining its temperature at 37 °C. Image acquisition was set to acquire a mosaic-set of pictures in a meandering fashion (3x3 images). This was repeated every 30 min. Self-written algorithms in ImageJ were used to batch-stitch mosaic images and to threshold and quantify fluorescence acquired.

4.8. NET confirmation using confocal laser scanning microscopy

For acquisition of NET images by immunofluorescence, neutrophils (10^6 per ml in Hank's) were first seeded into 24 well plates and were subsequently plasma-treated. Cell suspension was transferred into 12 well plates containing round coverslips and 12 well plates were incubated for 3 h at 37 °C. Plates were centrifuged (100 x g for 5 min) and media was gently removed. Coverslips were fixed with PFA for 20 min and washed with PBS. Cells were permeabilized with Triton-X 100 in PBS and washed with PBS. Coverslips were blocked with DAKO protein block. Cells were stained with polyclonal rabbit anti-human neutrophil

elastase in DAKO protein block (serum-free) for 1 h at 37 °C. Coverslips were washed with ELISA wash buffer. Afterwards, a secondary antibody (goat anti-rabbit Alexa Fluor 488 in DAKO protein block) was added and samples were incubated for 1 h at 37 °C. Coverslips were again washed in ELISA wash buffer, dipped several times in ddH₂O, and drained on KIM wipes. Finally, samples were mounted on microscopic slides using *Vectorshield* (containing DAPI) and sealed with nail polish. Samples were stored in the fridge in the dark until analysis by confocal laser scanning microscopy (using the 405 nm laser and the 488 nm laser, respectively).

5. Statistics

Graphing and statistical analysis was performed using prims 6.05 (graph pad software) and excel (Microsoft), and slope calculation was performed using UV Solutions 3.0. In general, and if not stated otherwise, *Student's* T test was used for statistical comparison between two sample groups. For statistical analysis between >2 groups, one-way analysis of variance (ANOVA) was used which compared treated samples to controls if not stated otherwise (*Dunnnett* post test to adjust for multiple comparison). If more than two groups were to be compared with more than two conditions for each group, two-way ANOVA was applied. According to number of comparisons or type of comparison, different post test were integrated into the statistical analysis (in most cases either *Tukey* or *Sidak*).

Throughout this work, significance levels were indicated as follows: $^*\alpha = 0.05$, $^{**}\alpha = 0.01$, and $^{***}\alpha = 0.001$.

Chapter 4. Aim of this work

In this work, human leukocytes were investigated after exposure to cold physical plasma. Cold plasma is a promising option in the treatment of chronic wounds. Key molecular events during different phases of wound healing are orchestrated by different cells of the immune system. Moreover, chronic wounds are frequently associated with mislead inflammation mediated by cells of the immune system. In order to estimate wound cell behavior in response to plasma, peripheral blood leukocytes were plasma-treated and their reactions investigated. Leukocytes consist of different subpopulations, each displaying highly specific effector functions. Moreover, previous studies investigating plasma-treated cells did not fully decipher how exactly cold physically plasma mediates its effects on cells. For this, two major questions were addressed in this thesis:

- i) What are the effects of plasma on human leukocytes and their subpopulations?
and
- ii) What are the underlying mechanisms of plasma effects on cells using the kinpen?

At the time when this project started, no scientific articles were available addressing the question of how and in what way cold physical plasma affects leukocyte or their subpopulations. Characterizing plasma effects is challenging due to interdisciplinary skills required in plasma treatment and subsequent assessment of various functions in different types of primary immune cells. Therefore, another aim was to establish an exact and reproducible plasma treatment together with robust biological downstream assays.

Altogether, this work was supposed to give a more detailed picture in basic research of plasma medicine and redox immunology alike in order to gain a better understanding of plasma applications in biology and medicine.

Chapter 5. Results

1. Characterization of cold plasma and plasma-treated liquids

The main questions of this thesis were: i) how is plasma affecting leukocyte viability and/or function, and ii) which components of cold physical plasma are important in affecting cells? Characterizing the kinpen plasma source used in this work was therefore vital to understand how it exerts its effects on cells. The plasma was generated in ambient air (the plasma gas phase) to affect molecules or cells in suspension (the liquid phase). Thus, investigating the plasma gas phase was important in order to understand how the liquid phase is affected. Characterizing the gas and liquid phases was also essential to define the operational setting for treatment of cells.

1.1. Molecular reactive species in the plasma gas phase

The plasma was ignited at the central electrode and driven out by an argon flux. It was hypothesized that, once in contact with ambient air, ionized argon species will react with molecular oxygen or nitrogen to form ROS or RNS, respectively. After excitation, the reactive molecular species switch back to stable energy levels emitting light of specific wavelengths, which are detectable by optical emission spectroscopy (OES). Using this method, emission peaks can be attributed to specific molecular species allowing semi-quantitative comparison of different settings.

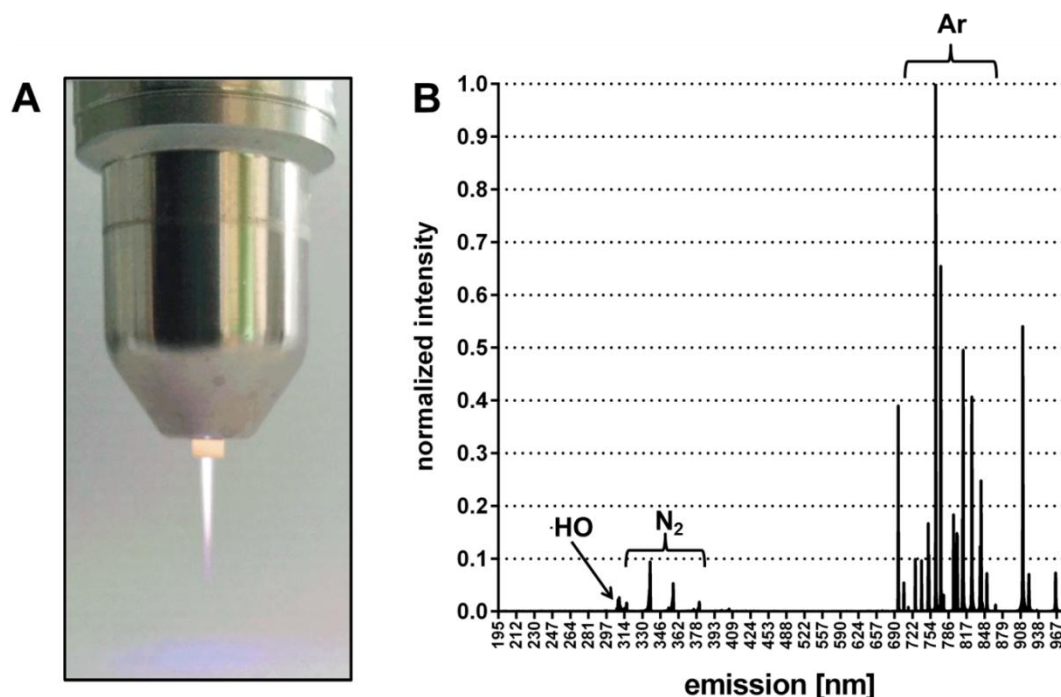


Fig. 8: Plasma effluent of the kinpen 09 and optical emission spectroscopy of its effluent.

Picture of the kinpen 09 operated at 3 standard liters per minute of dry and pure argon as feed gas (A). The plasma is cone shaped and appears white after being driven out of the ceramic nozzle. The violet tip indicates presence of UV radiation. Optical emission intensities were normalized to the highest peak (B). Distinct bands showed the presence of $\cdot\text{HO}$ (arrow, $\sim 307\text{--}310\text{ nm}$) and excited nitrogen molecules (second positive nitrogen system at $\sim 310\text{--}360\text{ nm}$). There was minimal emission in the range of visible light between $\sim 400\text{--}700\text{ nm}$. The near infrared ($700\text{--}1000\text{ nm}$) spectrum lines mainly represent excited argon molecules of the feed gas.

The emission spectrum of the argon plasma jet effluent showed several emission bands in the ultraviolet and near-infrared spectral range (Fig. 8B). Creation of reactive oxygen (e.g., $\cdot\text{HO}$) and nitrogen (second positive nitrogen system, N_2) species was apparent. Thus, highly energetic particles are emitted by plasma. In the NIR spectral range, various argon lines were observed. Also at 777 nm an atomic oxygen band appeared (small intensity and not highlighted). Atomic hydrogen was not detected (emission wavelengths: 410 nm , 434 nm , 486 nm , 656 nm). Of note, the emission profile was dependent on the composition of the feed gas used (appendix Fig. i p.127).

1.2. Plasma-treated buffered solutions

Next, liquids were treated with plasma and the plasma-treated liquids were investigated for the presence of reactive species and oxidants. This was of interest, as it is known that oxidants can affect cells in various ways.

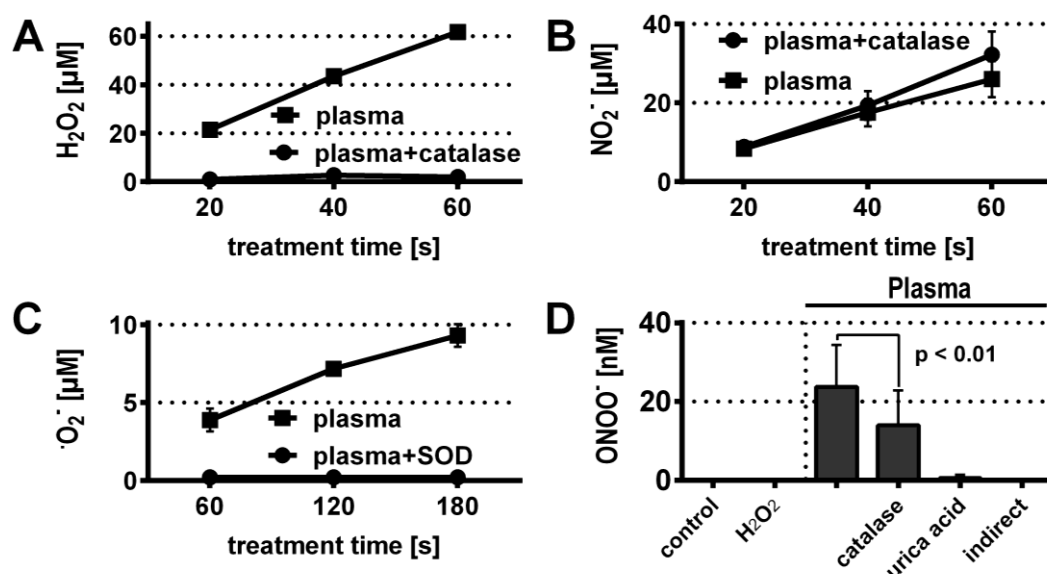


Fig. 9: Plasma generated reactive molecules in liquids.

Medium was plasma-treated for the indicated length of time and H_2O_2 (A*) or NO_2^- (B*) was immediately quantified using redox sensitive fluorescent probes. Catalase treatment confirmed H_2O_2 production (A*) and fluorescence of the NO_2^- -detecting reagent (B*). Generation of O_2^- was quantified by measuring cytochrome c absorbance, using the molar extinction coefficient of cytochrome c (C). Addition of superoxide dismutase (SOD) verified the specificity of the reaction with O_2^- . RNS/ ONOO^- (D*) was measured by spiking medium with tyrosine (1 mM) before exposure to plasma (60 s). 3-nitrotyrosine formation was quantified using LC/MS and calibrated with a standard. The amount of ONOO^- differed significantly between treated samples with and without catalase (paired t test). Data are presented as mean \pm SD of four independent experiments.

**adapted from (185) with permission from Informa Healthcare*

Plasma-treated liquid cell culture medium contained the long-lived oxidant H_2O_2 (Fig. 9A), and NO_2^- (Fig. 9B). The medium still contained about 20 % of initial H_2O_2 concentrations 24 h after exposure (appendix Fig. ii p.128). Also, significant amounts of O_2^- were generated (Fig. 9C). Generation of 3-nitrotyrosine (NY, Fig. 9D) strongly suggested the presence of ONOO^- . Interestingly, this process was reduced in presence of catalase but experimentally added H_2O_2 did not increase NY production. As expected, uric acid scavenged RNS and ONOO^- and diminished NY production almost completely. Likewise, addition of tyrosine 30 s

after plasma treatment of medium (indirect treatment) did not led to NY formation. Formation of 3-chlorotyrosine indicative of generation of $\cdot\text{OCl}$ was not detectedable (limit of detection 800 pM).

In summary, reactive species were generated in the plasma gas phase and the treated liquid cell culture medium contained significant amounts of oxidants known to oxidize biological components. The oxidation potential can be measured by using redox probes that fluoresce upon oxidation (Fig. 10 A, B). Cells use anti-oxidative defense systems to cope with redox stress. Free thiol groups play a central role here. The majority of intracellular free thiols are found on glutathione (GSH). It was therefore addressed whether plasma-treated liquids oxidized GSH (Fig. 10 C).

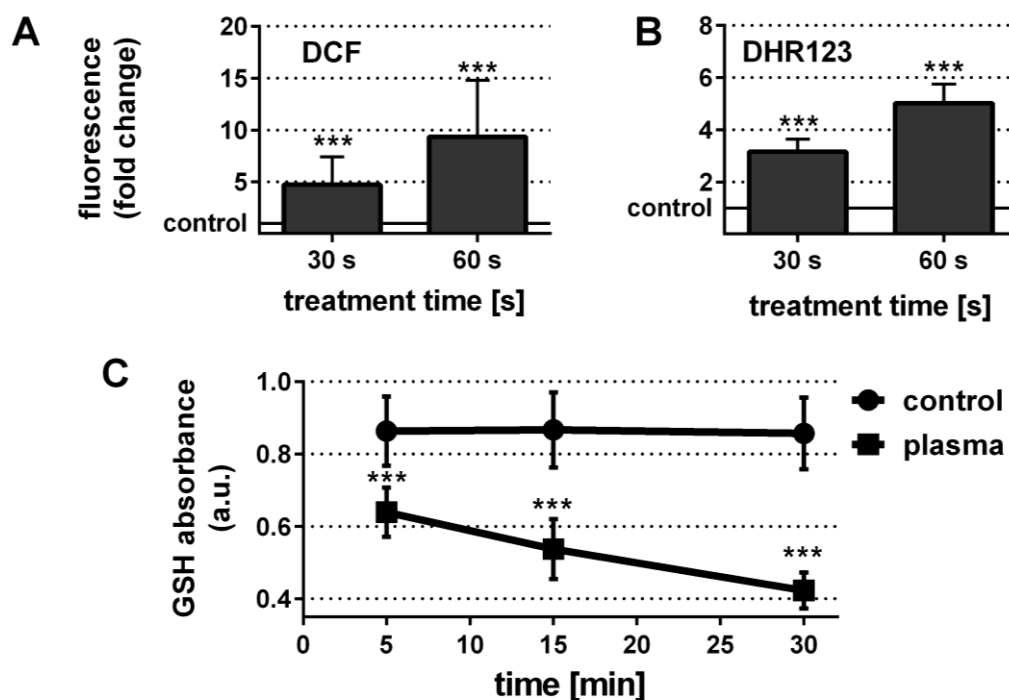


Fig. 10: Plasma treatment oxidized GSH and redox-sensitive fluorescent probes.

Medium was spiked with DCFH (A) or DHR123 (B) and directly plasma-treated. DCFH forms the fluorescent product DCF upon oxidation by various species but preferentially H_2O_2 . DHR123 forms the fluorescent product rhodamine 123 which fluoresces upon oxidation by various species but preferentially $\cdot\text{O}_2^-$. Fluorescence was recorded using a plate reader and depicted as fold change over fluorescence of non-treated control. Fluorescence of plasma-treated samples differed significantly from controls. For GSH experiments (C*), medium was spiked with GSH (final concentration 50 μM) and then plasma-treated. DTNB was added (final concentration 200 μM) to react with GSH to form a yellow product whose absorbance was measured over time using spectrophotometry. Reduced GSH significantly decreased after plasma exposure compared to control (C*). Data are presented as mean \pm SD of three independent experiments. Statistical analysis was performed using paired student's t test.

**adapted from (192) with permission from Begell House*

Two different redox-sensitive probes were used to assess plasma-mediated oxidation of medium. The fluorescence increase of these probes was measured after plasma exposure in a treatment time dependent manner (Fig. 10A and 10B). DCFH is sensitive to many different reactive species, including H_2O_2 -derived species such as $\cdot\text{HO}$, and is often used in cell biology to detect generalized oxidative stress. DHR123 also displays broad sensitivity and is often used in neutrophil biology to investigate the respiratory burst and its product superoxide. Compared to non-treated controls, plasma significantly oxidized GSH, an important molecule in the cell's antioxidative defense system (Fig. 10C). GSH levels decreased with incubation time after treatment which was indicative of a long-lived oxidant-mediated reaction.

1.1. Summary of results

In this section, plasma properties in the gas phase and their effects on liquids were investigated. It was shown that plasma generated various reactive molecular species in the gas phase. These molecules interacted with components of the liquid and generated other reactive species and oxidants such as H_2O_2 , NO_2^- , $\cdot\text{O}_2^-$, and RNS/ONOO^- . Plasma-derived species effectively oxidized fluorescent redox-sensitive probes and GSH in a treatment-time dependent fashion. In the next chapter, the effect of plasma on peripheral blood mononuclear cells (PBMCs) was therefore, investigated.

2. Effect of plasma on oxidation and viability of human PBMCs

PBMCs are a fraction of leukocytes containing mainly lymphocytes and monocytes. These cells are crucial in initiation and regulation of inflammation and immune responses. Prospective plasma applications potentially involve treatment of inflamed tissue, such as chronic wounds, and hence PBMCs were chosen to investigate plasma effects *in vitro*. Special attention was paid to CD4⁺ T helper (T_H) cells and monocytes which are assumed to be involved in non-healing wound pathophysiology, as outlined in the introductory section.

2.1. Oxidation and cellular damage were a consequence of exposure to plasma

As shown in the previous section, plasma readily oxidized fluorescent redox markers and GSH in liquid. It was hypothesized that oxidation would also take place in cells where GSH may be modulated. Two redox markers were used to assess changes in oxidation. DCF accumulates in the cytosol and serves as general redox indicator. *Mitotracker orange* (MTO) on the other hand, accumulates in mitochondria but also displays a general sensitivity to oxidation. For intracellular GSH measurement, the *thioltracker* probe was used which measures free intracellular reduced thiols. As the majority of thiols are present in the form of GSH, this probe can give an estimation of the intracellular concentration of this reductant.

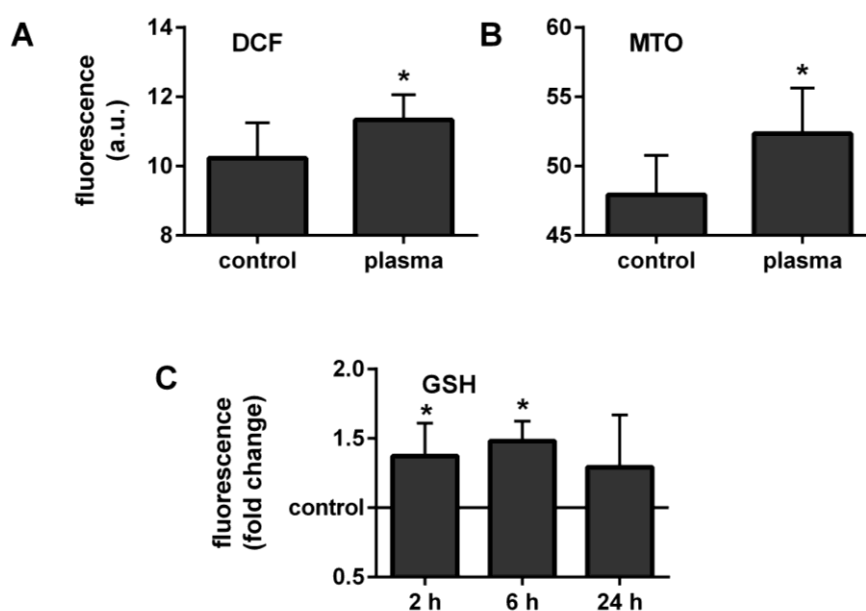


Fig. 11: Plasma treatment oxidized intracellular fluorescent probes but increased reduced concentrations of free thiols.

PBMCs in cell culture medium were stained with H₂DCFDA (A) or Mitotracker orange (MTO) dye (B) and directly plasma-treated (60 s). Cells were immediately harvested and fluorescence was measured by flow cytometry gating on CD4⁺ T_H cells. With both dyes a significant fluorescence increase was noted. To quantify intracellular free thiols (C*), cells were stained with thioltracker probe 2 h, 6 h, and 24h after plasma treatment (20 s). A significant fluorescence increase was measured in treated cells 2 h and 6 h after treatment and compared to controls. Data are presented as mean + SD of three independent experiments. Statistical analysis was performed using paired student's t test.

**adapted from (192) with permission from Begell House*

PBMCs were stained with probes accumulating in the cytosol (H₂DCFDA) or in the mitochondria (MTO) prior to plasma exposure. In plasma-treated cells, fluorescence increased significantly in both compartments compared to non-treated controls (Fig. 11A and Fig. 11B). Also, thiol content was assessed and found to be significantly increased 2 h and 6 h after treatment suggesting that GSH concentrations were elevated in plasma-treated T cells (Fig. 11C).

Cells were oxidized in the cytosol and mitochondria. Mitochondria are imperative in the cell's metabolism and an increase in oxidation within the mitochondria suggested potential damage. This was tested by measuring the mitochondrial membrane potential using JC-1. In live cells, JC-1 accumulates in mitochondria, exhibiting an orange-red fluorescence in its aggregated form. Upon mitochondrial damage, JC-1 disseminates in the cytosol, indicated by green fluorescence and both can be measured by flow cytometry.

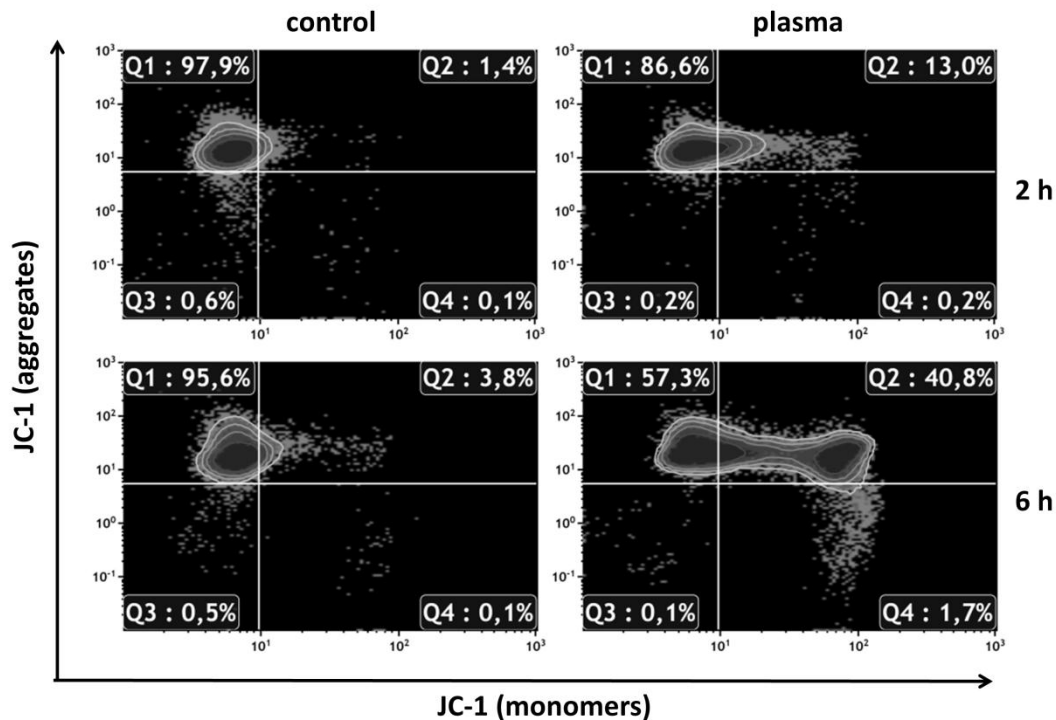


Fig. 12*: Loss of mitochondrial membrane potential in plasma-treated CD4⁺ T cells.

For measurement of mitochondrial membrane potential, PBMCs were treated with plasma (20 s), and incubated for 2 h or 6 h at 37 °C prior to staining with JC-1. Fluorescence was determined by flow cytometry and T_H cells were gated according to their expression of CD4. A decrease of cell numbers in dot plot quadrant Q1 and appearance of cells in quadrants Q2 and Q4 indicated loss of mitochondrial potential which was higher in plasma-treated cells. Five independent experiments were conducted, of which one representative result is shown.

**adapted from (192) with permission from Begell House*

PBMCs were plasma-treated and stained with JC-1 and CD4 to assess mitochondrial membrane potential in T_H cells. In plasma-treated cells with intact mitochondria (JC-1 aggregates, Q1 and Q2) there was a population also positive for JC-1 monomers (Q2). The effect was stronger after 6 h (40.8 %) compared to 2 h after treatment (13.0 %) (Fig. 12). This indicated a loss in mitochondrial membrane potential and suggested that plasma-induced oxidation was destructive to mitochondria. Damage would result in loss of metabolic activity which can be assessed and quantified using resazurin. This dye readily diffuses into cells where it is reduced to resorufin via NADPH generated by active mitochondria.

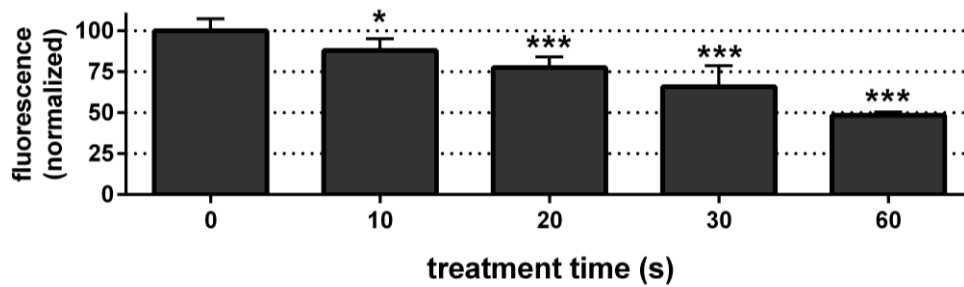


Fig. 13: Plasma treatment of PBMCs decreased their production of reduction equivalents.

PBMCs were plasma-treated and incubated for 16 h. Resazurin was added and fluorescence was measured using a plate reader after 8 h of incubation. Background was subtracted and fluorescence normalized to controls. Metabolic activity was significantly reduced (one-way ANOVA with Dunnett post test) in plasma-treated samples. Data are presented as mean + SD of three independent experiments.

PBMCs were plasma-treated and their metabolic activity assessed by measuring their transformation of resazurin to resorufin (Fig. 13). In plasma-treated cells, fluorescence was significantly decreased (Fig. 13). This was indicative of a decrease in metabolic activity of cells by plasma. To assess whether this was due to overall reduced cellular metabolism or induction of cell death, numbers and cell membrane permeability of T_H cells were evaluated.

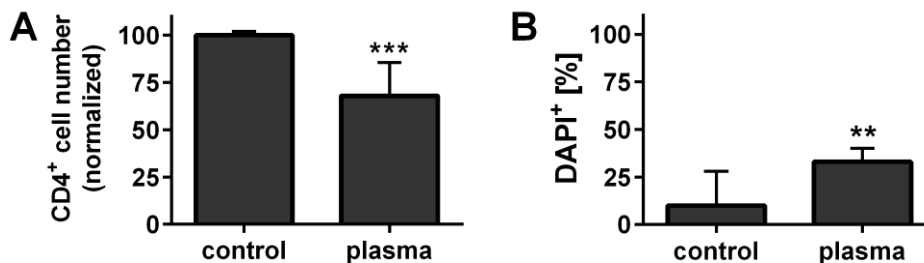


Fig. 14: Plasma treatment decreased cell numbers and induced membrane damage in $CD4^+$ T_H cells.

PBMCs were plasma-treated (60 s), incubated for 24 h, and $CD4^+$ cell numbers were evaluated by flow cytometry (A). A significant fraction of T_H cells were positive for DAPI indicating membrane damage in these cells (B). Data are presented as mean + SD of four independent experiments.

PBMCs were plasma-treated and 24 h later $CD4^+$ T_H cells were counted by flow cytometry. Significantly fewer T_H cells were present compared to control (Fig. 14A). Plasma also increased the percentage of DAPI⁺ (dead) cells 24 h after treatment (Fig. 14B). This led to the next question whether plasma-mediated cell death was a consequence of apoptosis or necrosis.

2.2. Cell death was a consequence of apoptosis but not necrosis

As cell viability was compromised after plasma treatment it was investigated whether this was due to necrosis. Necrosis can be characterized by an immediate loss of membrane integrity following direct physical insult and allowing viability dyes such as DAPI to penetrate into cells. DAPI itself is non-fluorescent and cannot cross the cell membrane of intact leukocytes at significant rates. Upon entering cells with compromised membranes and binding to the major groove of DNA it exhibits a conformational change and is converted to its fluorescent form which is detectable by flow cytometry.

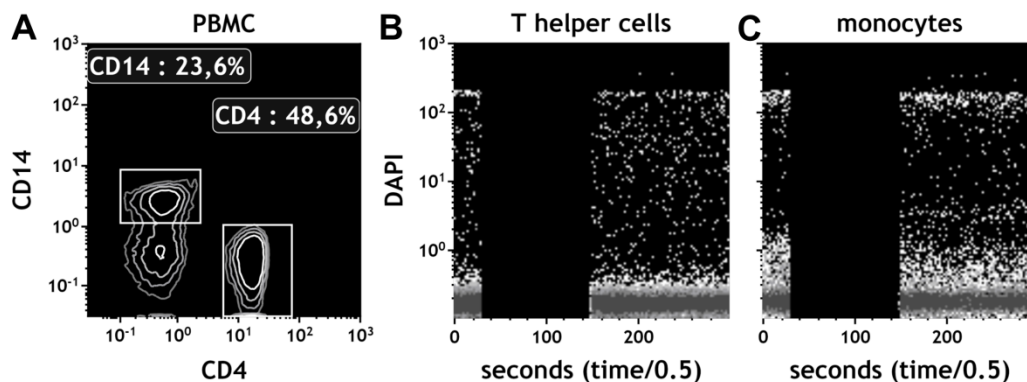


Fig. 15: Plasma treatment did not induce necrosis in PBMCs.

PBMCs were stained with anti-CD4 and anti-CD14 antibodies and were resuspended at 10⁶ per ml in medium (R10F). DAPI was added and a base line (15 s) of DAPI-positive cells was acquired by flow cytometry, and then paused. The cell suspension was plasma-treated for 60 s and flow cytometric measurement continued immediately. T_H cells and monocytes were analyzed (A) for DAPI fluorescence over time. Neither T_H cells (B) nor monocytes (C) showed instantaneous membrane damage after exposure to plasma. Shown are representative images of six independent experiments.

In previous experiments, plasma treatment resulted in a loss of mitochondrial membrane potential and elevated portions of dead cells 24 h after treatment, and it was investigated whether exposure to plasma immediately necrotized cells. DAPI positive T_H cells and monocytes (Fig. 15A) were measured by flow cytometry immediately after plasma treatment but no increase in penetration of DAPI into lymphocytes or monocytes was observable (Fig. 15B and 15C). Thus, necrosis was not likely to be responsible for plasma-induced cell damage. It was next investigated whether plasma treatment induced apoptosis. Apoptosis is a “silent”, non-inflammatory type of cell death in which cellular disintegration is carried out in an active and controlled manner.

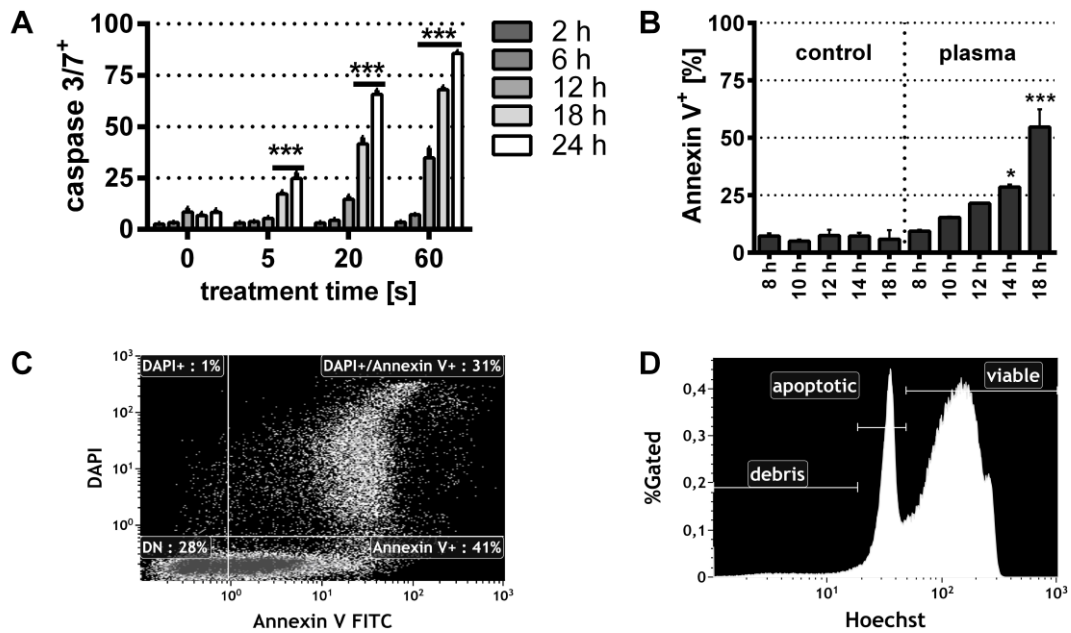


Fig. 16: Cell damage involved caspase activation and phosphatidylserine exposure.

PBMCs were plasma-treated and stained for caspase 3/7-activity after different time points. In flow cytometric analysis, gating on CD4⁺ T lymphocytes, cells displayed activated caspases from 12 h onwards after treatment (A*). For assessment of phosphatidylserine (PS) exposure, PBMCs were plasma-treated (60 s), harvested at various time points, and stained with Annexin V (B*). The percentage of T_H cells displaying PS increased between 8-10 h following exposure to plasma. For discrimination of early and late apoptosis, cells were plasma-treated and incubated for 24 h before staining with Annexin V and DAPI (C). Early (Annexin V⁺) and late (Annexin V⁺/DAPI⁺) apoptotic T_H cells were measured. Apoptotic cells were also identified by their reduced DNA content (Hoechst staining) 24 h after plasma treatment. Data are presented as mean + SD (A, B) or one representative (C, D) of three independent experiments. Statistical analysis was performed using two-way ANOVA (Sidak post test).

*adapted from (192) with permission from Begell House

PBMCs were plasma-treated and hallmarks of apoptosis were investigated in T_H cells. A significantly higher portion of T_H cells stained positive for active caspase 3/7 6 h after plasma treatment (60 s, Fig. 16A). At longer incubation times, plasma-treated cells stained positive for phosphatidylserine (PS) exposure (Fig. 16B). During the so-called early phase of apoptosis, PS was exposed on the outside of the membrane with the cellular membrane remaining intact thus excluding nucleic acid-binding fluorescent dyes such as DAPI (Fig. 16C). In later stages of apoptosis, the membrane lost its integrity and T lymphocytes stained positive for both Annexin V and DAPI (Fig. 16C). DNA fragmentation is a consequence of apoptosis and decreased DNA content was measured in apoptotic cells. To further confirm that plasma induced an active form of cell death, PBMCs were plasma-treated

and incubated for 24 h at different incubation temperatures (4 °C, 20 °C, 37 °C). Significantly fewer dead cells were measured in T_H cells when PBMCs were incubated at 4 °C or 20 °C compared to 37 °C (appendix Fig. iii p.129).

PBMCs contain many different populations and it was investigated whether there were differences in their sensitivity towards plasma treatment. The following subsets were studied: T helper cells, cytotoxic T cells, NK cells, B cells, and $\gamma\delta$ T cells. The subpopulations were discriminated by multicolor flow cytometry; the gating strategy is shown in the appendix (Fig. iv p.129).

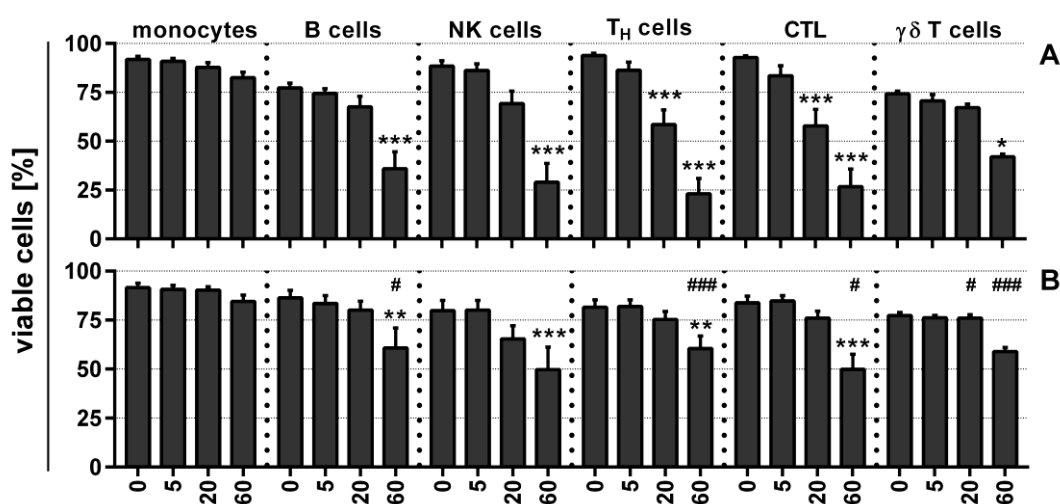


Fig. 17*: Plasma-induced cell death in subpopulations of immune cells.

PBMCs were isolated and incubated O/N with (B) or without (A) PHA (500 ng/ml) at 37 °C. Cells were plasma-treated, incubated for 24 h at 37 °C, and harvested. PBMCs were stained with Annexin V, DAPI, and antibodies and discriminated for different subpopulations. Specifically, cell types were positive for the following cell surface molecules: monocytes (CD14), B cells (CD19), NK cells (CD56, negative for CD3), T_H cells (CD3, CD4), cytotoxic T lymphocytes (CTL; CD3, CD8), $\gamma\delta$ T cells ($\gamma\delta$ TCR). The percentage of Annexin V / DAPI (viable) cells significantly (*, **, ***) decreased in lymphocytes and non-significantly decreased in monocytes in plasma-treated samples. Within lymphocytes there were only minor differences in viability with $\gamma\delta$ T cells being least affected after exposure to plasma. In plasma-treated samples, survival rates of activated cells (B) were significantly (#, ###) increased compared to those of non-activated (A) cells. Data are presented as mean + SE of four to twelve independent experiments. For comparison of survival rates of plasma-treated cells compared to their respective non-treated control a two-way ANOVA was used (Sidak post test). Unpaired student's t test was used for comparison between viability rates of non-activated and activated samples and separately for each treatment.

**adapted from (193) with permission from Begell House*

Plasma treatment induced apoptosis in all cell types investigated (Fig. 17). No subpopulation showed enhanced viability rates after exposure. Monocytes were least affected by plasma,

while lymphocytes displayed a greater effect with significantly compromised viability (Fig. 17A). Among the lymphocyte populations, $CD4^+$ T_H cells displayed the highest sensitivity after plasma treatment. To mimic conditioning in the wound environment, PBMCs were activated with PHA prior to plasma treatment. Lymphocyte activation was accompanied by upregulation of CD25 (appendix Fig. v p.130), confirming stimulation. Viability in PHA-activated control samples was reduced (Fig. 17B) as activation by mitogens can induce apoptosis (activation-induced cell death). Stimulation with PHA prior to plasma treatment enhanced survival rates considerably in all lymphocyte types investigated (Fig. 17B). In four of five lymphocyte populations, plasma exposure of 5 s did not induce any cytotoxicity as opposed to non-PHA pulsed PBMCs (Fig. 17A). Survival rates of monocytes did not change and always differed significantly from that of lymphocytes (appendix tab. i p.130). On the contrary, there were no significant differences between any two lymphocyte populations (appendix tab. i p.130). These results were independent of activation of PBMCs with PHA prior to plasma treatment.

The lectin PHA agglutinates and thereby broadly activates lymphocytes in experimental and laboratory conditions. In wounds, however, lymphocytes may encounter activating molecules of bacterial origin. Therefore, a common bacterial stimulus (staphylococcal superantigens) was used. Compared to control samples, superantigen-activated and plasma-treated T lymphocytes also displayed improved survival rates compared to non-activated but plasma-treated controls (appendix Fig. vi p.131). Special T lymphocyte subsets, e.g., $CD4^+$ effector/memory T_H cells are commonly associated with wound healing and were investigated next.

2.3. Plasma selectively inactivated effector/memory T_H cell subset

$CD4^+$ T_H cells can be divided into naïve cells, that have not encountered their antigen yet, and effector/memory cells. The cells can be distinguished by their reciprocal expression of CD45RA and CD45RO. The question addressed in this section was how cytotoxic is plasma to naïve and effector/memory T_H subpopulations.

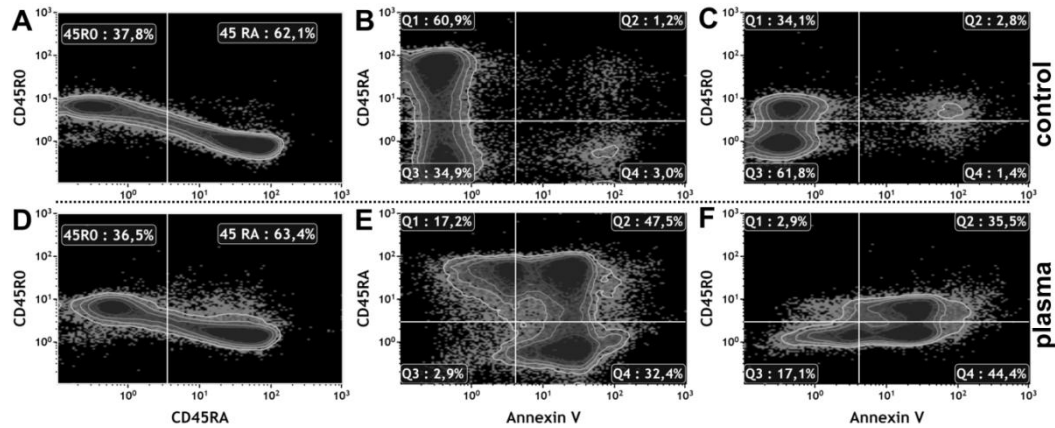


Fig. 18: CD45RA⁺ T lymphocytes showed better survival compared to CD45R0⁺ cells.

PBMCs (10^6 per ml in R10F) were plasma-treated (60 s), harvested after 24 h incubation at 37 °C, and stained for CD4, CD45R0, CD45RA, and Annexin V. Plasma treatment did not alter the expression of CD45R0 or CD45RA (A vs D). Viable (Annexin V) cells displayed a predominantly CD45RA⁺ (Q1 in E) / CD45R0⁻ (Q1 in F) phenotype after plasma treatment, while in controls both naïve (CD45RA⁺) and effector/memory T_H cells were present (Q1 and Q2 in B and C). Shown are dotplots of one representative of six independent experiments.

Two CD4⁺ T_H subsets, naïve and effector/memory cells, were investigated for their survival after plasma treatment. Naïve CD45RA⁺ cells were less prone to plasma-induced apoptosis (Fig. 18E and F) compared to effector/memory CD45R0⁺ cells, while total percentages of CD45RA⁺ to CD45R0⁺ cells did not change (Fig. 18A and B). These results suggested that, effector/memory T cells were much more susceptible to plasma treatment than naïve T cells. Effector/memory cells can be distinguished by expression of L-selectin (CD62L). CD62L⁺ cells can re-enter secondary lymphatic organs and CD62L⁻ cells primarily home to peripheral tissues. Lack of expression of L-selectin also marks a distinct effector memory T cell subset which is terminally differentiated and re-expresses CD45RA⁺ (TEMRA). Next, it was investigated how CD62L expression is related to apoptosis of CD45RA⁺ and CD45R0⁺ T_H cell subpopulations. CD62L⁻ cells (TEMRA) were enriched in CD45RA⁺ T cell populations after plasma treatment. In the CD45R0⁺ population, CD62L⁻ effector memory cells were apparently more robust to plasma exposure than the CD62L⁺ population. As CD45RA and CD45R0 are expressed in a reciprocal manner, CD45RA plots have been omitted for reasons of simplicity.

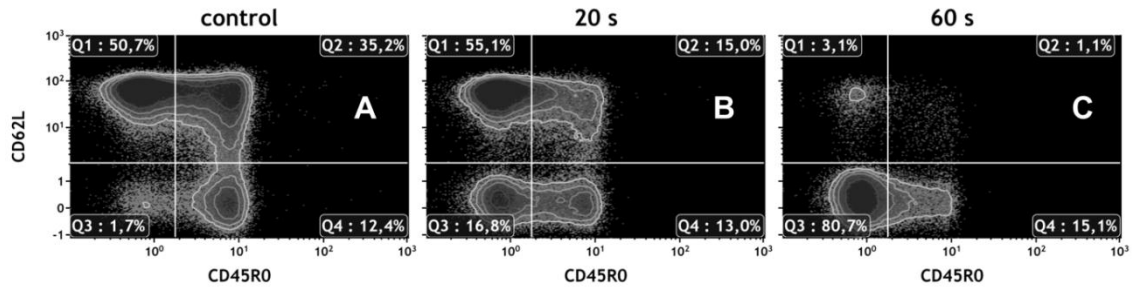


Fig. 19: Plasma-treated and viable CD4⁺ T_H cells displayed a CD62L⁻ phenotype.

PBMCs (10^6 per ml in R10F) were plasma-treated, incubated for 24 h at 37 °C, and stained with antibodies directed against CD3, CD4, CD45R0, CD45RA, and CD62L expression as well as Annexin V and caspase 3/7 detection reagent. Cells shown in the dotplots are CD3⁺/CD4⁺/Annexin V⁻/caspase 3/7⁻. In non-treated control PBMCs (A), the majority of viable T cells among CD45R0⁻ (CD45RA⁺) cells were positive for CD62L (naïve T cells). After plasma treatment (B, C), percentages of viable CD62L⁺ cells decreased in CD45R0⁺ and CD45R0⁻ T_H cells alike. Shown are dotplots of one representative of three independent experiments.

Independent of CD45RA or CD45R0 expression, viable CD4⁺ T_H cells were increasingly negative for CD62L 24 h after plasma treatment (Fig. 19C). However, CD62L surface expression is known to be actively regulated in T cells. Therefore, it was investigated whether the decrease of CD62L⁺ cells was either a result of apoptosis of CD62L⁺ cells or down-regulation of CD62L in CD62L⁺ T_H cells. Portion of naïve (CD62L⁺) cells among all viable CD45RA⁺ T_H cells were similar within 6 h after plasma treatment (Fig. vii p.131). Thus, plasma treatment induced preferential survival of the TEMRA phenotype in CD4⁺ T_H cells but no active regulation of CD62L expression.

2.4. Summary of results

In this section it was shown that plasma oxidized cells and induced cell death, mainly by apoptosis rather than necrosis. Only few monocytes became apoptotic after plasma treatment. By contrast, lymphocytes were strongly affected by exposure to plasma. Within lymphocytes, survival rates were similar between five populations investigated with $\gamma\delta$ cells showing the highest and CD4⁺ T cells showing the lowest viability. Preactivation of the immune cells, using PHA, improved survival, most prominently in CD4⁺ T_H cells. Among CD4⁺ T_H cells, CD62L⁻ cells showed better survival compared to CD62L⁺ cells in CD45RA⁺ and CD45R0⁺ cells alike.

3. Plasma treatment alters lymphocyte function and phenotype

In the previous section it was shown that plasma induced cellular oxidation and apoptosis, especially in lymphocytes. Lymphocytes are abundant during late phases of wound healing where they are thought to have regulatory functions and induce an immune response. Functional alterations induced by plasma treatment, including cell proliferation and cytokine secretion, are therefore of interest.

3.1. Proliferation was reduced but not halted in viable T lymphocytes

T lymphocytes proliferate upon antigen stimulation. This results in clonal expansion of antigen-specific T cells contributing to immune memory. In contrast, mitogens induce a polyclonal proliferation which is independent of the TCR-specificity. Two questions were raised in this context: i) is proliferation reduced after plasma treatment, and ii) does plasma induce proliferation in non-activated cells?

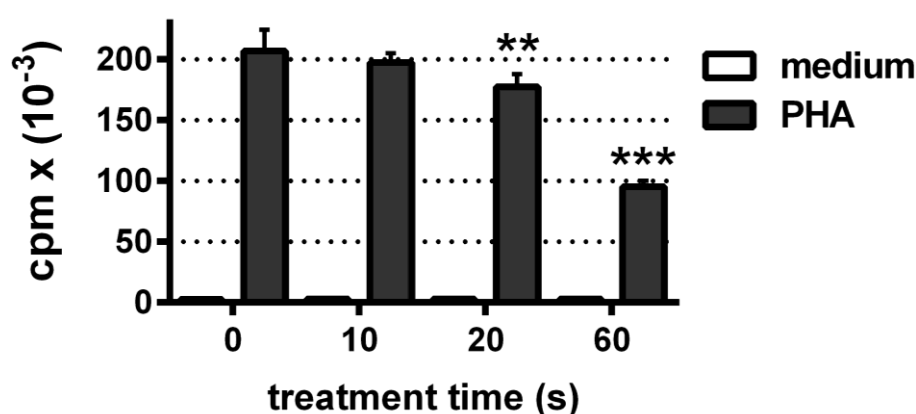


Fig. 20*: Plasma treatment reduced proliferation in mitogen-activated T lymphocytes.

PBMCs (10^6 per ml in R10F) were plasma-treated and cultured with or without PHA (500 ng/ml) for 72 h at 37 °C. ³H-methyl-thymidine (0.5 µCi per well) was added and cells were incubated for another 17 h. Thymidine incorporation was measured using a β-counter. In the absence of PHA cells did not proliferate, and plasma treatment did not change this. In PHA-activated cells plasma reduced the proliferative response in a significantly and dose-dependent manner. Data are presented as mean ± SD of three independent experiments. For statistical analysis, one-way ANOVA was performed (*Dunnnett* post test).

**adapted from (192) with permission from Wiley*

The proliferative response declined significantly but only partially in plasma-treated PBMCs (Fig. 20). Thus, plasma-treated T lymphocytes retain their ability to become activated, even if long-term exposure directed many cells to programmed cell death. Importantly, plasma treatment did not induce cell proliferation in non-activated cells. This indicated that oxidation did not randomly activate lymphocytes in an antigen-independent manner.

T cell activation induces signaling involving phosphorylation of NFκB and ERK1/2, triggering the MAP-kinase pathway. This leads to proliferation which was decreased in plasma-treated cells. Therefore, it was investigated next whether plasma treatment rendered T lymphocytes non-stimulable to activation via alteration of NFκB and/or ERK1/2 phosphorylation. PBMCs were plasma-treated and subsequently incubated for 15 min at 37 °C with or without PMA/Ionomycin. PMA and Ionomycin are small organic compounds that freely diffuse into cells and activate protein kinase C without the need of surface receptor stimulation. This ultimately leads to NFκB and ERK1/2 phosphorylation and is quicker when compared to PHA-stimulation that involves surface receptor cross-linking.

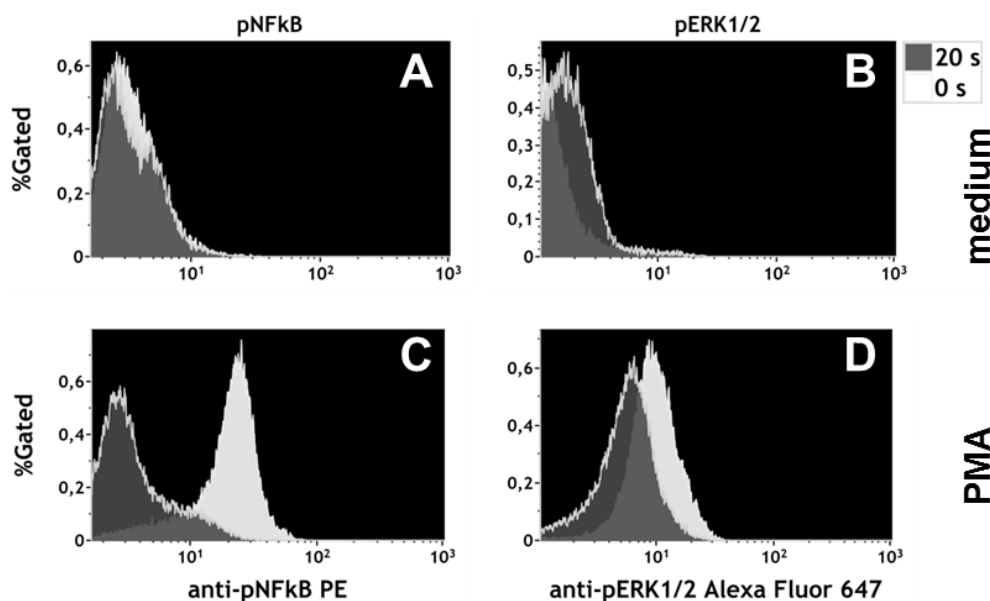


Fig. 21: Plasma treatment reduced the ability of T cells to become activated via NFκB and/or ERK1/2 signaling.

PBMCs (10⁶ cells per ml in R10F) were plasma-treated (20 s) and either PMA (50 ng/ml) and Ionomycin (1 μg/ml), or medium alone was added immediately. Cells were incubated for 15 min at 37 °C and fixed and permeabilized. Cells were then stained for cells surface markers and phosphorylated NFκB and ERK1/2, and evaluated by flow cytometry. Plasma treatment had no effect on NFκB phosphorylation (A) and a small effect on ERK1/2 phosphorylation (B). In contrast, plasma-treated CD4⁺ T_H cells were rendered less sensitive to PMA-activation as shown by reduced phosphorylation of NFκB and ERK1/2 (C, D). Shown is one representative of three independent experiments.

Confirming results of previous experiments, plasma did not activate T_H cells by itself as no phosphorylation of NFκB was observed (Fig. 21A). A small increase in phosphorylation of ERK1/2 was measured in plasma-treated CD4⁺ T_H compared to control cells (Fig. 21B). However, exposure to plasma strongly (NFκB, Fig. 21C) or partially (ERK1/2, Fig. 21D) reduced the ability of CD4⁺ T cells to become activated via PMA/Ionomycin stimulation. This suggested that plasma interferes with T cell signaling pathways contributing to the observed effects on proliferation in previous experiments. Investigating signaling pathways via flow cytometry was chosen due to the following advantages compared to traditional western blotting: i) it requires fewer sample handling, ii) it is quicker (within two hours), iii) it is more accurate as the phosphorylation is determined on a single cell level, and iv) phosphorylation can potentially also be determined in different populations at the same time by adding additional antibodies directed against surface molecules.

Next, it was examined whether already activated and subsequently plasma-treated cells continued proliferation. As ³H-methyl-thymidine incorporation measures total but not individual proliferation activity, proliferative responses were next investigated on a single cell level using flow cytometry. PBMCs were stained with CFSE and stimulated with PHA for 48 h prior to plasma treatment. Cells were then plasma treated and incubated for another 72 h prior to flow cytometric evaluation. The fluorescence intensity of CFSE-stained cells is bisected by each cell division. Therefore it is possible to estimate the number of proliferative cycles and the course of proliferation of activated T lymphocytes. The aim was to investigate the mechanism leading to the reduction in T cell proliferation observed in the ³H-methyl-thymidine experiments. Reduced proliferation could be due to increased cell death and/or a reduction in proliferation of viable cells.

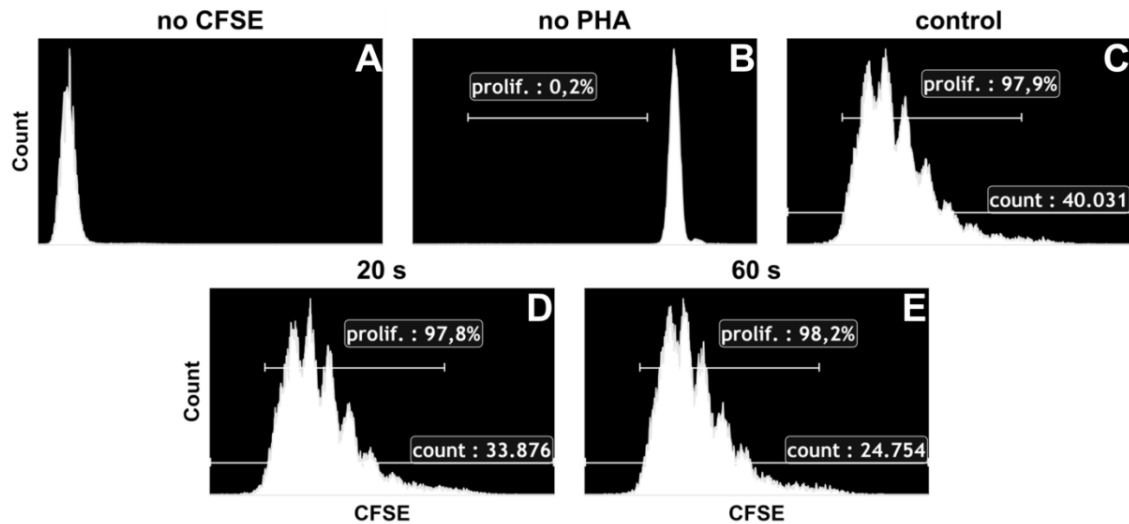


Fig. 22*: Plasma treatment did not mediate a blockage of proliferation in PHA-activated T lymphocytes.

PBMCs were stained with CFSE and incubated for 48 h with PHA (500 ng/ml) at 37 °C. Cells were then plasma-treated and incubated for 120 h. PBMCs were then stained with anti-CD3 APC antibodies and DAPI, and measured by volumetric flow cytometry (same acquisition volume for each sample). Unstained but PHA-pulsed cells remained non-fluorescent (**A**). Stained but non-activated cells were fluorescent but exhibited no proliferation response (single peak, **B**). Stained and PHA activated cells showed distinct proliferation pattern (multiple peaks) which are similar in intensity and portion (>97 %) for plasma-treated samples (**D**, **E**) and control (**C**). At the same time, the number of total viable T cells decreased in plasma-treated samples compared to control. Shown is one representative of three independent experiments.

*adapted from (194) *with permission from Wiley*

CFSE-stained PBMCs were PHA-stimulated, then plasma-treated, and cell fluorescence was measured after 120 h by volumetric flow cytometry. Unstained cells (fig 22A) exhibited only background fluorescence, while CFSE positive but not mitogen activated cells (Fig. 22B) remained highly fluorescent without showing the characteristic peak division profile of proliferating cell populations. In PHA-activated samples, almost all (>97 %) viable (DAPI) T cells (CD3⁺) of treated and control samples alike exhibited the characteristic peak division profile. Thus, despite high rates of apoptosis in plasma-treated samples, proliferation of the remaining and viable T lymphocytes continued unimpaired.

3.2. Cytokine expression was significantly altered in T lymphocytes

In the previous experiments, cells were activated with mitogens. T cell activation induces the secretion of cytokines. Cytokines are soluble low-molecular weight proteins which establish

cellular communication between adjacent but also distant sites. The two main cell populations in PBMCs, monocytes and T lymphocytes, are highly abundant in healing wounds. Depending on activation state and environmental conditions, they generate pro and anti-inflammatory cytokines. These cytokines greatly impact and drive immune responses, also in wound healing. As outlined in the introductory section, non-healing wounds are associated with delayed resolution of inflammation and an unbalanced inflammatory cytokine profile. It was therefore investigated whether plasma treatment altered cytokine responses of PBMCs.

Cytokines are produced in response to a stimulus. Depending on the type of cytokine, they can either increase inflammation or dampen it. Chronic inflammation is a key component in chronic wounds. Thus, PBMCs were exposed to plasma. After 48 h of incubation supernatants were investigated for cytokines relevant in wound healing.

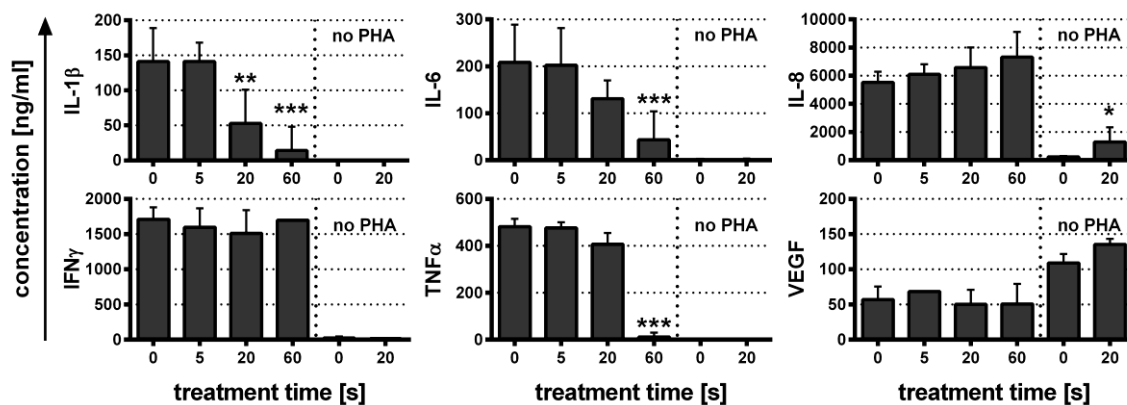


Fig. 23: Effects of plasma treatment on the release of cytokines.

PBMCs were cultured with or without PHA (500 ng/ml) O/N. Cells were plasma-treated for the indicated time periods and incubated for another 48 h. Supernatants were analyzed by ELISA. The concentrations of IL-1 β , IL-6, and TNF α decreased significantly following plasma treatment in a dose-dependent fashion. By contrast, secretion of IL-8 was elevated after plasma treatment, especially in resting PBMCs. The concentrations of IFN γ and VEGF were not affected by plasma exposure. Data are presented as mean + SD of three independent experiments. Statistical analysis was performed using one-way ANOVA (*Dunnett* post test; with PHA) or paired student's t test (without PHA).

In the supernatant of PHA-activated and plasma-treated cells, the cytokine profile was changed compared to untreated control cells (Fig. 23). Levels of highly pro-inflammatory IL-1 β and TNF α significantly decreased. Plasma treatment did not induce their release in

non-stimulated cells which was also the case for IFN γ . However, levels of pro-inflammatory IL-8 increased in activated and significantly in non-activated and plasma-treated PBMCs. All cytokines investigated in PBMCs supernatants are summarized in the appendix (tab. ii p.132). To identify the source of the cytokines in the PBMCs culture supernatants, cells were stained for intracellular cytokines and investigated by flow cytometry. First, human PBMCs were activated with PHA O/N. Then, the protein transport inhibitor (brefeldin A) was added and cells were subsequently plasma-treated. After 18 h of incubation, cells were harvested and percentages of CD3⁺ T lymphocytes that expressed cytokines were evaluated by multicolor flow cytometry.

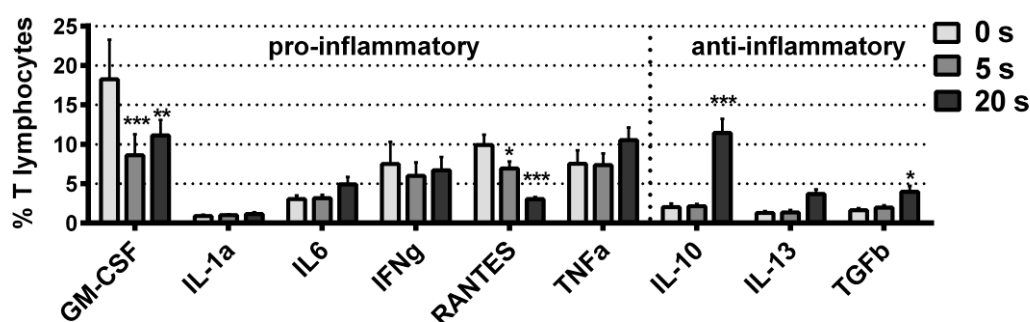


Fig. 24: Plasma induced a predominantly non-inflammatory cytokine response in T lymphocytes.

PBMCs were cultured with PHA (500 ng/ml) O/N at 37 °C. Brefeldin A was added and cells were plasma-treated. After 18 h of incubation, cells were harvested and stained for flow cytometric experiments. Dead cells were excluded by using fixable viability dyes. The percentage of GM-CSF- and RANTES-producing cells decreased significantly following plasma treatment. The fraction of T cells expressing the anti-inflammatory cytokines IL-10 and TGF β increased significantly. Data are presented as mean + SE of 2-4 independent experiments. Statistical analysis was performed using one-way ANOVA (*Dunnett* post test).

Similar to the cytokines measured by ELISA (Fig. 23), pro-inflammatory cytokines (GM-CSF, RANTES) were expressed less, while at the same time expression of anti-inflammatory cytokines (IL-10, IL-13, TGF β) was increased (Fig. 24). TNF α - and IL-6 expression profiles differed from the results of the extracellular cytokine measurements. These cytokines, including IL-1 β , are thought to derive from innate immune cells. Accordingly, monocyte cytokine responses after plasma treatment were measured next.

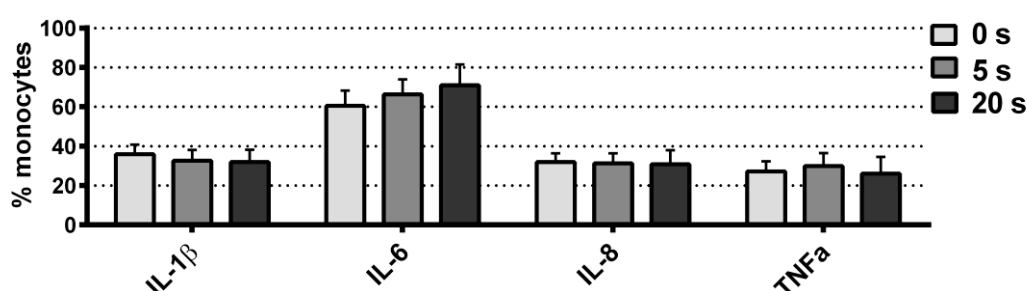


Fig. 25: Plasma treatment did not alter the cytokine responses of activated monocytes.

PBMCs were cultured with LPS (10 ng/ml) and brefeldin A for 1 h at 37 °C. Cells were plasma-treated and incubated for another 5 h. Percentages of cytokine-positive monocytes were assessed by multicolor flow cytometry. Dead cells were excluded from analysis using fixable viability dyes. Percentages of cells positive for any cytokines investigated did not change significantly between plasma-treated and control samples. Data are presented as mean + SE of 7 independent experiments.

Compared to untreated control cells, expression levels of IL1- β , IL-6, IL-8, and TNF α in LPS-stimulated monocytes were not significantly affected 5 h after plasma treatment (fig 25).

3.3. Summary of results

It was shown in this section that plasma treatment altered the cellular behavior of T lymphocytes. Plasma exposure reduced lymphocyte activation by blocking NF κ B and ERK1/2 signaling. In pre-activated T cells, however, proliferation was not affected by plasma in viable cells. Lymphocyte activation is associated with cytokine secretion and the cytokine profile of plasma-treated cells was largely non-inflammatory.

4. What are the mechanisms of the effects of plasma on immune cells?

Different properties of cold physical plasma have been suggested to have an impact on cells. Among them are electrical fields, UV-radiation, thermal stress, and oxidants or reactive species. In this section, a series of experiments are described, which were conducted to decipher the mechanism(s) by which plasma exerted cytotoxic effects on PBMCs and especially T_H cells.

4.1. Cytotoxicity effects were dependent on plasma treatment conditions

Plasma induced apoptosis in T lymphocytes. To understand the relationship between plasma treatment and cytotoxicity, the treatment conditions for PBMCs were altered. This included total volume, cell concentration, distance of the jet, and protein-content of the medium.

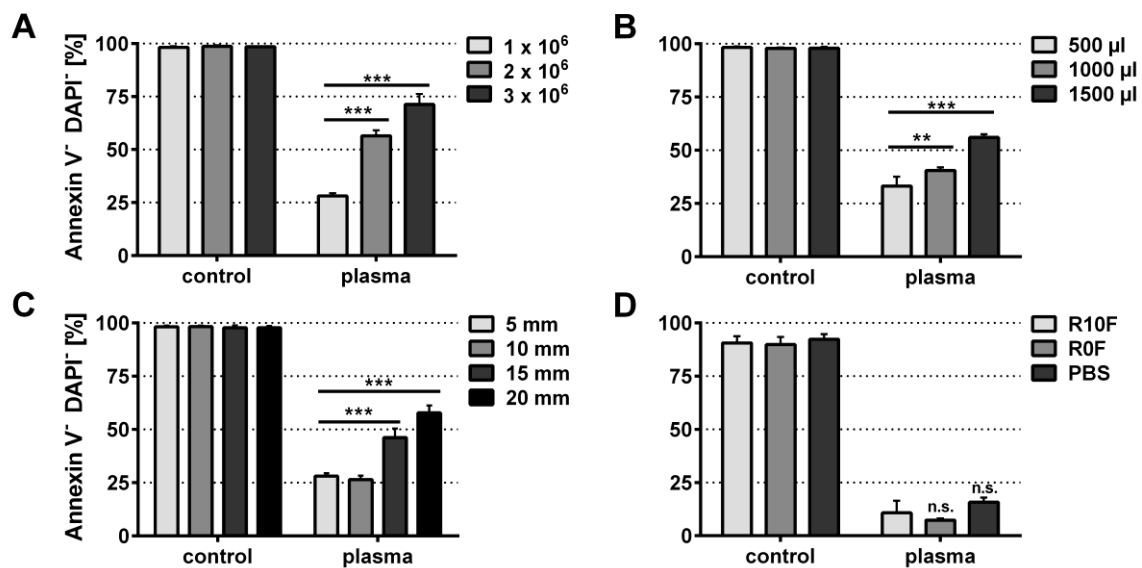


Fig. 26: Plasma toxicity was dependent on total volume and cell concentration but not protein content.

In all experiments, PBMCs were plasma-treated and stained with Annexin V, DAPI, and anti-CD4 antibodies after 24 h of incubation. Cell concentration had a significant effect on cytotoxicity (A). Using the same cell concentration but treating different volumes of cell suspension also significantly altered cell survival (B). Increasing the distance between the plasma jet and cell suspension produced significantly less (15 mm, 20 mm) toxic effects (C). The conditions of the medium did not affect cell viability (D). Data are presented as mean + SD of three independent experiments. Statistical analysis was done using one-way ANOVA comparing different treatment conditions against the first condition shown in the graph (*Dunnett* post test).

To determine what parameters were important in plasma-mediated cytotoxicity, plasma treatment conditions were varied (Fig. 26 and appendix Fig. ix p.134). Cell concentration (Fig. 26A), cell volume (Fig. 26B), and distance of the jet to the liquid (Fig. 26C) significantly influenced the percentage of viable T_H cells. The condition of the medium in which PBMCs were treated (medium with or without FCS and PBS) had no influence on viability (Fig. 26D). Previous experiments showed a treatment-time dependent induction of apoptosis in lymphocytes (Fig. 16). Here, using the same treatment time and volume of the medium, plasma cytotoxicity was dependent on cell concentration (Fig. 26A). Likewise, using the same treatment time and cell concentration, less apoptosis was induced if the total volume treated was increased (Fig. 26B). Both results indicated that cytotoxic plasma agent(s) were inactivated by or reacted with cells and showed a concentration-dependent effect. Additionally, close proximity of the jet enhanced its cytotoxic effects (Fig. 26C).

It appeared that the effect of plasma on liquid determined the degree of cytotoxicity. In experiments investigating plasma-treated liquids alone (Fig. 9), substantial concentrations of short and long-lived reactive molecules were found. In order to determine the contribution of short-lived reactive species such as $\cdot O_2^-$ or $ONOO^-$ to cytotoxicity, medium alone was plasma-treated and subsequently added to PBMCs.

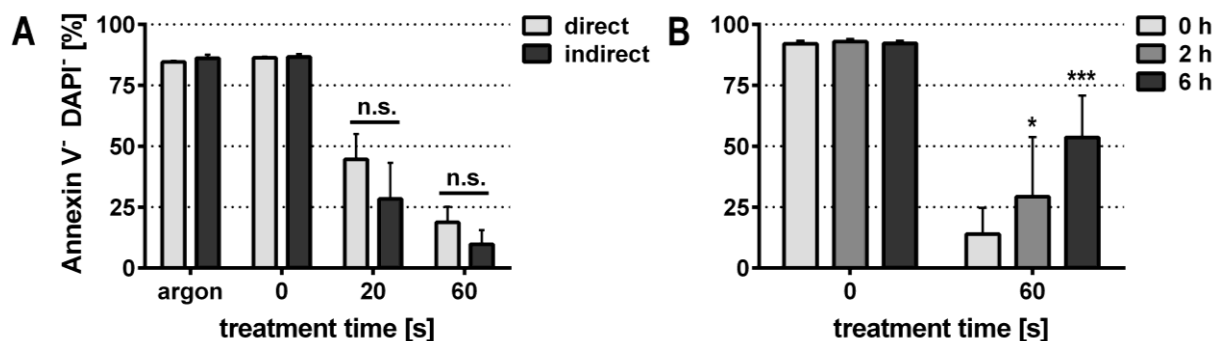


Fig. 27: Plasma-treated medium alone also displayed cytotoxic activities.

PBMCs were either directly plasma-treated or medium alone was exposed to plasma before adding to cells immediately (indirect treatment). For indirect treatment, 1 ml of medium was treated twice as long as for direct treatment and 500 μ l of medium was added to 500 μ l of PBMCs suspension at 2×10^6 per ml in medium. After 24 h of incubation, PBMCs were stained (anti-CD4 antibodies, Annexin V, and DAPI) and percentages of viable $CD4^+$ T_H cells measured by flow cytometry. Cytotoxicity of both treatment regimens was similar and differences were non-significant (A). Plasma-treated medium was given at different time points to cells (B). Medium significantly lost activity after 2 h and 6 h of incubation. Data are presented as mean + SD of three independent experiments. Statistical analysis was performed using two-way ANOVA (Dunnett post test).

Direct and indirect plasma treatment yielded similar toxicity in CD4⁺ T_H cells (Fig. 27A). Even 6 h after treatment and incubation at 37 °C, plasma-treated medium still displayed cytotoxic effects although to a significantly lesser extent compared to freshly treated medium (Fig. 27B). These results made action of a stable oxidant, such as hydrogen peroxide, likely and its specific contribution to plasma-mediated cytotoxicity was tested next.

4.2. Hydrogen peroxide was central in plasma-mediated cytotoxicity

In the preceding section it was concluded that the plasma-mediated cytotoxicity was most likely elicited by a stable oxidant. Hydrogen peroxide displays a long half-life in solution and is known to be cytotoxic. Hence, it was investigated which portion of plasma-mediated cell death may be due to H₂O₂ deposition by plasma. RNS and superoxide were also scavenged to confirm their negligible direct role in plasma-mediated apoptosis as suggested by indirect plasma treatment (Fig. 27).

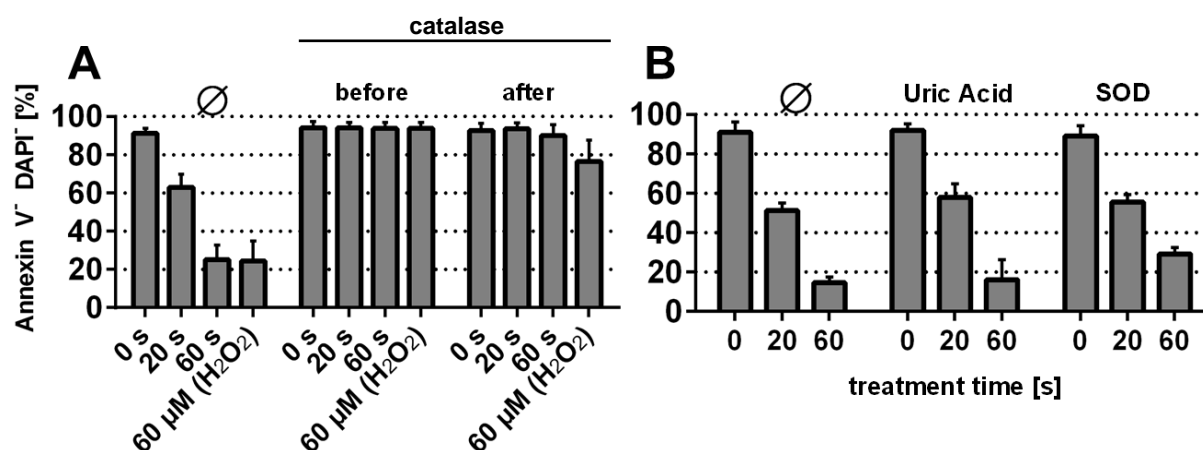


Fig. 28: H₂O₂ was the main cytotoxic plasma agent.

PBMCs were directly plasma-treated in the presence of antioxidant enzymes or proteins, or vehicle controls. Viability of CD4⁺ T_H cells was assessed by Annexin V / DAPI staining after 24 h of incubation at 37 °C. Addition of catalase prior to plasma treatment fully protected cells to plasma cytotoxicity (A*). Supplementation of catalase immediately after treatment greatly improved viability. H₂O₂ alone also induced apoptosis in vehicle controls only, while addition of uric acid or superoxide dismutase prior to plasma exposure showed similarly decreased viability as in vehicle controls (B). Data are presented as mean + SD of three independent experiments.

**adapted from (185) with permission from Informa Healthcare*

To investigate the contribution of different plasma-derived reactive molecules, PBMCs were plasma-treated in the presence of species-degrading enzymes or an antioxidant. Catalase inactivates hydrogen peroxide (H_2O_2), while superoxide dismutase (SOD) inactivates superoxide. Uric acid scavenges RNS such as peroxynitrite. Uric acid or SOD showed no protective effect (Fig. 28B) but catalase fully protected plasma-treated CD4^+ T_H cells (representatively shown for lymphocytes) when added before exposure (Fig. 28A). Adding catalase after treatment yielded very low apoptosis.

The cells were also exposed to experimentally added H_2O_2 (Fig. 28A) using a treatment time matched concentration calculated from initial experiments measuring H_2O_2 in plasma-treated medium alone (Fig. 9A). Experimentally added H_2O_2 led to similar survival rates compared to plasma treatment underlining its central part in cytotoxicity. It was also indirectly shown that H_2O_2 reacted with the cells as its concentration was lower in supernatants of plasma-treated PBMCs (1 h: 25 μM and 24 h: 3 μM) compared to plasma-treated medium alone (1 h: 60 μM ; 24 h: 9 μM) alone (Fig. 9A and appendix Fig. viii p.133). Further, it was the specific enzymatic activity of catalase that provided protection as no H_2O_2 was measured in supernatants of plasma-treated PBMCs in the presence of catalase (appendix Fig. viii p.133).

Catalase protected CD4^+ T_H cells from apoptosis and no change in the CD45RA/CD45RO/CD62L expression pattern of plasma-treated but catalase protected T_H cells was observed (not shown).

How was H_2O_2 mediating cellular damage? It is a relatively slow reacting oxidant and not toxic *per se*. Presence of metal ions such as Fe^{2+} , however, leads to generation of $\cdot\text{HO}$ (*Fenton* reaction) which rapidly oxidizes biological molecules. A second possibility was that monocyte/macrophage myeloperoxidase (MPO) further oxidized H_2O_2 to $\cdot\text{OCl}$ which is highly toxic. To test this hypothesis, PBMCs were incubated with the MPO inhibitor 4-ABAH prior to plasma treatment (Fig. 29).

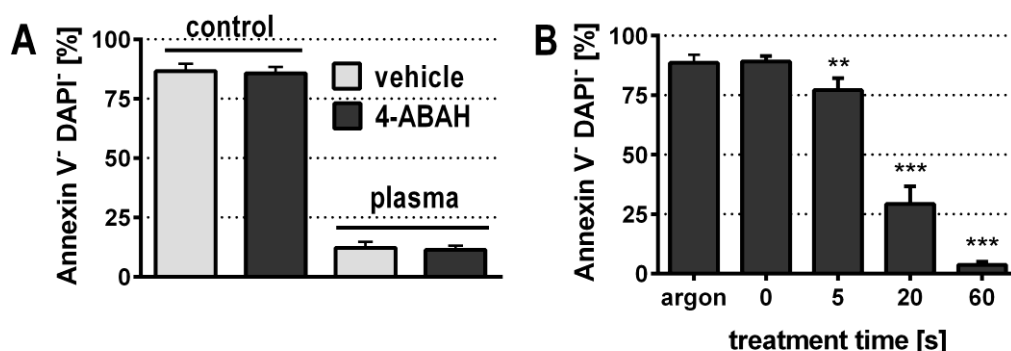


Fig. 29: H₂O₂-induced lymphocyte death is independent of MPO.

PBMCs were incubated with 100 μ M of the MPO-inhibitor 4-ABAH or vehicle control, directly plasma-treated, and CD4⁺ T lymphocyte viability was assessed using Annexin V and DAPI after 24 h of incubation. MPO-inhibition did not protect cells from cytotoxic plasma effects (A). Absence of monocytes led to plasma-induced cell death in fluorescence-activated-cell-sorted CD4⁺ T lymphocytes (purity >98 %) (B). Data are presented as mean + SD of two (A) and four (B) independent experiments. Statistical analysis was done using one-way ANOVA (*Dunnnett* post test).

MPO is not involved in plasma-mediated cytotoxicity as its inhibition lead to similar cell viability in plasma-treated cells (Fig. 29A) compared to PBMCs treated without MPO inhibition. This finding was supported by plasma exposure of highly purified CD4⁺ T cell suspensions devoid of monocytes/macrophages. Significant percentages of plasma-treated CD4⁺ T cells were apoptotic (Fig. 29B). Thus, plasma-deposited H₂O₂ did not act indirectly via its conversion to [•]OCl. As described in the introduction, [•]HO in the gas phase is thought to generate H₂O₂ in the gas and liquid phase of plasma. As H₂O₂ was important in plasma-mediated cytotoxicity it was next investigated whether there were alternative routes of H₂O₂ production.

Generation of [•]HO in the gas phase is dependent on the presence of oxygen. The plasma setup was modified in a way that allowed controlling the influx of ambient air species into the plasma effluent by using a gas shielding device (appendix Fig. ix p.133). N₂ (2 slm) was used as the curtain gas and argon (1 slm) served as the feed gas. The plasma effluent was operated in close proximity to the liquid. This setup allowed complete exclusion of any oxygen to interfere with plasma in the gas phase. As N₂ served as the shielding gas, no ROS and only RNS were generated in the plasma gas phase. The cytotoxicity of this setup was evaluated 24 h after plasma-treatment of PBMCs.

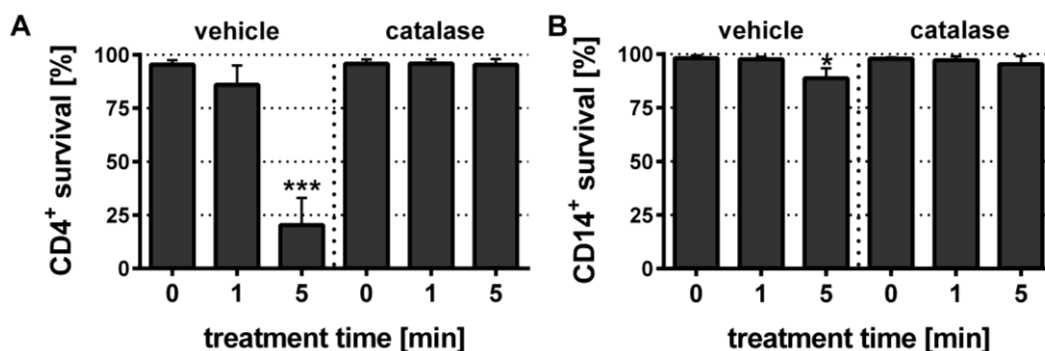


Fig. 30*: Oxygen was dispensable for plasma cytotoxicity.

N₂-shielded plasma was used to treat PBMCs and evaluate T_H (CD4⁺, **A**) and monocyte (CD14⁺, **B**) survival after 24 h of incubation using Annexin V and DAPI. Plasma was cytotoxic but the presence of catalase abrogated harmful plasma effects in both cell types. Data are presented as mean + SD of four independent experiments.

**adapted from (195) with permission from IEEE*

It was investigated whether gas-phase derived O₂ was essential in plasma-mediated cytotoxicity to CD4⁺ T_H cells (Fig. 30A) or monocytes (Fig. 30B) in PBMCs. Plasma was cytotoxic to CD4⁺ T_H cells but to a lesser extent compared to the setup used normally throughout this work. Also, catalase protected lymphocytes and monocytes from toxic plasma effects in this alternative treatment regime, making a ROS-independent pathway of generation of H₂O₂ likely. Together, H₂O₂ was identified as the central cytotoxic agent in plasma-treated lymphocytes and monocytes.

4.3. H₂O₂ was the main but not the only oxidizing agent in cells

Plasma-induced apoptosis was highly dependent on the presence of H₂O₂. Next, it was investigated whether H₂O₂ was also central in mediating oxidation in cells. Species, such as superoxide, were detected (Fig. 9C) in plasma-treated medium but did not contribute to toxicity in plasma-treated cells (Fig. 28B). However, they could mediate cell oxidation. Additionally, and considering the wealth of species being created by plasma in the gas phase, it was hypothesized that H₂O₂-independent oxidation was present. To dissect the effects of H₂O₂ alone, catalase and concentration-matched experimentally added H₂O₂ were used as controls.

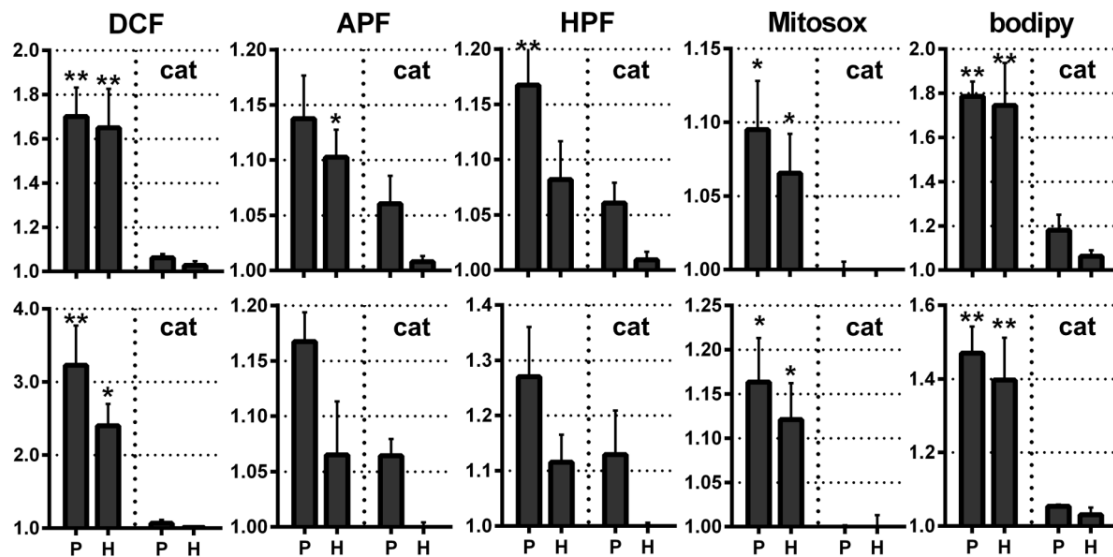


Fig. 31*: Plasma-induced oxidation in cell membranes, cytosol and mitochondria was reduced by catalase.

PBMCs were stained with five different redox dyes and anti-CD4 and anti CD14 antibodies to discriminate their fluorescence in CD4⁺ T_H cells (**upper graphs**) and monocytes (**lower graphs**). Directly after plasma treatment, cells were harvested, washed and fluorescence measured by multicolor flow cytometry. Fluorescence increase was similar in CD4⁺ T_H cells and monocytes, and fold increase over control (= 1) of 60 s of plasma (P) or 60 μM of H₂O₂ (H) treated cells is shown. Prior to treatment, catalase (cat) was added as control. Statistical significance of plasma or H₂O₂ treated samples refers to MFI increase compared to each respective catalase treatment (two-way ANOVA, *Sidak* post test). Data are presented as mean + SE of three to seven independent experiments.

**adapted from (185) with permission from Informa Healthcare*

PBMCs were stained separately with five different redox-sensitive probes and exposed to plasma (60 s) or treated with a treatment-time matched concentration of H₂O₂ (60 μM). Fluorescence was recorded gating on T_H cells (Fig. 31, upper graphs) and monocytes (Fig. 31, lower graphs). Similar fluorescence patterns were observed in CD4⁺ T_H cells and monocytes for all dyes used. Three different compartments were investigated: cell membrane (bodipy), cytoplasm (DCF, APF, HPF), and mitochondria (Mitosox). All probes responded to plasma and H₂O₂ treatment but plasma treatment always induced a higher fluorescence increase compared to H₂O₂ treatment. As both treatments induced cell death to a similar extent this pointed to an impact of species other than H₂O₂. Also, fluorescence increase differed significantly (DCF, mitosox, bodipy) or non-significantly (APF, HPF) between samples with and without catalase, independent of plasma or H₂O₂ treatment. While catalase fully protected oxidation of mitosox (present in mitochondria), only partial protection of oxidation was observed in the cell membrane and cytosol.

4.4. Summary of results

In this section, it was investigated how plasma mediated its effects on cells. Plasma-induced apoptosis was dependent on cell concentration and the total volume treated suggesting a dose-like relationship in cytotoxicity on cells. Also, plasma-treated medium alone exhibited similar cytotoxic properties compared to cells being directly exposed to plasma. This made a direct contribution of UV-radiation, elevated temperatures, or electrical fields to plasma cytotoxicity unlikely. Cytotoxicity of plasma-treated medium was effective for many hours, arguing for action of a long-lived oxidant. Accordingly, the role of hydrogen peroxide was investigated and found to be the main cytotoxic agent inducing apoptosis in plasma-treated cells. The contribution of other species to toxicity such as hypochlorous acid, superoxide, or RNS was found to be minor. Use of redox-sensitive probes indicative of oxidation revealed a plasma-induced, but H_2O_2 -independent, oxidation at the membrane and in the cytosol without cytotoxic consequences.

Up to now in this study, PBMCs were investigated and it was shown how they were affected by plasma treatment and by which mechanisms the reactions were possibly mediated. Monocytes and lymphocytes migrate into the wound bed during the late phase of inflammation. Intriguingly, non-healing wounds are frequently associated with chronic inflammation which is thought to be a neutrophil-driven process. Neutrophil granulocytes have a sophisticated arsenal of toxic molecules to fight infections but these can also mediate tissue destruction. Therefore, neutrophils were investigated next to decipher by what means exposure to plasma modulated their behavior *in vitro*.

5. Plasma treatment of human neutrophils

Plasma treatment of PBMCs induced oxidative stress and apoptosis, especially in lymphocytes. Exposure to plasma also modulated their cytokine response towards a non-inflammatory profile. Hyper inflammation is thought to play a crucial role in chronic wounds. It prolongs the inflammatory phase in wound healing and subsequently inhibits its transition towards a pro-resolving phenotype. An important cell type mediating inflammation is the neutrophil granulocytes. Neutrophils effectively kill microorganisms in an oxidant-dependent or -independent manner leading to inflammation in tissues but potentially also destruction. Elevated numbers of neutrophils are associated with non-healing wounds. Plasma is a promising treatment option in this disease and it was therefore vital to investigate the neutrophil response to plasma treatment. In all experiments, polymorpho-nuclear cells (PMNs) were isolated by dextran sedimentation followed by ficoll centrifugation, thereby separating PMNs from PBMCs. The dominant cell population in PMNs is neutrophils with usually less than 5 % eosinophils (appendix Fig. xi p.134). Exclusion of DAPI (>95 %), purity in terms of PBMCs contamination (<5 %), and percentage of eosinophils (1-10 %) was always assessed by flow cytometry to quality control successful isolation of PMNs. The aim of this section was to examine whether plasma treatment had an influence on neutrophil behavior and/or function associated with their pivotal role in wound healing.

5.1. Plasma oxidized neutrophils but only partially induced apoptosis

Oxidation and apoptosis induction was shown in plasma-treated PBMCs. However, neutrophil biology strongly differs from lymphocyte biology. Under cell culture conditions, neutrophils are short-lived cells with a half-life of 6-8 h. During cell isolation procedures they can easily become primed and extreme care must be taken during further handling to avoid activation and aggregation. Moreover, neutrophils are potent producers of ROS which in turn also play a central role in neutrophil biology and physiology. These considerations were important in designing experiments to assess viability and oxidation.

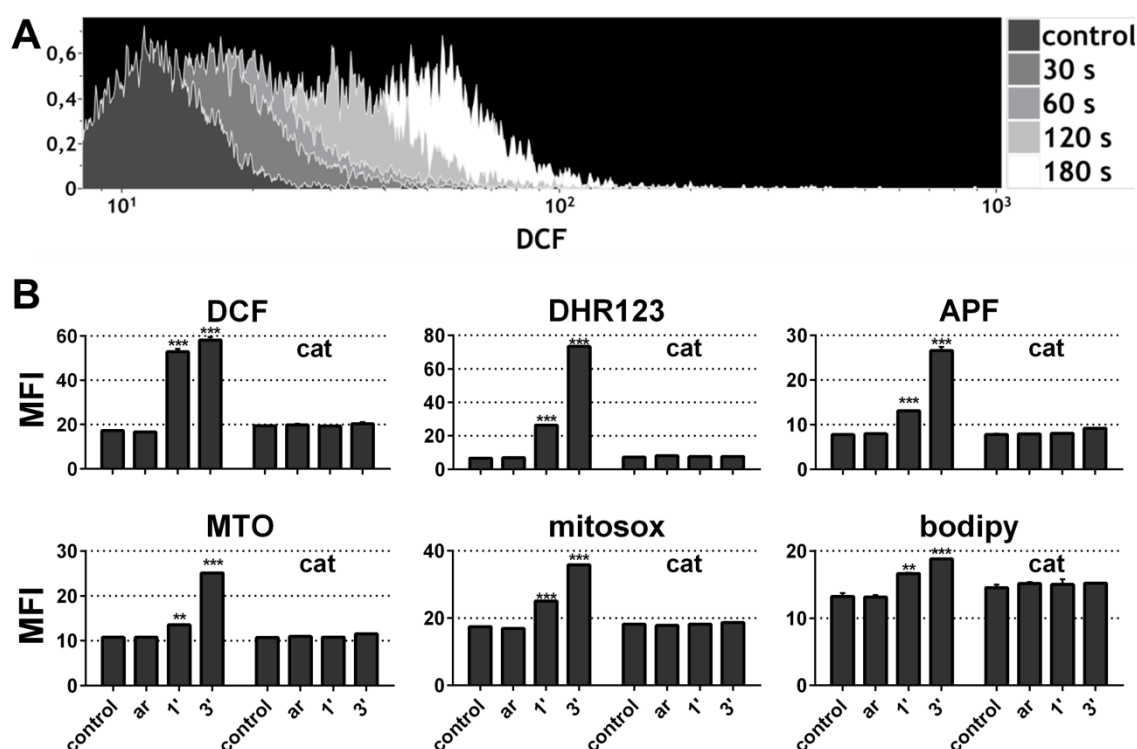


Fig. 32: Plasma oxidized PMNs in a H_2O_2 -dependent manner.

PMNs were separately stained with six different redox-sensitive dyes, treated with plasma, and mean fluorescence was acquired by flow cytometry. A strong fluorescent increase was observed, e.g., in DCF (representative overlay **A**). Oxidation was measured in different cellular compartments using the following dyes: cytosol (DCF, DHR123, APF), mitochondria (*Mitotracker* orange, mitosox), and cell membrane (bodipy) (**B**). Three min of plasma exposure strongly increased mean fluorescence, especially of cytosolic probes. Addition of catalase prior to exposure resulted in fluorescence intensities similar to controls. Argon gas (ar) treatment (1 min) alone did not induce any oxidation. Data are presented as mean + SD of duplicates of one representative of three independent experiments. Statistical analysis was done using one-way ANOVA (*Dunnnett* post test).

PMNs were stained with different redox-sensitive probes prior to plasma treatment and fluorescence was acquired using flow cytometry. Plasma-treated cells displayed a H_2O_2 -dependent oxidation in all cellular compartments investigated (cell membrane: bodipy; cytosol: DCF, DHR123, APF; mitochondria: mitosox, *Mitotracker* orange) (Fig. 32B). Although neutrophils are known to be prone to shear forces and consequently can become activated, 1 min of argon gas treatment was assessed. Argon treatment did not result in a fluorescence increase indicative of spontaneous cellular activation. This was an important consideration for further experiments. As oxidation and cell death correlated well in experiments of plasma-treated lymphocytes, it was next investigated whether plasma also induced apoptosis in neutrophils.

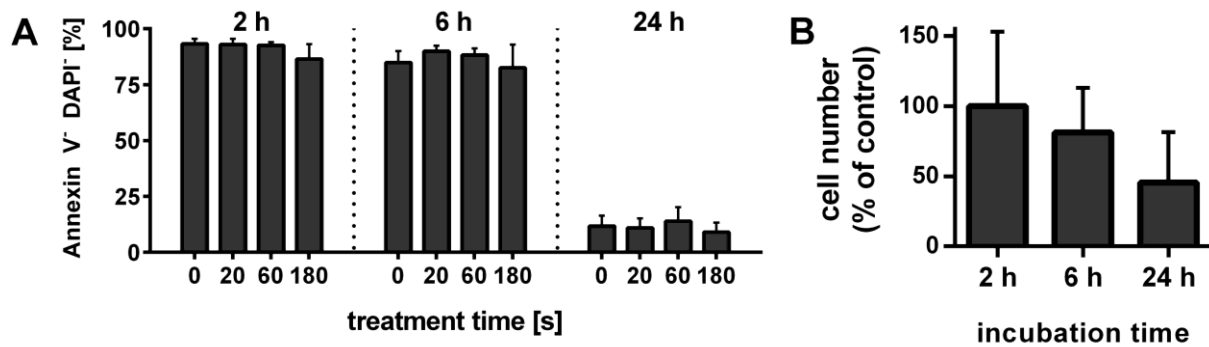


Fig. 33: Plasma treatment led to decreased neutrophil numbers but did not induce apoptosis.

PMNs were plasma-treated, incubated at 37 °C, and percentages of viable (Annexin V⁻/DAPI⁺) cells measured after different time points. An increase in induction of apoptosis in plasma-treated compared to control cells was not observed for any time point tested (A). Cell numbers of plasma-treated (3 min) samples decreased after 6 h and 24 h, respectively (B). Data are presented as mean + SD of five independent experiments.

Plasma treatment oxidized neutrophils. Therefore, it was assessed whether their viability was compromised. Exposure to plasma showed no significant effects on cell viability (Fig. 33A) but fewer cells were recovered with increasing incubation time after plasma treatment (Fig. 33B). Isolated neutrophils undergo major spontaneous apoptosis, making it difficult to determine if plasmas treatment enhances that rate. As it was not clear whether the loss of cells (Fig. 33B) was due to increased attachment of the cells or necrosis, supernatants of plasma-treated cells were taken and analyzed for the presence of lactate dehydrogenase indicative of cell membrane damage. All samples tested were negative for LDHB up to 48 h after plasma treatment (appendix Fig. xii p.135). As this made plasma-induced necrosis in neutrophils implausible it was more likely that plasma-treated neutrophils may have adhered to the cell culture plastic or were otherwise altered, making them hard to recover for flow cytometry. Therefore, another viability assay was used measuring metabolic turnover from resazurin to resorufin. This method gave a measure of all cells per well and not only cells that could be recovered for flow cytometry.

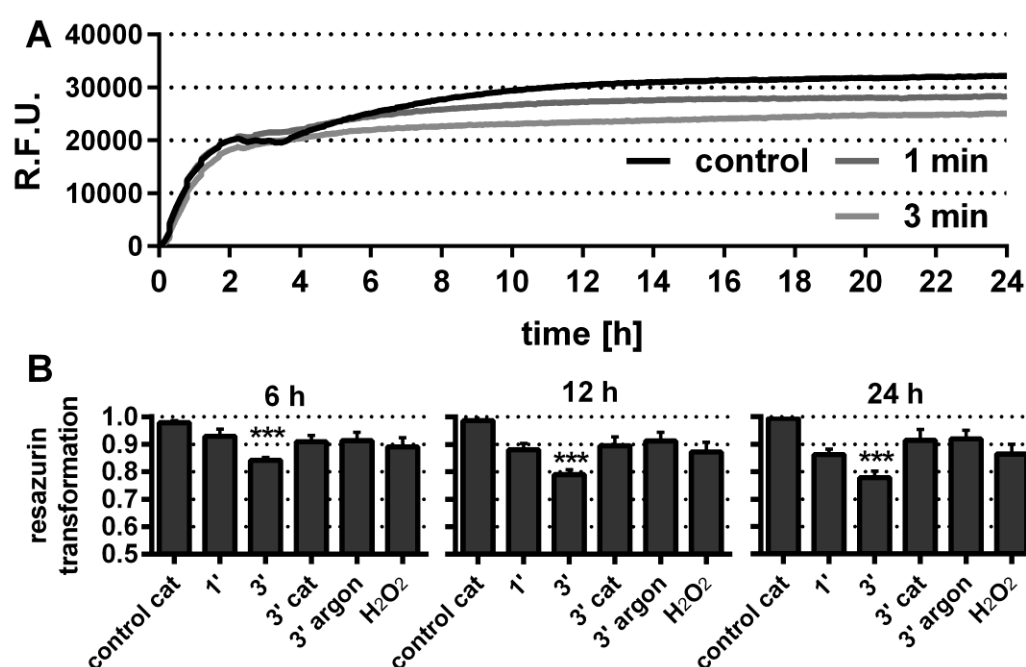


Fig. 34: Metabolic activity decreased significantly in plasma-treated PMNs.

PMNs were plasma-treated and immediately aliquoted (4 replicates per sample) into 96 well plates. Resazurin was added (final concentration 200 μ M) and fluorescence monitored over 24 h at 37 °C using a plate reader. The representative kinetic showed increased metabolic activity in control for the first 10 h of reading, while in samples exposed to 3 min of plasma the fluorescence signal stagnated 4-6 h after seeding (A). R.F.U. were normalized to controls and quantification at three different time points revealed a significant difference for 3 min plasma-treated samples only (B). Data are presented as mean + SE of four to eight independent experiments.

Metabolic activity was significantly lower in plasma-treated cells compared to controls (Fig. 34). This effect was only partially abrogated by catalase, while H₂O₂ or argon gas treatment had no significant effect on activity. The rate of resazurin transformation was the highest within the first 2-3 h after seeding (Fig. 34A) and plasma-treated cells only showed effects different from controls after 4-8 h of incubation. As no apoptosis was present at that time it was concluded that, at least in part, exposure to plasma altered the cellular phenotype or activity which was investigated next.

5.2. Cellular oxidative burst remained functional after plasma treatment

Compared to the effect of plasma on the viability of PBMCs, PMNs viability was only marginally altered. It was thus the question whether plasma treatment manipulates effector

functions of neutrophils. In response to stimulation, neutrophils can quickly assemble Nox2-related proteins at the cell membrane, ultimately inducing a quick (seconds to minutes) respiratory burst resulting in production of superoxide. It was investigated whether neutrophil burst activity was affected after plasma treatment.

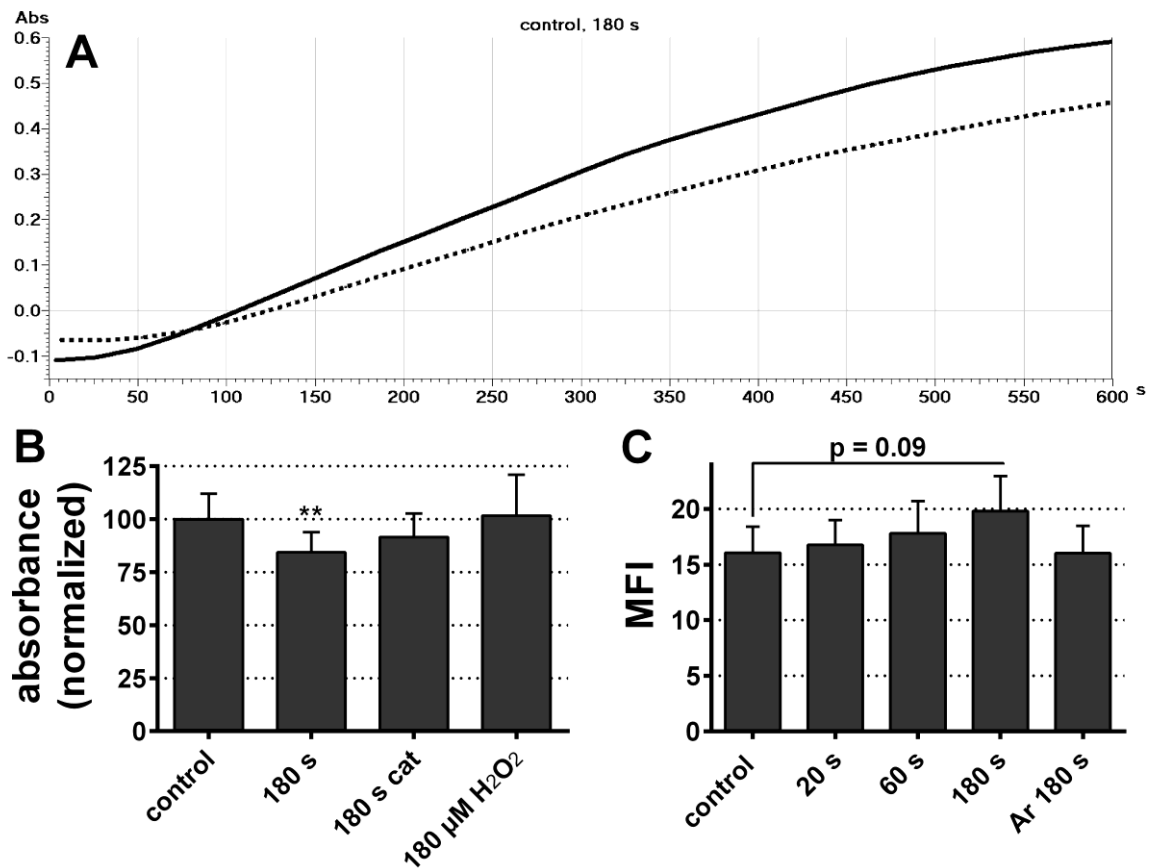


Fig. 35: Exposure to plasma attenuated the oxidative burst

For assessment of superoxide production, PMNs were plasma-treated and immediately added to cuvettes incubated at 37 °C. PMA was added (100 nM final concentration) and absorbance measured at 550 nm over 10 min (**A**). The slope of control cells (black line) was slightly steeper compared to plasma-treated cells (dotted line). Quantification and normalization of slopes revealed a significant decrease for 3 min plasma-treated samples (**B**). Controls produced $\sim 6 \mu M \cdot O_2^- / \text{min} / 10^6$ cells. Neutrophils were also stained with the redox-sensitive probe DHR123 and incubated with opsonized bacteria (*Escherichia coli*) for 10 min at 37 °C. The mean fluorescence of the oxidative burst in response to phagocytosed bacteria was slightly increased in plasma-treated samples but not argon gas controls (**C**). Data are presented as mean + SD of four (**B**) and three (**C**) independent experiments. Statistical analysis was carried using one-way ANOVA (Dunnett post test).

Neutrophil respiratory burst was tested by measuring superoxide production after PMA-stimulation and DHR123 fluorescence after incubation with *Escherichia coli*. Plasma treatment had a subtle but significantly reducing effect on the oxidative burst after PMA

activation (Fig. 35B). Cell counts were similar in all samples (appendix Fig. xiii p.135) excluding the possibility that during plasma treatment neutrophils became increasingly adherent which would have affected the number of cells transferred to the cuvettes for analysis of superoxide production. In contrast to PMA-stimulation, oxidative burst was slightly increased in response to physiological stimulus (*Escherichia coli*, Fig. 35C). The oxidative burst of is one important feature of the neutrophil antimicrobial defense system, bacterial phagocytosis and killing are others. Accordingly, it was tested whether plasma treatment altered neutrophil's ability to take up and subsequently kill engulfed bacteria.

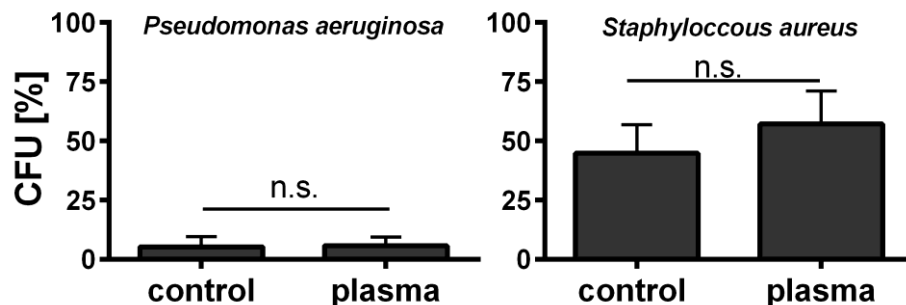


Fig. 36: Neutrophil bacterial killing was not significantly impeded by plasma treatment.

Bacteria were opsonized in autologous serum for 30 min at 37 °C. Neutrophils were seeded into wells of a 24 well plate (10^7 per ml in Hank's containing 10 % autologous serum) and plasma-treated (3 min). Immediately after treatment, bacteria (10^8 in total) were added to each well and also to one well containing Hank's only. Cell suspensions were transferred to 1.5 ml Eppendorf tubes and incubated for 30-45 min, while rotating in an incubator. Neutrophils were lysed and diluted suspensions then plated on blood agar. Plates were incubated O/N at 37 °C and colonies were counted and normalized to plates with bacteria incubated without neutrophils (100 %). Killing of *Pseudomonas aeruginosa* (*p.a.*) and *Staphylococcus aureus* (*s.a.*) was similarly effective in plasma-treated and control cells. Data are presented as mean + SD of two (*p.a.*) and three (*s.a.*) independent experiments. Statistical analysis was done using unpaired student's t test.

Neutrophil killing of bacteria was neither significantly enhanced nor reduced by plasma treatment (Fig. 36). This again suggested that neutrophil activity was not severely impaired by plasma treatment. Apart from phagocytosis and intracellular killing, neutrophils have evolved several other mechanisms to inactivate or kill invading bacteria. Among them is the formation of extracellular structures (NETs) that efficiently entrap microorganisms and whose formation is linked to the generation of reactive species by neutrophils. It was thus investigated whether exposure to plasma may elicit the production of these NETs.

5.3. Plasma treatment induced neutrophil extracellular trap formation

One of the major findings in neutrophil biology in the past decade was the cell's extrusion of cellular DNA to the extracellular space. These structures are called neutrophil extracellular traps (NETs) and serve as a host defense mechanism to trap pathogens, thereby inhibiting their proliferation. This is an active process and elicited in response to various stimuli. Decreasing cell numbers but not increasing apoptosis already suggested cellular aggregation which is typical for NET formation. Light microscopic evaluation further demonstrated the increased presence of large aggregates of neutrophils in plasma-treated cell suspensions compared to controls. It was thus investigated next whether exposure to plasma stimulated neutrophils to make NETs.

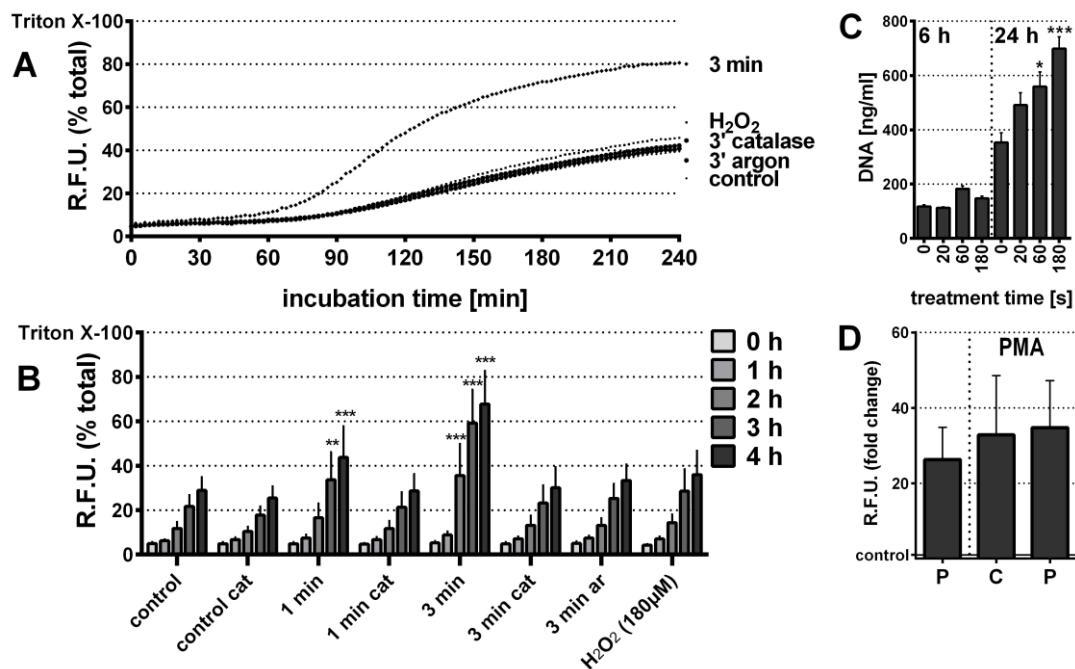


Fig. 37: Plasma-treated neutrophils and their supernatants stained positive for DNA.

Neutrophils were plasma-treated, immediately seeded into black 96 well plates containing Sytox orange, and fluorescence monitored for 4 h at 37 °C using a plate reader (A). One representative of eight independent experiments is shown. Plasma induced stronger fluorescence and argon-, H₂O₂-, or catalase controls were similar to non-treated cells. Quantification revealed significantly increasing fluorescence for 1 min and 3 min of plasma treatment only and for incubation times exceeding 2 h after exposure (B). DNA in supernatants of treated cells was not significantly elevated after 6 h but was after 24 h of treatment compared to controls (C). If cell suspensions were treated with DNase 3 h after exposure to plasma (P), a 20-fold increase in DNA-fluorescence was observed compared to control (Y-axis) and comparable to PMA-induced NET production (D). Data are presented as mean + SD of eight (B), three (C), and four (D) independent experiments. Statistical analysis was performed using one-way (C) or two-way (B) ANOVA, respectively.

Already 1 h after exposure, PMNs showed enhanced DNA fluorescence compared to control (Fig. 37A). This process was not inducible by H_2O_2 or argon gas treatment alone but was catalase-inhibitable (Fig. 37B). H_2O_2 was added in three different ways: at once (a bolus), 6x 30 μM , or in addition to argon gas control (appendix Fig. xiv p.136). The effect of a split dosage of H_2O_2 was not different from effects when it was given as a bolus. As argon gas or H_2O_2 alone led to a subtle increase in fluorescence it was investigated whether their combination may increase neutrophil responses. H_2O_2 given during the argon gas treatment resulted in a very similar fluorescence increase compared to argon gas treatment alone (appendix Fig. xiv p.136). Moreover, MPO inhibition using 4-ABAH did not increase or decrease the fluorescence of plasma-treated cells (appendix Fig. xiv p.136) pointing to an MPO-independent reaction. Fluorescence, as measured in the plate reader, does not discriminate between nuclear DNA from non-viable cells and extracellular DNA. Therefore, supernatants were investigated for DNA content. After 6 h, no additional DNA was measured but a significant increase was measured in supernatants taken after 24 h (Fig. 37C). However, if DNase was added to neutrophils 3 h after plasma treatment and supernatants were stained with Sytox green, a very strong increase in fluorescence over control was observable (Fig. 37D). The increase was similar when PMA was added, a known inducer of NETs. These results provided strong evidence that the observed fluorescence increase was due to NETs. To confirm this hypothesis, PMNs were plasma-treated and incubated at 37 °C in a live cell microscope with frequent image acquisition of mosaic patterns (3x3). After batch stitching and cropping, an algorithm was written that excluded low fluorescence (background) as well as high fluorescence (nuclei) to perform quantitative image analysis for total NET-area.

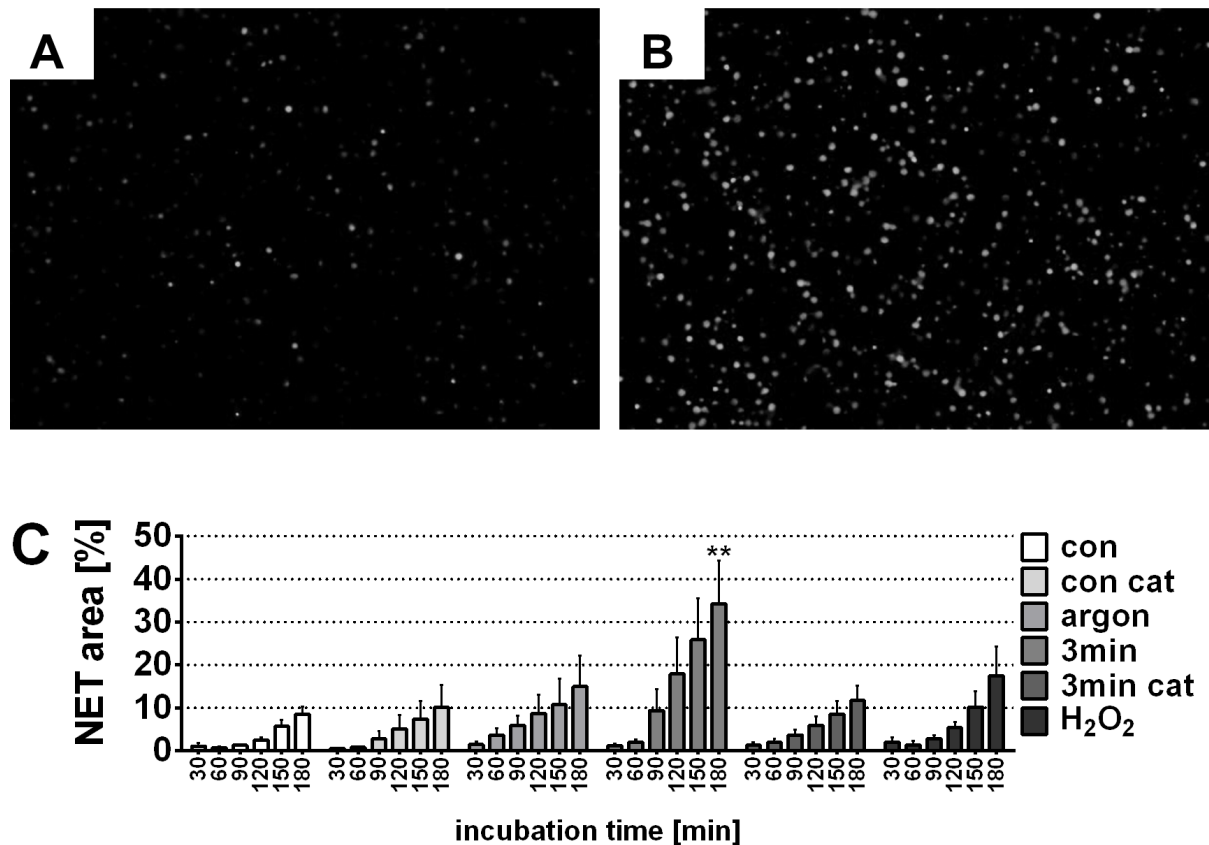


Fig. 38: Quantitative image analysis of total NET area.

Neutrophils were plasma-treated and DNA fluorescence acquired every 30 min. Shown are representative images of control (A) and plasma-treated (B) PMNs after 3 h of incubation. Here, NET area of plasma-treated but not argon gas or H₂O₂ (180 μ M) treated cells increased significantly compared to control cells (C). Data are presented as mean + SD of four to six independent experiments. Statistical analysis was performed using two-way ANOVA comparing all means and applying *Tukey* post-test.

Plasma treatment of neutrophils led to significantly increased total NET-area (Fig. 38C). Catalase abrogated this effect but addition of exogenous H₂O₂ did not initiate it. Diffuse structures formed around cells between 60-90 min after treatment which were enumerated as NETs. It is described that long, string-like NETs are an experimental artefact rather than a long-distance expulsion from neutrophils. To verify that DNA was not expelled accidentally but was due to an active process (NETosis) neutrophils were plasma-treated, stained against DNA and neutrophil elastase, and imaged using confocal laser scanning microscopy. Elastase is a serine proteinase and associated with neutrophil azurophilic granules. It destroys bacteria but also host tissue and is associated with prolonged inflammation. NETs are decorated with elastase which confers some of their antibacterial activity. Elastase is therefore a suitable co-stain to confirm the presence of NETs.

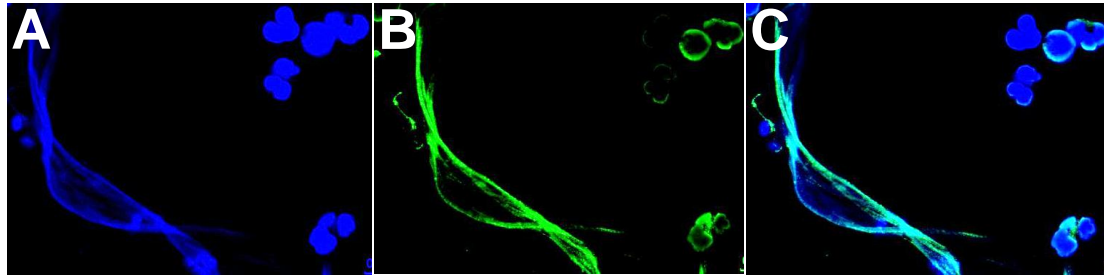


Fig. 39: Verification of NET structures after plasma treatment.

Neutrophils were plasma-treated, incubated for 2 h, and stained for DNA (DAPI, **A**) and elastase (anti-elastase antibody, **B**). Overlay of both signals showed congruent staining and thereby confirmed the presence of NETs after plasma treatment (**C**). Structures shown were frequently present in fixed preparations of plasma-treated samples but not in controls.

String-like DNA (observed when preparations are subject to disturbance when fixing and staining) was associated with elastase (Fig. 39C) verifying that the structures released upon plasma treatment were neutrophil extracellular traps, a product of neutrophil ETosis. Thus, plasma induced a NET-response observable from 60-90 min after exposure and with a consistent increase after that. NETs are also decorated with antibacterial proteins, e.g., the reactive oxidant-producing enzyme myeloperoxidase (MPO). MPO is stored in primary granules and can be released independently of NETs by degranulation. Likewise, various inflammatory cytokines can be released by neutrophils upon activation. It was, therefore, investigated in the following section how plasma-treated neutrophils manipulated their environment in addition to release of extracellular traps.

5.4. Neutrophil cytokine and MPO release was also modulated after exposure to plasma

Neutrophils release NETs, cytokines, and antibacterial proteins, such as MPO in response to stimulus, directly or indirectly resulting in enhanced bacterial clearance but also hyper-inflammation and tissue destruction. Using neutrophil supernatants, the presence of soluble inflammatory mediators was investigated as these also play a pivotal role in wound healing. IL-8 for example can induce NET-release and IL-1 β , IL-6, and TNF α are associated with slow-healing wounds and prolonged inflammatory responses.

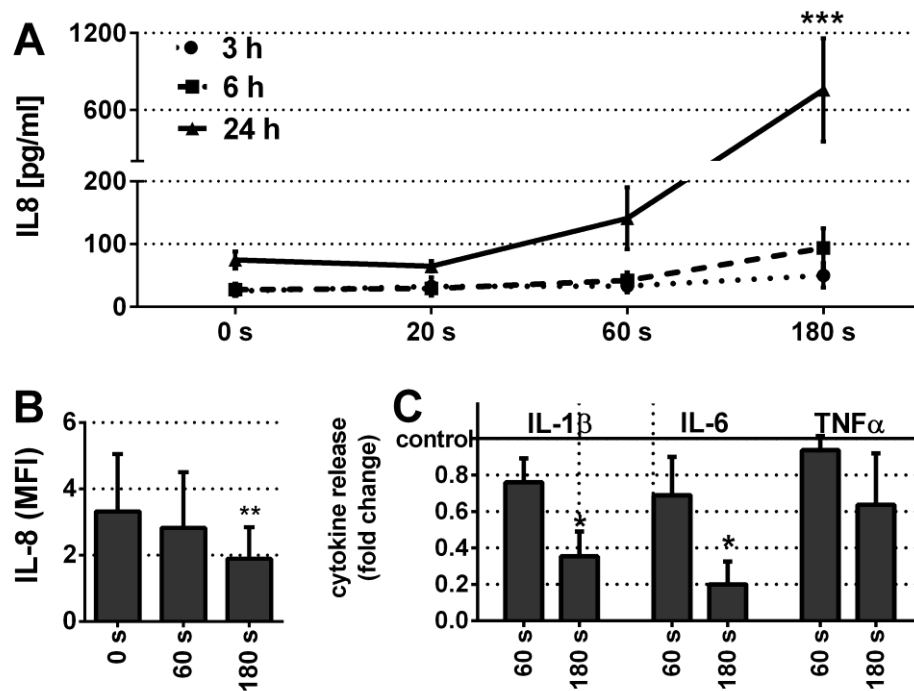


Fig. 40: Cytokine response of plasma-treated neutrophils.

Neutrophils (10^6 per ml in R10F) were plasma-treated and supernatants collected after 3 h, 6 h, and 24 h. Using ELISA, IL-8 concentration was quantified against a known standard and showed increased IL-8 levels with increased incubation and plasma treatment time (A). Intracellular cytokine measurements using flow cytometry verified neutrophils to be the origin of IL-8 as levels decreased in plasma-treated cells 24 h after exposure (B). Investigation of other inflammatory cytokines using Luminex technology showed significantly decreased levels of IL-1 β and IL-6 24 h after exposure (C). Data are presented as mean + SD of replicates of four (A, B) or three (C) different donors. Statistical analysis was performed using two-way ANOVA comparing treated samples to control (0 s, *Dunnett* post test, A) or using paired student's T test (B, C).

IL-8 release increased in plasma-treated samples but only significantly 24 h after exposure, thereby IL-8 release was not linked to NET-induction (Fig. 40A). Monocytes/macrophages also produce IL-8 and as isolation procedures never yield 100 % pure neutrophil suspensions, intracellular IL-8 was measured in neutrophils by flow cytometry to verify these cells as the source. Cells were incubated without protein transport inhibitors, allowing the release of IL-8. Accordingly, the mean fluorescence of IL-8 in neutrophils (Fig. 40B) decreased, arguing for its release which was measured by ELISA. The cytokines IL-1 β , IL-6, and TNF α are associated with neutrophils and inflammation and their levels in supernatants decreased with increasing treatment time (Fig. 40C). A summary of all cytokines investigated in supernatants of plasma-treated neutrophils can be found in the appendix (tab. iii p.137).

Neutrophils not only mediate inflammation by cytokine release but also by degranulation. Primary granules, containing for example MPO, can be quickly released upon activation. Therefore, the presence of MPO was assessed in neutrophil supernatants as a measure of degranulation.

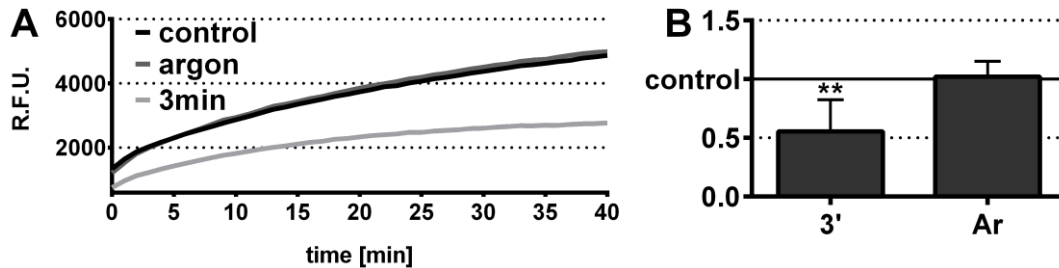


Fig. 41: Extracellular MPO activity is decreased after plasma treatment.

Neutrophils (10^6 per ml in Hank's) were plasma-treated and supernatants collected after 1 h incubation at 37 °C. Amplex ultra red and H_2O_2 was added to supernatants and the fluorescence increase recorded over 40 min in a plate reader (A). Plasma- but not argon gas treatment reduced MPO enzymatic activity in neutrophil supernatants. Data are presented for one representative (A) or mean + SD (B) of three experiments from different donors.

MPO activity was found to be decreased by half in plasma-treated supernatants and argon gas treatment had no effect (Fig. 41B). As this assay determines MPO-activity but not concentration results can be due either to reduced MPO activity, reduced MPO-concentration, or both. Regardless of this, results suggest a decreased inflammatory potential.

5.5. Summary of results

Although plasma treatment induced strong oxidation in human neutrophils their viability and function (oxidative burst, phagocytosis) was only marginally compromised. Plasma also induced formation of extracellular traps, accompanied by an increase of IL-8 but decrease of inflammatory mediators such as MPO, IL-1 β , IL-6, and TNF α . Taken together these results suggest a gain of function (NETs) while not spurring further inflammation.

Chapter 6. Discussion

1. Generation of reactive species by plasma, and their interplay

In this work, human leukocytes in liquid suspension were treated by an atmospheric pressure argon plasma jet. Plasma is an ionized gas and mediates its effects, at least in part, by creating reactive species in the gas phase. Species then diffuse into the liquid, ultimately reaching the cells. Firstly, it was investigated what species were present after plasma treatment. Several **biologically-relevant reactive species** were identified which are normally present in mitochondria and fought by (anti-)oxidative defense systems of eukaryotes but were generated by plasma in this work: hydrogen peroxide (H_2O_2), nitrite (NO_2^-), peroxynitrite (ONOO^-), and superoxide (O_2^-) (Fig. 9 p.56).

Hydrogen peroxide is central in oxidative stress and cytotoxic at higher concentrations (174). Its generation was likely a product of two hydroxyl radicals (Fig. 8B p.55) associating via a collision partner (196,197). Unexpectedly, addition of oxygen to the feed gas yielded significantly less H_2O_2 in liquids although H_2O_2 can be a product of direct two-electron reduction of oxygen (198). The ability to modulate H_2O_2 concentrations generated by plasma could be beneficial in tailoring plasma according to a given application.

The inert inorganic anion **nitrite** was formed by plasma treatment and its concentration was also modulated by the feed gas composition (appendix Fig. ii p.128). NO_2^- is non-toxic and a byproduct of nitric oxide production *in vivo* (199). However, it can also be recycled to form nitric oxide especially under hypoxic conditions (200). Nitric oxide has pro-angiogenic properties beneficial in wound healing (201). Plasma-deposited NO_2^- could have been formed by autoxidation of nitric oxide (202), or was a possible reaction product of nitric oxide with singlet oxygen (203) which were both detected previously in the plasma gas phase (80,204).

The finding that tyrosine was converted to 3-nitrotyrosine (NY) supported the notion that RNS such as **peroxynitrite** were formed by plasma (Fig. 9D p.56). High concentrations of ONOO^- are cytotoxic (205), partially due to its ability to form hydroxyl radicals (206). NY

was detected only during direct, but not after indirect, plasma exposure of tyrosine in solution. Due to its short-lived nature ($t_{1/2} = 1.9$ s) RNS would have rapidly decomposed to give nitrite (205) during indirect treatment which was indeed present after plasma treatment (Fig. 9B p.56). ONOO^- could have been formed from H_2O_2 and nitrite under acidic conditions (207). Both PBS and media are buffered solutions but it is hypothesized that plasma creates a local and very short drop in pH, thereby possibly allowing this reaction (208). The finding that the H_2O_2 -scavenging enzyme catalase partially but significantly reduced NY-formation in PBS and medium alike, supports this possibility.

Superoxide was also deposited by plasma into liquids (Fig. 9C p.56). It is assumed to be toxic to cells (209). O_2^- is created by adding one electron to oxygen, and is hypothesized to derive from the hydroperoxyl radical which itself may be a product of photoreactions with H_2O in the plasma gas phase (77).

Plasma treatment effectively oxidized not only fluorescent redox-sensitive probes but also glutathione (GSH) (Fig. 10 p.57) which is an important part of the oxidant-detoxification system (210). Accordingly, it was likely that plasma induced oxidative stress in leukocytes.

2. Behavior of monocytes and lymphocytes in response to plasma treatment

Leukocytes can be subdivided into PBMCs, containing monocytes and lymphocytes, and granulocytes. Both monocytes and lymphocytes are long-lived cells with a life-span of days to years. In contrast, neutrophil granulocytes only have a short half-life of 6-8 h in the blood and their purpose after immigration to the wound site is bacterial clearance and ultimately cell death. Attributing to these fundamentally different, almost opposite, patterns of cell viability this work was bisected into investigating the impact of plasma on PBMCs on the one hand, and studying its effects on neutrophils on the other hand. Determining the cellular responses towards plasma is important for understanding the modulating effect of plasma on wound environment.

2.1. The redox modulation after plasma treatment

Plasma generated various reactive components in the gas phase which were transported into the liquid, thereby creating an oxidative environment. Cells feature several protective mechanisms including **glutathione** (GSH) to counter-act oxidative stress (211). GSH constitutes and regenerates the majority of free thiols in cells to maintain redox homeostasis (212). Measuring the intracellular free thiol content in living cells using a suitable fluorescent probe (213), an significant increase was observed 2 h and 6 h after plasma treatment compared to controls (Fig. 11C p.60). This was unexpected, but suggests an active GSH synthesis in response to plasma treatment since the cell culture medium and cells were likely to be oxidized by reactive species. Supporting this notion, thiol-upregulation in oxidatively stressed T lymphocytes has been shown before (in presence of dendritic cells) (214). Upregulation of GSH was also shown to be beneficial in survival of IL-2 deprived T lymphocytes in response to growth factors (215). In general, GSH is important for lymphocyte activation and proliferation (216) and low levels are associated with apoptosis in T cells (217). Increased GSH-levels were found in viable T cells 24 h after plasma treatment (Fig. 11C p.60) which suggests an active protection mechanisms of these cells against oxidative stress.

To confirm that plasma really induced cellular oxidative stress, several **redox-sensitive probes** were employed (Fig. 31 p.82). Interestingly, oxidation patterns in cell membrane, cytosol, and mitochondria were similar in lymphocytes and monocytes although the latter are themselves equipped with a ROS-generating molecular machinery (105). This indicates i) that endogenous monocyte-derived ROS did not significantly contribute to cellular oxidative stress, and ii) that plasma did not induce an oxidative burst in monocytes. An increase in the fluorescence of bodipy probe indicated membrane oxidation which can have consequences beyond the biomembrane itself (218), including ROS amplification, changes in membrane fluidity, or impairment of lipid-protein interactions (219). ROS generate lipid-peroxides in the cell membrane of T cells (220) which, in turn, can oxidize intracellular or near-membrane molecules (221). Indeed, oxidative stress was propagated in the cytosol as measured by increased fluorescence of DCF, indicative of cell damage (222) mediated by plasma

treatment. Also, mitochondria were oxidized and loss of **mitochondrial membrane potential** was measured in plasma-treated cells (Fig. 12 p.61). Taken together, these results show that plasma seemed to alter cellular redox hemostasis and mitochondrial integrity, pointing to damage of cells and a possible loss in viability.

2.2. Plasma treatment and apoptosis

After plasma treatment, PBMCs showed lower cell metabolism (Fig. 13 p.62) indicative of cell damage. Plasma was previously shown to induce transient cell poration (223) possibly leading to necrotic damage. Accordingly, necrosis was looked for and found to be at negligible levels (Fig. 15 p.63), making plasma-mediated induction of apoptosis likely. However, necrosis can also occur at later stages and hours after physical insult. Yet, also other findings pointed to **apoptosis** including increased levels of GSH (Fig. 11C p.60) and mitochondrial membrane depolarization (Fig. 12 p.61) (224,225). Apoptosis is an active and tightly controlled cellular process requiring energy (176). This explains the presence of intact and damaged mitochondria in the same cell, because ATP production by mitochondria is required at least during the first 2 h of apoptosis (226). Enzymes involved in apoptosis display the highest activity at 37 °C. Cell death in lymphocytes was reduced at lower temperatures (appendix Fig. iii p.129), supporting the notion of an active process such as apoptosis. Nonetheless, an inhibition of caspases would further strengthen this finding. A molecular hallmark of apoptosis is the activation of executioner caspase 3 as its protease activity is indispensable in chromatin condensation and DNA fragmentation (227). Six to twelve hours after plasma treatment, caspase 3 was found to be activated (Fig. 16A p.64). Previous studies linking caspase 3 activation to redox modulation support this finding (228). Parallel to caspase activation, phosphatidylserine (PS) exposure on the outer membrane is considered another early marker of apoptosis (229). Its expression was measured 10-12 h after treatment and increased with incubation time (Fig. 16B p.64). Taken together, these findings clearly showed that plasma treatment induced apoptosis. This is of importance as apoptosis is regarded a “silent” form of death. PS exposure facilitates uptake of dead cells by macrophages that then will not mount an inflammatory response. By contrast, necrosis causes inflammation

by releasing intracellular content to the extracellular space (180). Apoptosis was a product of redox stress with oxidation and cell death increasing in a treatment-time dependent fashion.

2.3. Differences in apoptotic responses between PBMCs subpopulations after plasma treatment

Monocytes and lymphocytes enter the wound at different stages of healing, and different site-specific functions are attributed to them (143). There are several subpopulations within the lymphocytes at the chronic wound, among them CD4⁺ T cells, CD8⁺ T cells, B cells, and NK cells (230,231). In addition, $\gamma\delta$ T cells are abundant in skin and actively contribute to wound repair (232). Monocytes/Macrophages are also attributed a central role in wound healing (233). Characterizing their susceptibility towards plasma was critical in understanding how they might be affected during treatment of chronic wounds.

Monocytes were the most robust population in plasma-treated PBMCs, while apoptosis induction in all other cell types investigated was significantly enhanced (Fig. 17 p.65). Within lymphocytes, $\gamma\delta$ T cells displayed the highest survival rates, suggesting an enhanced resistance towards oxidative stress. This could possibly be due to their physiological location in skin and gut (234), environments that both are naturally enriched for oxidative stressors (235,236). Recent studies attributed them a distinct role in cutaneous wound healing: upon tissue injury, keratinocytes display $\gamma\delta$ T cell ligands (237) and activate $\gamma\delta$ T cells to release keratinocyte growth factors (238). Compared to $\gamma\delta$ T cells, cytotoxic effects in CD4⁺ T_H cell were almost twice as high but were significantly reduced in PHA-activated cells (Fig. 17 p.65). PHA leads to broad activation of all lymphocytes in a PKC-dependent manner and was used to mimic activation of cells in wounds (239). Similar results were obtained for staphylococcal superantigens (appendix Fig. vi 131) which activate about 20 % of T cells by cross-linking TCR and MHC molecules (240).

This survival advantage might be due to an enhanced anti-oxidative defense which is upregulated during activation and subsequent increase in ROS production (241). Alternatively, lymphocyte activation or cytokines induced anti-apoptotic signaling, possibly resulting in enhanced survival after plasma exposure (242,243). Substantial amounts of IL-2,

TNF α , and IFN- γ were detected in supernatants of PBMCs cultured with PHA (appendix tab. ii p.132) which may have rendered lymphocytes more resistant to plasma cytotoxicity. For example, IL-2 enhances survival and proliferation of activated T cells after binding to their IL-2 receptor (244). However, activation with PHA can also induce activation-induced cell death (245) and there were fewer viable T lymphocytes in controls. PHA addition did not significantly affect monocyte survival rates.

Monocyte were largely resistant to plasma-induced apoptosis and their survival rates differed significantly from survival of any other subpopulations investigated (tab. i p.130). This could be due to differences in oxidation-induced pro (MEK1/2, ERK1/2) and anti-apoptotic (p38 MAPK, JNK1/2) signaling events previously implicated in a comparison between two cell lines; Jurkat T lymphocytes and THP-1 monocytes (246). Another possibility may be a more potent antioxidative defense system which under physiological conditions protects these phagocytes against self-produced ROS during oxidative burst (105).

CD4⁺ T_H cells were shown to be relevant in wound (247). Human naïve and memory T cells can be distinguished by the reciprocal expression of CD45RA or CD45R0, respectively (109). Most CD45RA⁺ cells are naïve (they express CD62L) and apoptosis induction was stronger in CD45R0⁺ cells compared to CD45RA⁺ cells after plasma treatment (Fig. 18 p.67). Interestingly, CD45R0⁺ memory T cells are predominantly found in pathological skin (248,249) and thus could be a potential target for plasma treatment. Further, CD45RA⁺ or CD45R0⁺ cells surviving the plasma exposure were predominantly negative for CD62L (Fig. 19C p.68). T cells can actively down-regulate CD62L surface expression (250) and this possibility was excluded (Fig. vii p.131). L-selectin allows lymphocytes to home into secondary lymphoid tissues. Most T cells (>80 %) in normal skin are CD62L⁺ (T_{em}) (251) and plasma would preferentially inactivate the remaining CD45R0⁺/CD62L⁺ T_{em}. Yet, there are no studies about the detailed T cell subset distribution in chronic wounds.

If CD4⁺ T cells recognize their cognate antigen-MHC II complex, and receive proper co-stimulation by the antigen-presenting cell, they proliferate. Plasma treatment reduced overall lymphocyte proliferation (Fig. 20 p.69). Detailed investigations showed that this reduction was not due to decelerated proliferation of all cells. Instead, most plasma-treated cells were not stimulated as results investigating NF κ B phosphorylation indicated (Fig. 21A

p.70). Also previous studies suggested a block of T cell NF κ B activation by oxidative stress (252). In TCR-dependent T cell activation, linker of activation (LAT) is rendered by ROS, and signaling is not transduced to the nucleus (253). Moreover, if cells were activated first and plasma-treated second, mitosis was not halted in non-apoptotic cells (Fig. 22 p.72) suggesting that plasma might not strongly interfere with T cell proliferation after antigen recognition. Therefore, plasma treatment mitogen stimulation interfered with signaling associated with T cell activation and cell cycle progression. By contrast, plasma-treatment did not inhibit proliferation in mitogen stimulated T cells.

2.4. The effect of plasma on cytokine and chemokine production

Cytokines are key regulatory molecules in wound pathology. Compared to acute wounds, non-healing wounds are frequently associated with altered cytokine signatures, e.g., increased levels of IL-1 β (157), IL-6 (254), and TNF α (255). IL-1 β attracts neutrophils to the wound site (256). TNF α and IL-1 β upregulate matrix-metalloproteinase (MMP) expression and excessive amounts of MMPs are associated with non-healing wounds (257). Likewise, IL-6 is monocyte/macrophage derived and acts as a systemic inflammation marker. Plasma treatment reduced the production of these cytokines in activated immune cells. Hence, it could counteract pathological inflammation in chronic wounds. Levels of IFN γ , a pro-inflammatory cytokine, were not modulated (Fig. 23 p.73). Similarly, VEGF concentrations did not change, indicating that plasma probably would not interfere with VEGF-spurred angiogenesis. The only molecule found to be increased significantly in supernatants of plasma-treated PBMCs was neutrophil-attracting IL-8. IL-8 release upon redox stress has been observed before, e.g., in keratinocytes (258), dendritic cells (259), and endothelial cells (260).

Intracellular cytokine measurements revealed that GM-CSF and RANTES were significantly reduced in plasma-treated T lymphocytes (Fig. 24 p.74). Since GM-CSF prolongs the life-span of neutrophils and induces their differentiation in the bone marrow (261), plasma treatment could attenuate the neutrophil response. Reduced RANTES on the other hand may decrease lymphocyte immigration to the wound site as it aids in endothelial homing (262).

The anti-inflammatory cytokines IL-10 and TGF β were significantly increased in

plasma-treated T lymphocyte (Fig. 24 p.74). IL-10 decreases production of pro-inflammatory cytokines such as IL-1 β by monocytes (263). This may have contributed to the reduction of IL-1 β , IL-6, and TNF α release by plasma-treated cells. TGF β enhances expression of VEGF (264) and its lack of expression is associated with delayed wound healing (265), attributing a positive role to enhanced TGF β release after plasma treatment. Altogether, exposure to plasma induced a distinct cytokine signature in activated PBMCs: levels of IL-8 (facilitating neutrophil recruitment) and anti-inflammatory cytokines IL-10 and TGF β were significantly enhanced, while the production of inflammatory cytokines was significantly decreased. As chronic wounds are linked to chronic inflammation, plasma treatment may be a treatment option to reduce inflammation and improve healing.

2.5. The role of H₂O₂ in plasma-mediated oxidative stress and cell death

A number of results argued for a central role of a long-lived oxidant such as H₂O₂ to be responsible for mediating toxic effects of plasma on cells: a) physical mixing of cell suspension increased cytotoxicity (Fig. 26C p.76 and appendix Fig. x p.134); b) plasma-treated cell culture medium was similarly cytotoxic to cells compared with direct exposure to cells (Fig. 26A p.77); c) plasma cytotoxicity was dependent on cell concentration and the total volume of cell suspension (Fig. 26 p.76); d) GSH was continuously oxidized in plasma-treated medium (Fig. 10C p.57); e) a treatment-time matched concentration of experimentally added H₂O₂ was similarly cytotoxic compared to plasma (Fig. 28A p.78); and f) presence of catalase during treatment fully abrogated cell death (Fig. 28A p.78). These findings also excluded effects of UV-radiation, thermal radiation, and electrical fields as directly damaging the cells.

Several routes may account for H₂O₂ generation. Both ROS (e.g., $\cdot\text{O}_2^-$) (266) and RNS (e.g., ONOO \cdot) (267) can aid in H₂O₂ production. Scavenging of $\cdot\text{O}_2^-$ and RNS did not improve cell viability (Fig. 28B p.78) arguing for their negligible role in H₂O₂ generation in liquids. Likewise, plasma-treated medium without fetal calf serum yielded similar levels of H₂O₂ (appendix Fig. ii p.128) and cell death (appendix Fig. x p.134) compared to fully supplemented medium. This means it is unlikely that secondary reactions of oxidized proteins

made a significant contribution to plasma cytotoxicity. In this study (appendix Fig. i p.127 and appendix Fig. ii p.128) and in previous work (78), increasing the humidity in the feed gas positively correlated with increased levels of gaseous $\cdot\text{HO}$ and H_2O_2 in liquids. The oxygen originated from vaporized water or room air molecular oxygen. However, despite complete exclusion of oxygen (195) and gaseous $\cdot\text{HO}$, cell death was dependent on H_2O_2 (Fig. 30 p.81). This suggested alternative routes of generation of H_2O_2 in liquids, e.g., by UV radiation (267). Results using catalase also indicated negligible toxicity of highly energetic nitrogen metastables which were previously detected in this setup (195).

Hydrogen peroxide is intra- and extracellular as it readily diffuses through water channels of cell membranes (268). Its low molecular weight and neutral charge contribute to the molecule's stability allowing long distance diffusion (269). H_2O_2 is a mildly oxidizing species and does not directly oxidize most biological molecules (270). H_2O_2 cytotoxicity is assumed to be mediated by highly reactive hydroxyl radicals (271). This species can be generated from H_2O_2 by UV-radiation (272). However, similar toxicity to cells that were directly and indirectly exposed to plasma (Fig. 26A p.77) makes it unlikely that this is a relevant mechanisms in this case. Alternatively, the jet generates substantial amounts of ozone (74) which may contribute to H_2O_2 -reactivity generating $\cdot\text{HO}$ (272). Yet, the most probable reaction accounting for H_2O_2 cytotoxicity might be the Fenton reaction where $\cdot\text{HO}$ is created via small transition metals (273). $\cdot\text{HO}$ reacts in a local and non-selective manner and cannot be enzymatically detoxified (274). H_2O_2 can be converted to highly toxic $\cdot\text{OCl}$ by monocyte myeloperoxidase (MPO) (275). Inhibition of MPO by 4-ABAH prior to plasma treatment showed similar cytotoxic effects suggesting no significant contribution of MPO/ $\cdot\text{OCl}$ to the apoptosis induction observed (Fig. 29 p.80). This was supported by the finding that plasma was also toxic to purified T_H cells with not monocytes present.

H_2O_2 was the main cytotoxic agent. However, catalase did not fully prevent cell oxidation by plasma (Fig. 31 p.82). This made a non-lethal oxidation of reactive molecules other than H_2O_2 such as $\cdot\text{O}_2^-$ or ONOO^- (Fig. 9 p. 56) likely. This was supported by the notion that plasma-treatment always induced higher fluorescence increase compared to exposure to concentration-matched H_2O_2 . Bodipy responds well to lipid-peroxidation products (276) which were created in an H_2O_2 -dependent and -independent manner in plasma-treated cells.

Likewise, it can be speculated that APF and HPF fluorescence in catalase protected cells could have been due to species such as peroxynitrite or hydroxyl radical but not $\cdot\text{OCl}$, as HPF was found to be insensitive to the latter (189). The lack of formation of 3-chlorotyrosine as measured by LC/MS supports this view as $\cdot\text{OCl}$ mediates the chlorination of tyrosine (277).

3. The Neutrophil response after exposure to plasma

Neutrophils are unique in their biology. They are short-lived and it is their purpose to migrate to the site of infection to exert their antimicrobial action and to die in this process. In the inflammatory phase of wound healing, neutrophils are the first to arrive, followed by monocytes and lymphocytes. Although neutrophil influx has been found indispensable for proper wound healing (278) their sustained presence is associated with non-healing wounds (279). Neutrophils' powerful arsenal of digestive and ROS-producing enzymes is toxic to bacteria and host tissue alike, and contributes to continuous inflammation which a major trait associated with chronic wounds. Investigating neutrophils treated with cold physical plasma was done here for the first time to determine their responses with wound healing in mind.

3.1. The effect of plasma on neutrophil function and cytokine release

Immediately after plasma treatment, total $\cdot\text{O}_2^-$ production by PMA-stimulated neutrophils was significantly reduced (Fig. 35 p.88). This implicated a quick signaling response in neutrophils and was not due to transfer of fewer neutrophils in case of spontaneous adhesion to cell culture in plasma-treated cells (appendix Fig. xiii p.135). PMA-induced $\cdot\text{O}_2^-$ production is mediated via protein kinase-C activation and rapid assembly of the $\text{p47/67}^{\text{phox}}$ to the plasma membrane (and phagosomes) (280). It can be speculated whether reduced $\cdot\text{O}_2^-$ production was due to plasma-mediated alterations in PKC-activation, resulting in fewer neutrophils bursting in response to PMA. Quicker removal of $\text{p47/67}^{\text{phox}}$ from the cell membrane in plasma-treated cells, leading to early termination of burst activity in plasma-treated cells, was unlikely due to similar kinetics of $\cdot\text{O}_2^-$ production over 10 min of measurement (Fig. 35A p.88). $\cdot\text{O}_2^-$ is an oxidative stressor and its hampered generation by activated neutrophils may be beneficial in

healing of oxidatively stressed wounds. Interestingly, the intracellular oxidative burst in response to *Escherichia coli* was not affected. In line with this finding, intracellular killing of two common (281) wound pathogens also did not change (Fig. 36 p.89). Thus, plasma treatment of wound neutrophils may not interfere with phagocytosis or killing of bacteria.

The cytokine response of neutrophils was significantly altered (Fig. 40 p.94 and tab. iii p.137). Significantly decreased concentrations of the pro-inflammatory mediators IL-1 β and IL-6, and decreased levels of TNF α were found in supernatants of plasma-treated neutrophils compared to non-treated controls. All three cytokines are relevant in wound healing (282) and these results suggest that plasma treatment could dampen inflammation. On the other hand, concentrations of IL-8 were markedly increased in supernatants of plasma-treated neutrophils compared to control cells. IL-8 is the main chemotactic molecule for neutrophils and increased concentrations would suggest enhanced neutrophil immigration to the wound site, possibly adding insult to injury (283).

3.2. Neutrophil viability and extracellular trap formation after plasma treatment

Lactate dehydrogenase (LDH), a marker of necrosis and inflammation (284), was not released from plasma-treated neutrophils (appendix Fig. xii p.135). Plasma treatment strongly oxidized neutrophils in a H₂O₂-dependent manner (Fig. 32B p.85) but no difference was observed in neutrophil phosphatidylserine expression after plasma treatment compared to non-treated cells (Fig. 33B p.86). Yet, isolated neutrophils undergo major apoptosis spontaneous apoptosis, making it difficult to determine if plasma enhances that rate. Nonetheless and in line with the findings, previous studies showed that H₂O₂ at relatively low concentrations were not toxic to neutrophils (285) while higher concentrations (> 500 μ M) induce apoptosis in neutrophils (286). Yet, total cell numbers (Fig. 33A p.86) and metabolic respiration were significantly lower in plasma-treated neutrophils (Fig. 34B p.87). This indicated that plasma rendered cells inactive.

The formation of neutrophil extracellular traps (NETs) after plasma treatment may account for these findings. Pathogens, but also host cells, can become entangled in these web-like

structures consisting of highly decondensed chromatin and decorated with antimicrobial proteins (139). Plasma treatment significantly increased presence of extracellular DNA (Fig. 37 p.90), and confocal laser scanning microscopy confirmed that NETs had been formed (Fig. 39 p.93). Catalase prevented extrusion of DNA which is agreement with reports that ROS are necessary for NET formation (287). However, direct addition of H₂O₂ showed no significant increase of extracellular DNA.

A combination of mechanisms may account for the NET response after plasma treatment. First, neutrophils are easily primed or activated by shear-forces and argon gas treatment alone caused a non-significant increase in total NET area (Fig. 38 p.92). Second, the induction of NETs was treatment-time dependent (Fig. 37 p.90), implying a graded-response to plasma in neutrophils. Third, IL-8 is known to induce NETs (288) and significant amounts were found in supernatants of plasma-treated neutrophils (Fig. 40 p.94) although at later time points compared to NET-release. Last, plasma-produced reactive species other than H₂O₂ may also be play a role.

Different proteins are bound to NETs, among them MPO (289). Compared to controls, supernatants of plasma-treated neutrophils contained less MPO (Fig. 41 p.95). A possible mechanism could be a decreased (MPO-containing) primary granule (290) efflux. If this was to retain MPO intracellularly in order to increase its concentration on NETs, this finding would add a new attribute to NETosis. However, neutrophil elastase, also stored in primary granules, was not detected in plasma-treated or control supernatants (appendix tab. ii p.132). Further research is needed to elucidate the *in vivo* significance of NET formation in wounds on the one hand and after plasma treatment of wounds on the other.

4. Leukocyte responses after cold plasma treatment: implications and potential significance in chronic wounds

Non-healing wounds are stuck in a low-grade inflammatory phase without transitioning to the proliferative or remodeling phase (231). Lymphocytes are indispensable in wound healing (282). However, pathologically increased subsets have been associated with chronic wounds (291), including B cells, CD8⁺ T cells, and CD45R0⁺ CD4⁺ T cells (248,231). Plasma

treatment effectively induced apoptosis in those cell types. It also generated large amounts of nitrite which inhibits T cell activity (292). *In vivo*, depletion of the CD8⁺ T cells results in a marked enhancement of wound healing in mice (293) and rats (294). By contrast, $\gamma\delta$ T cells are assumed to be beneficial in wound healing (295) and plasma only moderately induced apoptosis in this cell type. T cell proliferation, attributed to initiation of immune responses to wound-resident pathogens, was not halted in plasma-treated lymphocytes. Altogether, these results argue for a positive effect of cold plasma in wound healing.

In acute wound healing, phagocytes are the first to arrive first at the site of injury but they are also strongly associated with chronic wounds (231). Neither monocyte nor neutrophil viability was substantially compromised by plasma treatment. Yet, neutrophils are thought to have a short half-life but recent evidence suggests that they become resistant to apoptosis in environments subject to chronic inflammation (296). In this view, it may be beneficial that plasma induced neutrophils extracellular traps. This may contribute to wound resolution by i) increased neutrophil inactivation via NETosis, and ii) formation of antibacterial DNA-clots serving as a scaffold for other skin-resident cells.

In wounds, influx of leukocytes from the blood to the wound site is constantly facilitated via cytokine gradients. Elevated levels of IL-1, IL-6, and TNF α are present in chronic but not acute wound fluid (297). Interestingly, these cytokines were significantly down-regulated in plasma-treated PBMCs and also neutrophils. At the same time, the anti-inflammatory cytokines IL-10 and TGF β were increased. TGF β and IL-10 are both strongly associated with enhanced wound healing and resolution of inflammation (298,299). However, concentrations of IL-8 were also increased which is associated with an increased neutrophil influx *in vivo*. IFN γ , a potent inhibitor of fibroblast proliferation and collagen synthesis (300), was not decreased in supernatants of PHA-activated PBMCs. Nonetheless, the majority of inflammatory cytokines and chemokines investigated were down-regulated in plasma-treated cells (appendix tab. i p.132 and appendix tab. iii p.137).

In summary and with the exception of IL-8, plasma treatment predominantly decreased inflammatory cytokines. Together with distinctive cytotoxic effects in lymphocytes and induction of NETosis, the experiments of this thesis indicate a potentially beneficial role of cold physical plasma in treatment of chronic inflammation such as in non-healing wounds.

Chapter 7. Summary

Non-healing wounds pose a major burden to patients and health care systems alike. These wounds are chronically stuck in the inflammatory phase of the healing process without transitioning to the proliferative phase. They are also characterized by the excessive presence of leukocytes which are assumed to provoke the persistent inflammation observed in pathological wound healing. Recent studies suggested a beneficial role of cold physical plasma in the treatment of chronic wounds. Hence, it was the central question, whether exposure to cold physical plasma would affect the viability and/or function of human leukocytes.

Cold plasma displays various properties of which the generation of reactive molecules, such as reactive oxygen and nitrogen species (ROS/RNS), were found to be central in mediating redox changes in leukocytes. Oxidative stress was present especially in lymphocytes that readily underwent apoptosis after exposure to plasma. This was largely a direct consequence of plasma-generated hydrogen peroxide but not superoxide or RNS. Amount of apoptosis was comparable among several lymphocyte subpopulations, with the wound healing-relevant $\gamma\delta$ T cells being least affected. Lymphocyte apoptosis was accompanied by mitochondrial membrane depolarization, caspase 3 activation, DNA fragmentation, and phosphatidylserine exposure. These results are in line with previous characterizations of the intrinsic apoptotic pathway in redox biology, and suggest that plasma-induced apoptosis was not mediated by alternative molecular mechanisms. An important immune response mechanism, the proliferation of lymphocytes, was not interrupted in plasma-treated but non-apoptotic cells.

In wounds, a central role of leukocytes is to orchestrate the healing response via the release of small communication molecules called cytokines. Non-healing wounds are associated with elevated amounts of pro-inflammatory IL-1 β , IL-6, and TNF α , and plasma-treatment of

leukocytes strongly decreased their concentrations. At the same time, the expression of anti-inflammatory cytokines (IL-10, TGF β) was markedly increased. The pro-inflammatory chemokine IL-8 was the only molecule to be significantly increased in supernatants of plasma-treated cells. IL-8 is the major chemo-attractant for neutrophil granulocytes.

Neutrophils are frequently associated with non-healing wounds. These professional phagocytes are the first to migrate to the site of injury where they inactivate invading pathogens by various mechanisms. Importantly, highly relevant effector functions remained mostly unaffected by plasma treatment: the phagocytosis of bacteria, the oxidative burst, and the intracellular killing of microbes. Of note, plasma induced a strong induction of neutrophil extracellular traps (NETs). Decorated with antimicrobial proteins, NETs are web-like chromatin extrusions that entrap pathogens.

These results have several implications for wound healing. Plasma-treated neutrophils were still capable of eradicating bacteria, which are frequently associated with non-healing wounds. In addition, plasma-induced NETs could aid in wound healing by providing an antibacterial scaffold to safeguard against further dissemination of microorganisms. Chronic wounds display a state of sustained inflammation and plasma induced apoptosis but not necrosis in lymphocytes. This was an important finding as necrosis, the involuntary cell death, is associated with the release of intracellular content, enhancing inflammation. By contrast, apoptosis dampens it as dead cells are cleared by macrophages inducing anti-inflammatory responses. Further, the cytokine signature of plasma-treated leukocytes was largely non-inflammatory, which could further decrease inflammation in wounds.

Altogether, this work provided first insight with regard to effects and mechanisms of cold physical plasma treatment of wound-relevant leukocytes. Generally, these cells were affected by a plasma-mediated modulation of their redox state. Future studies should include the possibility of redox modulation into their experimental approach to further elucidate the role of ROS/RNS in inflammation and possibly to improve existing wound healing therapies.

Chapter 8. References

1. Crookes W. 1879. On radiant matter. *Journal of the Franklin Institute* 108: 305-316
2. Langmuir I. 1928. Oscillations in Ionized Gases. *Proceedings of the National Academy of Sciences* 14: 627-637
3. Fridman A. Plasma Chemistry. Philadelphia, USA: Cambridge University Press; 2008.
4. Graves DB. 2012. The emerging role of reactive oxygen and nitrogen species in redox biology and some implications for plasma applications to medicine and biology. *Journal of Physics D-Applied Physics* 45: 263001-263042
5. Lieberman MA, Lichtenberg AJ. 1994. Principles of plasma discharges and materials processing. *MRS Bulletin* 30: 899-901
6. Morfill G, Kong M, Zimmermann J. 2009. Focus on Plasma Medicine. *New Journal of Physics* 11: 115011
7. Vasilets VN, Gutsol A, Shekhter AB, Fridman A. 2009. Plasma medicine. *High Energy Chemistry* 43: 229-233
8. Siemens DF, Halake A. 1902. Technische Chemie.
9. Boucher R. 1985. State of the art in gas plasma sterilization. *Medical Device and Diagnostic Industry* 7: 51-56
10. Holler C, Martiny H, Christiansen B, Ruden H, Gundermann KO. 1993. The efficacy of low temperature plasma (LTP) sterilization, a new sterilization technique. *Zentralbl Hyg Umweltmed* 194: 380-391
11. Laroussi M. 2008. The biomedical applications of plasma: a brief history of the development of a new field of research. *IEEE Transactions on Plasma Science* 36: 1612-1614
12. Sladek REJ, Filoche SK, Sissons CH, Stoffels E. 2007. Treatment of *Streptococcus mutans* biofilms with a nonthermal atmospheric plasma. *Letters in Applied Microbiology* 45: 318-323
13. Matthes R, Bekeschus S, Bender C, Koban I, Hubner NO, Kramer A. 2012. Pilot-study on the influence of carrier gas and plasma application (open resp. delimited) modifications on physical plasma and its antimicrobial effect against *Pseudomonas aeruginosa* and *Staphylococcus aureus*. *GMS Krankenhhyg Interdiszip* 7: Doc02
14. Matthes R, Hubner NO, Bender C, Koban I, Horn S, Bekeschus S, Weltmann KD, Kocher T, Kramer A, Assadian O. 2014. Efficacy of different carrier gases for barrier discharge plasma generation compared to chlorhexidine on the survival of *Pseudomonas aeruginosa* embedded in biofilm in vitro. *Skin Pharmacol Physiol* 27: 148-157
15. Boxhammer V, Morfill GE, Jokipii JR, Shimizu T, Klampfl T, Li YF, Koritzer J, Schlegel J, Zimmermann JL. 2012. Bactericidal action of cold atmospheric plasma in solution. *New Journal of Physics* 14: 113042
16. Daeschlein G, Scholz S, Arnold A, von Woedke T, Kindel E, Niggemeier M, Weltmann KD, Junger M. 2010. In Vitro Activity of Atmospheric Pressure Plasma Jet (APPJ) Plasma Against Clinical Isolates of *Demodex Folliculorum*. *IEEE Transactions on Plasma Science* 38: 2969-2973
17. Koban I, Matthes R, Hubner NO, Welk A, Meisel P, Holtfreter B, Sietmann R, Kindel E, Weltmann KD, Kramer A, Kocher T. 2010. Treatment of *Candida albicans* biofilms with low-temperature plasma induced by dielectric barrier discharge and atmospheric pressure plasma jet. *New Journal of Physics* 12: 1367-2630
18. Alekseev O, Donovan K, Limonnik V, Azizkhan-Clifford J. 2014. Nonthermal Dielectric Barrier Discharge (DBD) Plasma Suppresses Herpes Simplex Virus Type 1 (HSV-1) Replication in Corneal Epithelium. *Transl Vis Sci Technol* 3: 2
19. OConnell D, Cox L, Hyland W, McMahon S, Reuter S, Graham W, Gans T, Currell F. 2011. Cold atmospheric pressure plasma jet interactions with plasmid DNA. *Applied Physics Letters* 98: 043701
20. Bayliss DL, Walsh JL, Shama G, Iza F, Kong MG. 2009. Reduction and degradation of amyloid aggregates by a pulsed radio-frequency cold atmospheric plasma jet. *New Journal of Physics* 11: 115024
21. Zimmermann J, Shimizu T, Schmidt H, Li Y, Morfill G, Isbary G. 2012. Test for bacterial resistance build-up against plasma treatment. *New Journal of Physics* 14: 073037
22. Perni S, Shama G, Kong MG. 2008. Cold atmospheric plasma disinfection of cut fruit surfaces contaminated with migrating microorganisms. *Journal of Food Protection* 71: 1619-1625

References

23. Kanemitsu K, Imasaka T, Ishikawa S, Kunishima H, Harigae H, Ueno K, Takemura H, Hirayama Y, Kaku M. 2005. A comparative study of ethylene oxide gas, hydrogen peroxide gas plasma, and low-temperature steam formaldehyde sterilization. *Infection Control and Hospital Epidemiology* 26: 486-489
24. Sipoldova Z, Machala Z. 2011. Biodecontamination of Plastic and Dental Surfaces With Atmospheric Pressure Air DC Discharges. *IEEE Transactions on Plasma Science* 39: 2970-2971
25. Müller S, Zahn RJ. 2007. Air Pollution Control by Non Thermal Plasma. *Contributions to Plasma Physics* 47: 520-529
26. Laroussi M, Mendis DA, Rosenberg M. 2003. Plasma interaction with microbes. *New Journal of Physics* 5: 41.41-41.10
27. Oehmigen K, Hähnel M, Brandenburg R, Wilke C, K.-D. Weltmann, Woedtke Tv. 2010. The Role of Acidification for Antimicrobial Activity of Atmospheric Pressure Plasma in Liquids. *Plasma Processes and Polymers* 7: 250-257
28. Rowan NJ, Espie S, Harrower J, Anderson JG, Marsili L, MacGregor SJ. 2007. Pulsed-plasma gas-discharge inactivation of microbial pathogens in chilled poultry wash water. *Journal of Food Protection* 70: 2805-2810
29. Shimizu T, Nosenko T, Morfill GE, Sato T, Schmidt H-U, Urayama T. 2010. Characterization of Low-Temperature Microwave Plasma Treatment With and Without UV Light for Disinfection. *Plasma Processes and Polymers* 7: 288-293
30. Sosnin EA, Stoffels E, Erofeev MV, Kieft IE, Kunts SE. 2004. The effects of UV irradiation and gas plasma treatment on living mammalian cells and bacteria: a comparative approach. *IEEE Transactions on Plasma Science* 32: 1544-1550
31. von Woedtke T, Oehmigen K, Brandenburg R, Hoder T, Wilke C, Hähnel M, Weltmann KD. 2012. Plasma-Liquid Interactions: Chemistry and Antimicrobial Effects. *Plasma for Bio-Decontamination, Medicine and Food Security* NATO Science for Peace and Security Series A: Chemistry and Biology: 67-78
32. Daeschlein G, Napp M, von Podewils S, Lutze S, Emmert S, Lange A, Klare I, Haase H, Gumbel D, von Woedtke T, Junger M. 2014. In Vitro Susceptibility of Multidrug Resistant Skin and Wound Pathogens Against Low Temperature Atmospheric Pressure Plasma Jet (APPJ) and Dielectric Barrier Discharge Plasma (DBD). *Plasma Processes and Polymers* 11: 175-183
33. Ermolaeva SA, Varfolomeev AF, Chernukha MY, Yurov DS, Vasiliev MM, Kaminskaya AA, Moisenovich MM, Romanova JM, Murashev AN, Selezneva, II, Shimizu T, Sysolyatina EV, Shaginyan IA, Petrov OF, Mayevsky EI, Fortov VE, Morfill GE, Naroditsky BS, Gintsburg AL. 2011. Bactericidal effects of non-thermal argon plasma in vitro, in biofilms and in the animal model of infected wounds. *J Med Microbiol* 60: 75-83
34. Daeschlein G, Scholz S, Ahmed R, von Woedtke T, Haase H, Niggemeier M, Kindel E, Brandenburg R, Weltmann KD, Juenger M. 2012. Skin decontamination by low-temperature atmospheric pressure plasma jet and dielectric barrier discharge plasma. *J Hosp Infect* 81: 177-183
35. Maisch T, Shimizu T, Li Y-F, Heinlin J, Karrer S, Morfill G, Zimmermann JL. 2012. Decolonisation of MRSA, S. aureus and E. coli by cold-atmospheric plasma using a porcine skin model in vitro. *PLoS One* 7: e34610
36. Liebmann J, Scherer J, Bibinov N, Rajasekaran P, Kovacs R, Gesche R, Awakowicz P, Kolb-Bachofen V. 2011. Biological effects of nitric oxide generated by an atmospheric pressure gas-plasma on human skin cells. *Nitric Oxide* 1: 8-16
37. Brun P, Pathak S, Castagliuolo I, Palu G, Brun P, Zuin M, Cavazzana R, Martinez E. 2014. Helium generated cold plasma finely regulates activation of human fibroblast-like primary cells. *PLoS One* 9: e104397
38. Plewa J-M, Yousfi M, Frongia C, Eichwald O, Ducommun B, Merbahi N, Lobjois V. 2014. Low-temperature plasma-induced antiproliferative effects on multi-cellular tumor spheroids. *New Journal of Physics* 16: 043027
39. Tanaka H, Mizuno M, Ishikawa K, Nakamura K, Kajiyama H, Kano H, Kikkawa F, Hori M. 2011. Plasma-Activated Medium Selectively Kills Glioblastoma Brain Tumor Cells by Down-Regulating a Survival Signaling Molecule, AKT Kinase. *Plasma Medicine* 1: 265-277
40. Zirnheld JL, Zucker SN, DiSanto TM, Berezney R, Etemadi K. 2010. Nonthermal plasma needle: development and targeting of melanoma cells. *IEEE transactions on Plasma Science* 38: 948-952
41. Arjunan KP, Friedman G, Fridman A, Clyne AM. 2012. Non-thermal dielectric barrier discharge plasma induces angiogenesis through reactive oxygen species. *J R Soc Interface* 9: 147-157
42. Ngo M-HT, Liao J-D, Shao P-L, Weng C-C, Chang C-Y. 2014. Increased Fibroblast Cell Proliferation and Migration Using Atmospheric N₂/Ar Micro-Plasma for the Stimulated Release of Fibroblast Growth Factor-7. *Plasma Processes and Polymers* 11: 80-88
43. Ahn HJ, Kim KI, Hoan NN, Kim CH, Moon E, Choi KS, Yang SS, Lee JS. 2014. Targeting cancer cells with reactive oxygen and nitrogen species generated by atmospheric-pressure air plasma. *PLoS One* 9: e86173

44. Joh HM, Choi JY, Kim SJ, Chung T, Kang T-H. 2014. Effect of additive oxygen gas on cellular response of lung cancer cells induced by atmospheric pressure helium plasma jet. *Scientific reports* 4: 1-9
45. Lee SY, Kang SU, Kim KI, Kang S, Shin YS, Chang JW, Yang SS, Lee K, Lee J-S, Moon E. 2014. Nonthermal Plasma Induces Apoptosis in ATC Cells: Involvement of JNK and p38 MAPK-Dependent ROS. *Yonsei Medical Journal* 55: 1640-1647
46. Arndt S, Unger P, Wacker E, Shimizu T, Heinlin J, Li YF, Thomas HM, Morfill GE, Zimmermann JL, Bosserhoff AK, Karrer S. 2013. Cold atmospheric plasma (CAP) changes gene expression of key molecules of the wound healing machinery and improves wound healing in vitro and in vivo. *PLoS One* 8: e79325
47. Dobrynin D, Wasko K, Friedman G, Fridman AA, Fridman G. 2011. Cold Plasma Sterilization of Open Wounds: Live Rat Model. *Plasma Medicine* 1: 109-114
48. Dobrynin D, Wu A, Kalghatgi S, Park S, Shainsky N, Wasko K, Dumani E, Ownbey R, Joshi S, Sensenig R. 2011. Live pig skin tissue and wound toxicity of cold plasma treatment. *Plasma Medicine* 1: 93-108
49. Garcia-Alcantara E, Lopez-Callejas R, Morales-Ramirez PR, Pena-Eguiluz R, Fajardo-Munoz R, Mercado-Cabrera A, Barocio SR, Valencia-Alvarado R, Rodriguez-Mendez BG, Munoz-Castro AE, de la Piedad-Beneitez A, Rojas-Olmedo IA. 2013. Accelerated mice skin acute wound healing in vivo by combined treatment of argon and helium plasma needle. *Arch Med Res* 44: 169-177
50. Kramer A, Lademann J, Bender C, Sckell A, Hartmann B, Münch S, Hinz P, Ekkernkamp A, Matthes R, Koban I, Partecke I, Heidecke CD, Masur K, Reuter S, Weltmann KD, Koch S, Assadian O. 2013. Suitability of tissue tolerable plasmas (TTP) for the management of chronic wounds. *Clinical Plasma Medicine* 1: 11-18
51. Martines E, Zuin M, Cavazzana R, Gazza E, Serianni G, Spagnolo S, Spolaore M, Leonardi A, Deligianni V, Brun P, Aragona M, Castagliuolo I. 2009. A novel plasma source for sterilization of living tissues. *New Journal of Physics* 11: 115014
52. Ngo M-H, Shao P-L, Liao J-D, Lin C-CK, Yip H-K. 2014. Enhancement of Angiogenesis and Epithelialization Processes in Mice with Burn Wounds through ROS/RNS Signals Generated by Non-Thermal N₂/Ar Micro-Plasma. *Plasma Processes and Polymers* DOI: 10.1002/ppap.201400072:
53. Nasruddin, Nakajima Y, Mukai K, Rahayu HSE, Nur M, Ishijima T, Enomoto H, Uesugi Y, Sugama J, Nakatani T. 2014. Cold plasma on full-thickness cutaneous wound accelerates healing through promoting inflammation, re-epithelialization and wound contraction. *Clinical Plasma Medicine* 2: 28-35
54. Vandamme M, Robert E, Dozias S, Sobilo J, Lerondel S, Le Pape A, Pouvesle J-M. 2011. Response of human glioma U87 xenografted on mice to non thermal plasma treatment. *Plasma Medicine* 1: 27-43
55. Yajima I, Iida M, Kumasaka MY, Omata Y, Ohgami N, Chang J, Ichihara S, Hori M, Kato M. 2014. Non-equilibrium atmospheric pressure plasmas modulate cell cycle-related gene expressions in melanocytic tumors of RET-transgenic mice. *Experimental Dermatology* 23: 424-425
56. Daeschlein G, Scholz S, Ahmed R, Majumdar A, von Woedtke T, Haase H, Niggemeier M, Kindel E, Brandenburg R, Weltmann KD, Junger M. 2012. Cold plasma is well-tolerated and does not disturb skin barrier or reduce skin moisture. *J Dtsch Dermatol Ges* 10: 509-515
57. Lademann J, Richter H, Alborova A, Humme D, Patzelt A, Kramer A, Weltmann KD, Hartmann B, Ottomann C, Fluhr JW, Hinz P, Hubner G, Lademann O. 2009. Risk assessment of the application of a plasma jet in dermatology. *J Biomed Opt* 14: 054025
58. Lademann O, Richter H, Patzelt A, Alborova A, Humme D, Weltmann KD, Hartmann B, Hinz P, Kramer A, Koch S. 2010. Application of a plasma-jet for skin antisepsis: analysis of the thermal action of the plasma by laser scanning microscopy. *Laser Physics Letters* 7: 458-462
59. Isbary G, Koeritzer J, Mitra A, Li Y-F, Shimizu T, Schroeder J, Schlegel J, Morfill G, Stolz W, Zimmermann J. 2013. Ex vivo human skin experiments for the evaluation of safety of new cold atmospheric plasma devices. *Clinical Plasma Medicine* 1: 36-44
60. Lademann J, Richter H, Schanzer S, Patzelt A, Thiede G, Kramer A, Weltmann KD, Hartmann B, Lange-Asschenfeldt B. 2012. Comparison of the antiseptic efficacy of tissue-tolerable plasma and an octenidine hydrochloride-based wound antiseptic on human skin. *Skin Pharmacol Physiol* 25: 100-106
61. Lademann O, Kramer A, Richter H, Patzelt A, Meinke MC, Roewert-Huber J, Czaika V, Weltmann KD, Hartmann B, Koch S. 2011. Antisepsis of the follicular reservoir by treatment with tissue-tolerable plasma (TTP). *Laser Physics Letters* 8: 313-317
62. Isbary G, Heinlin J, Shimizu T, Zimmermann JL, Morfill G, Schmidt HU, Monetti R, Steffes B, Bunk W, Li Y, Klaempfl T, Karrer S, Landthaler M, Stolz W. 2012. Successful and safe use of 2 min cold atmospheric argon plasma in chronic wounds: results of a randomized controlled trial. *Br J Dermatol* 167: 404-410

63. Isbary G, Morfill G, Schmidt HU, Georgi M, Ramrath K, Heinlin J, Karrer S, Landthaler M, Shimizu T, Steffes B, Bunk W, Monetti R, Zimmermann JL, Pompl R, Stolz W. 2010. A first prospective randomized controlled trial to decrease bacterial load using cold atmospheric argon plasma on chronic wounds in patients. *Br J Dermatol* 163: 78-82
64. Heinlin J, Zimmermann JL, Zeman F, Bunk W, Isbary G, Landthaler M, Maisch T, Monetti R, Morfill G, Shimizu T, Steinbauer J, Stolz W, Karrer S. 2013. Randomized placebo-controlled human pilot study of cold atmospheric argon plasma on skin graft donor sites. *Wound Repair Regen* 21: 800-807
65. Heinlin J, Isbary G, Stolz W, Zeman F, Landthaler M, Morfill G, Shimizu T, Zimmermann JL, Karrer S. 2013. A randomized two-sided placebo-controlled study on the efficacy and safety of atmospheric non-thermal argon plasma for pruritus. *J Eur Acad Dermatol Venereol* 27: 324-331
66. Lademann O, Richter H, Meinke MC, Patzelt A, Kramer A, Hinz P, Weltmann K-D, Hartmann B, Koch S. 2011. Drug delivery through the skin barrier enhanced by treatment with tissue-tolerable plasma. *Experimental Dermatology* 20: 488-490
67. Duske K, Koban I, Kindel E, Schroder K, Nebe B, Holtfrete B, Jablonowski L, Weltmann KD, Kocher T. 2012. Atmospheric plasma enhances wettability and cell spreading on dental implant metals. *J Clin Periodontol* 39: 400-407
68. Fricke K, Koban I, Tresp H, Jablonowski L, Schroder K, Kramer A, Weltmann KD, von Woedtke T, Kocher T. 2012. Atmospheric pressure plasma: a high-performance tool for the efficient removal of biofilms. *PLoS One* 7: e42539
69. Koban I, Geisel MH, Holtfrete B, Jablonowski L, Hübner N-O, Matthes R, Masur K, Weltmann K-D, Kramer A, Kocher T. 2013. Synergistic Effects of Nonthermal Plasma and Disinfecting Agents against Dental Biofilms In Vitro. *ISRN Dentistry* 2013: 1-10
70. Boxhammer V, Li YF, Koritzer J, Shimizu T, Maisch T, Thomas HM, Schlegel J, Morfill GE, Zimmermann JL. 2013. Investigation of the mutagenic potential of cold atmospheric plasma at bactericidal dosages. *Mutat Res* 753: 23-28
71. Jatsch L. Etablierung eines HPRT-Genmutationstests in V79-Zellen für die Untersuchung von Atmosphärendruck-Niedertemperaturplasmen (diploma thesis). University of Greifswald: Leibniz Institute for Plasma and Technology; 2013. 56 p.
72. Metelmann H-R, Vu TT, Do HT, Le TNB, Hoang THA, Phi TTT, Luong TML, Doan VT, Nguyen TTH, Nguyen THM. 2013. Scar formation of laser skin lesions after cold atmospheric pressure plasma (CAP) treatment: A clinical long term observation. *Clinical Plasma Medicine* 1: 30-35
73. Weltmann KD, Kindel E, Brandenburg R, Meyer C, Bussiahn R, Wilke C, von Woedtke T. 2009. Atmospheric Pressure Plasma Jet for Medical Therapy: Plasma Parameters and Risk Estimation. *Contributions to Plasma Physics* 49: 631-640
74. Reuter S, Winter J, Iseni S, Peters S, Schmidt-Bleker A, Dünnbier M, Schäfer J, Foest R, Weltmann K-D. 2012. Detection of ozone in a MHz argon plasma bullet jet. *Plasma Sources Science and Technology* 21: 034015
75. Weltmann K, von Woedtke T. 2011. Basic requirements for plasma sources in medicine. *European Physical Journal - Applied Physics* 55: 13807
76. Reuter S, Winter J, Schmidt-Bleker A, Tresp H, Hammer MU, Weltmann KD. 2012. Controlling the Ambient Air Affected Reactive Species Composition in the Effluent of an Argon Plasma Jet. *Ieee Transactions on Plasma Science* 40: 2788-2794
77. Schmidt-Bleker A, Winter J, Iseni S, Dünnbier M, Weltmann K, Reuter S. 2014. Reactive species output of a plasma jet with a shielding gas device—combination of FTIR absorption spectroscopy and gas phase modelling. *Journal of Physics D: Applied Physics* 47: 145201
78. Winter J, Wende K, Masur K, Iseni S, Dünnbier M, Hammer MU, Tresp H, Weltmann KD, Reuter S. 2013. Feed gas humidity: a vital parameter affecting a cold atmospheric-pressure plasma jet and plasma-treated human skin cells. *Journal of Physics D-Applied Physics* 46: 295401
79. Fridman G, Friedman G, Gutsol A, Shekhter AB, Vasilets VN, Fridman A. 2008. Applied plasma medicine. *Plasma Processes and Polymers* 5: 503-533
80. Pipa A, Reuter S, Foest R, Weltmann K. 2012. Controlling the NO production of an atmospheric pressure plasma jet. *Journal of Physics D: Applied Physics* 45: 085201
81. Verreycken T, Mensink R, Horst Rvd, Sadeghi N, Bruggeman PJ. 2013. Absolute OH density measurements in the effluent of a cold atmospheric-pressure Ar–H₂O RF plasma jet in air. *Plasma Sources Science and Technology* 22: 055014
82. Bruce RL, Kai-Yuan S. 2011. Review of the methods to form hydrogen peroxide in electrical discharge plasma with liquid water. *Plasma Sources Science and Technology* 20: 034006
83. Winterbourn CC. 2014. The challenges of using fluorescent probes to detect and quantify specific reactive oxygen species in living cells. *Biochim Biophys Acta* 1840: 730-738

84. Lange H, Foest R, Schafer J, Weltmann KD. 2009. Vacuum UV Radiation of a Plasma Jet Operated With Rare Gases at Atmospheric Pressure. *IEEE Transactions on Plasma Science* 37: 859-865
85. Reuter S, Niemi K, Gathen VS-vd, Döbele H. 2009. Generation of atomic oxygen in the effluent of an atmospheric pressure plasma jet. *Plasma Sources Science and Technology* 18: 015006
86. Daeschlein G, von Woedtke T, Kindel E, Brandenburg R, Weltmann KD, Junger M. 2010. Antibacterial Activity of an Atmospheric Pressure Plasma Jet Against Relevant Wound Pathogens in vitro on a Simulated Wound Environment. *Plasma Processes and Polymers* 7: 224-230
87. Winter T, Winter J, Polak M, Kusch K, Mäder U, Sietmann R, Ehlbeck J, van Hijum S, Weltmann K-D, Hecker M, Kusch H. 2011. Characterization of the global impact of low temperature gas plasma on vegetative microorganisms. *Proteomics* 11: 3518-3530
88. Wende K, Reuter S, von Woedtke T, Weltmann KD, Masur K. 2014. Redox-Based Assay for Assessment of Biological Impact of Plasma Treatment. *Plasma Processes and Polymers* 11: 655-663
89. Wende K, Straßburg S, Haertel B, Harms M, Holtz S, Barton A, Masur K, von Woedtke T, Lindequist U. 2014. Atmospheric pressure plasma jet treatment evokes transient oxidative stress in HaCaT keratinocytes and influences cell physiology. *Cell Biology International* 38: 412-425
90. Schmidt A, Wende K, Bekeschus S, Bundscherer L, Barton A, Ottmüller K, Weltmann KD, Masur K. 2013. Non-thermal plasma treatment is associated with changes in transcriptome of human epithelial skin cells. *Free Radical Research* 47: 577-592
91. Wende K, Barton A, Bekeschus S, Bundscherer L, Schmidt A, Weltmann KD, Masur K. 2013. Proteomic tools to characterize non-thermal plasma effects in eukaryotic cells. *Plasma Med* 3: 81-95
92. Bender C, Matthes R, Kindel E, Kramer A, Lademann J, Weltmann KD, Eisenbeiss W, Hubner NO. 2010. The Irritation Potential of Nonthermal Atmospheric Pressure Plasma in the HET-CAM. *Plasma Processes and Polymers* 7: 318-326
93. Bender C, Partecke LI, Kindel E, Döring F, Lademann J, Heidecke CD, Kramer A, Hubner NO. 2011. The modified HET-CAM as a model for the assessment of the inflammatory response to tissue tolerable plasma. *Toxicol In Vitro* 25: 530-537
94. Partecke L, Evert K, Haug J, Doering F, Normann L, Diedrich S, Weiss F-U, Evert M, Huebner N, Guenther C, Heidecke C, Kramer A, Bussiahn R, Weltmann K-D, Pati O, Bender C, von Bernstorff W. 2012. Tissue tolerable plasma (TTP) induces apoptosis in pancreatic cancer cells in vitro and in vivo. *BMC Cancer* 12: 473-482
95. Lademann J, Richter H, Patzelt A, Meinke MC, Fluhr JW, Kramer A, Weltmann K-D, Lademann O. Antisepsis of the Skin by Treatment with Tissue-Tolerable Plasma (TTP): Risk Assessment and Perspectives. *Plasma for Bio-Decontamination, Medicine and Food Security*: Springer; 2012. p 281-291.
96. Lademann J, Ulrich C, Patzelt A, Richter H, Kluschke F, Klebes M, Lademann O, Kramer A, Weltmann K, Lange-Asschenfeldt B. 2013. Risk assessment of the application of tissue-tolerable plasma on human skin. *Clinical Plasma Medicine* 1: 5-10
97. Metelmann HR, von Woedtke T, Bussiahn R, Weltmann KD, Rieck M, Khalili R, Podmelle F, Waite PD. 2012. Experimental Recovery of CO₂-Laser Skin Lesions by Plasma Stimulation. *American Journal of Cosmetic Surgery* 29: 52-56
98. Shi XM, Zhang GJ, Yuan YK, Ma Y, Xu GM, Yang Y. 2008. Effects of Low-Temperature Atmospheric Air Plasmas on the Activity and Function of Human Lymphocytes. *Plasma Processes and Polymers* 5: 482-488
99. Abbas AK, Lichtman AH, Pillai S. Cellular and Molecular Immunology. Elsevier Health Sciences; 2011.
100. Murphy KM, Travers W, Walport M. Janeway's Immuno Biology. Garland W, editor. New York, London: Garland Science; 2012.
101. Schütt C, Bröker B. Grundwissen Immunologie. Spektrum-Akademischer Vlg; 2009.
102. Autissier P, Soulas C, Burdo TH, Williams KC. 2010. Evaluation of a 12-color flow cytometry panel to study lymphocyte, monocyte, and dendritic cell subsets in humans. *Cytometry A* 77: 410-419
103. Ziegler-Heitbrock H. 2000. Definition of human blood monocytes. *Journal of Leukocyte Biology* 67: 603-606
104. Adamson R. 2009. Role of macrophages in normal wound healing: an overview. *J Wound Care* 18: 349-351
105. Schütt C, Schilling T, Krüger C. 1991. sCD14 prevents endotoxin inducible oxidative burst response of human monocytes. *Allergie und Immunologie* 37: 159-164
106. Kantari C, Pederzoli-Ribeil M, Witko-Sarsat V. 2008. The Role of Neutrophils and Monocytes in Innate Immunity. *Trends in Innate Immunology* 15: 118-146

References

107. Toulon A, Breton L, Taylor KR, Tenenhaus M, Bhavsar D, Lanigan C, Rudolph R, Jameson J, Havran WL. 2009. A role for human skin-resident T cells in wound healing. *The Journal of Experimental Medicine* 206: 743-750
108. Nakayamada S, Takahashi H, Kanno Y, O'Shea JJ. 2012. Helper T cell diversity and plasticity. *Current Opinion in Immunology* 24: 297-302
109. Michie CA, McLean A, Alcock C, Beverley PC. 1992. Lifespan of human lymphocyte subsets defined by CD45 isoforms. *Nature* 360: 264-265
110. Kaibuchi K, Takai Y, Nishizuka Y. 1985. Protein kinase C and calcium ion in mitogenic response of macrophage-depleted human peripheral lymphocytes. *Journal of Biological Chemistry* 260: 1366-1369
111. Hilchey SP, Bernstein SH. 2007. Use of CFSE to monitor ex vivo regulatory T-cell suppression of CD4+ and CD8+ T-cell proliferation within unseparated mononuclear cells from malignant and non-malignant human lymph node biopsies. *Immunol Invest* 36: 629-648
112. Schoenberger S, Toes R, van der Voort E, Offringa R, Melief C. 1998. T-cell help for cytotoxic T lymphocytes is mediated by CD40-CD40L interactions. *Nature* 393: 480-483
113. Vivier E, Tomasello E, Baratin M, Walzer T, Ugolini S. 2008. Functions of natural killer cells. *Nature Immunology* 9: 503-510
114. Dancey JT, Deubelbeiss KA, Harker LA, Finch CA. 1976. Neutrophil kinetics in man. *J Clin Invest* 58: 705-715
115. Lapinet JA, Scapini P, Calzetti F, Pérez O, Cassatella MA. 2000. Gene expression and production of tumor necrosis factor alpha, interleukin-1 β (IL-1 β), IL-8, macrophage inflammatory protein 1 α (MIP-1 α), MIP-1 β , and gamma interferon-inducible protein 10 by human neutrophils stimulated with group B meningococcal outer membrane vesicles. *Infection and Immunity* 68: 6917-6923
116. Yamashiro S, Kamohara H, Wang J-M, Yang D, Gong W-H, Yoshimura T. 2001. Phenotypic and functional change of cytokine-activated neutrophils: inflammatory neutrophils are heterogeneous and enhance adaptive immune responses. *Journal of Leukocyte Biology* 69: 698-704
117. Ley K. 2002. Integration of inflammatory signals by rolling neutrophils. *Immunological Reviews* 186: 8-18
118. Faurschou M, Borregaard N. 2003. Neutrophil granules and secretory vesicles in inflammation. *Microbes Infect* 5: 1317-1327
119. Lacy P. 2005. The role of Rho GTPases and SNAREs in mediator release from granulocytes. *Pharmacology and Therapeutics* 107: 358-376
120. Nüsse O, Lindau M. 1988. The dynamics of exocytosis in human neutrophils. *The Journal of Cell Biology* 107: 2117-2123
121. Amulic B, Cazalet C, Hayes GL, Metzler KD, Zychlinsky A. 2012. Neutrophil function: from mechanisms to disease. *Annu Rev Immunol* 30: 459-489
122. Hampton MB, Kettle AJ, Winterbourn CC. 1998. Inside the neutrophil phagosome: oxidants, myeloperoxidase, and bacterial killing. *Blood* 92: 3007-3017
123. Prokopowicz Z, Marcinkiewicz J, Katz D, Chain B. 2012. Neutrophil Myeloperoxidase: Soldier and Statesman. *Archivum Immunologiae et Therapia Experimentalis* 60: 43-54
124. Winterbourn CC, Hampton MB, Livesey JH, Kettle AJ. 2006. Modeling the Reactions of Superoxide and Myeloperoxidase in the Neutrophil Phagosome IMPLICATIONS FOR MICROBIAL KILLING. *Journal of Biological Chemistry* 281: 39860-39869
125. Bianchi M, Hakkim A, Brinkmann V, Siler U, Seger RA, Zychlinsky A, Reichenbach J. 2009. Restoration of NET formation by gene therapy in CGD controls aspergillosis. *Blood* 114: 2619-2622
126. Kobayashi SD, Voyich JM, Buhl CL, Stahl RM, DeLeo FR. 2002. Global changes in gene expression by human polymorphonuclear leukocytes during receptor-mediated phagocytosis: cell fate is regulated at the level of gene expression. *Proceedings of the National Academy of Sciences* 99: 6901-6906
127. Romani L, Mencacci A, Cenci E, Spaccapelo R, Del Sero G, Nicoletti I, Trinchieri G, Bistoni F, Puccetti P. 1997. Neutrophil production of IL-12 and IL-10 in candidiasis and efficacy of IL-12 therapy in neutropenic mice. *The Journal of Immunology* 158: 5349-5356
128. Ellis TN, Beaman BL. 2004. Interferon-gamma activation of polymorphonuclear neutrophil function. *Immunology* 112: 2-12
129. Radsak M, Iking-Konert C, Stegmaier S, Andrassy K, Hänsch G. 2000. Polymorphonuclear neutrophils as accessory cells for T-cell activation: major histocompatibility complex class II restricted antigen-dependent induction of T-cell proliferation. *Immunology* 101: 521-530

130. Beauvillain C, Delneste Y, Scotet M, Peres A, Gascan H, Guernonprez P, Barnaba V, Jeannin P. 2007. Neutrophils efficiently cross-prime naive T cells in vivo. *Blood* 110: 2965-2973
131. Brinkmann V, Reichard U, Goosmann C, Fauler B, Uhlemann Y, Weiss DS, Weinrauch Y, Zychlinsky A. 2004. Neutrophil extracellular traps kill bacteria. *Science* 303: 1532-1535
132. Yousefi S, Mihalache C, Kozlowski E, Schmid I, Simon H. 2009. Viable neutrophils release mitochondrial DNA to form neutrophil extracellular traps. *Cell Death & Differentiation* 16: 1438-1444
133. Urban CF, Ermert D, Schmid M, Abu-Abed U, Goosmann C, Nacken W, Brinkmann V, Jungblut PR, Zychlinsky A. 2009. Neutrophil extracellular traps contain calprotectin, a cytosolic protein complex involved in host defense against *Candida albicans*. *Plos Pathogens* 5: e1000639
134. Fuchs TA, Abed U, Goosmann C, Hurwitz R, Schulze I, Wahn V, Weinrauch Y, Brinkmann V, Zychlinsky A. 2007. Novel cell death program leads to neutrophil extracellular traps. *J Cell Biol* 176: 231-241
135. Metzler KD, Fuchs TA, Nauseef WM, Reumaux D, Roesler J, Schulze I, Wahn V, Papayannopoulos V, Zychlinsky A. 2011. Myeloperoxidase is required for neutrophil extracellular trap formation: implications for innate immunity. *Blood* 117: 953-959
136. Papayannopoulos V, Metzler KD, Hakkim A, Zychlinsky A. 2010. Neutrophil elastase and myeloperoxidase regulate the formation of neutrophil extracellular traps. *J Cell Biol* 191: 677-691
137. Farley K, Stolley JM, Zhao P, Cooley J, Remold-O'Donnell E. 2012. A serpinB1 regulatory mechanism is essential for restricting neutrophil extracellular trap generation. *J Immunol* 189: 4574-4581
138. Beiter K, Wartha F, Albiger B, Normark S, Zychlinsky A, Henriques-Normark B. 2006. An endonuclease allows *Streptococcus pneumoniae* to escape from neutrophil extracellular traps. *Curr Biol* 16: 401-407
139. Brinkmann V, Zychlinsky A. 2007. Beneficial suicide: why neutrophils die to make NETs. *Nat Rev Microbiol* 5: 577-582
140. Kennedy AD, DeLeo FR. 2009. Neutrophil apoptosis and the resolution of infection. *Journal of Immunological Research* 43: 25-61
141. Fuchs TA, Brill A, Duerschmied D, Schatzberg D, Monestier M, Myers DD, Jr., Wroblewski SK, Wakefield TW, Hartwig JH, Wagner DD. 2010. Extracellular DNA traps promote thrombosis. *Proc Natl Acad Sci U S A* 107: 15880-15885
142. Guo S, Dipietro LA. 2010. Factors affecting wound healing. *J Dent Res* 89: 219-229
143. Witte MB, Barbul A. 1997. General principles of wound healing. *Surgical Clinics of North America* 77: 509-528
144. Hattori K, Heissig B, Wu Y, Dias S, Tejada R, Ferris B, Hicklin D, Zhu Z, Bohlen P, Witte L, Hendriks J, Hackett N, Crystal R, Moore M, Werb Z, Lyden D, Rafii S. 2002. Placental growth factor reconstitutes hematopoiesis by recruiting VEGFR1(1) stem cells from bone-marrow micro-environment. *Nature Medicine* 8: 841-849
145. Raja S, MS G, Isseroff R. 2007. Wound reepithelialization: modulating keratinocyte migration in wound healing. *Frontiers in Bioscience* 12: 2849-2868
146. Wu WK, Llewellyn OPC, Bates DO, Nicholson LB, Dick AD. 2010. IL-10 regulation of macrophage VEGF production is dependent on macrophage polarisation and hypoxia. *Immunobiology* 215: 796-803
147. Park JE, Barbul A. 2004. Understanding the role of immune regulation in wound healing. *Am J Surg* 187: 11S-16S
148. Swift ME, Burns AL, Gray KL, DiPietro LA. 2001. Age-related alterations in the inflammatory response to dermal injury. *Journal of Investigative Dermatology* 117: 1027-1035
149. Jameson JM, Sharp LL, Witherden DA, Havran WL. 2004. Regulation of skin cell homeostasis by gamma delta T cells. *Frontiers in Bioscience* 9: 2640-2651
150. Epstein FH, Singer AJ, Clark RAF. 1999. Cutaneous wound healing. *The New England Journal of Medicine* 341: 738-746
151. Menke NB, Ward KR, Witten TM, Bonchev DG, Diegelmann RF. 2007. Impaired wound healing. *Clin Dermatol* 25: 19-25
152. Nwomeh BC, Yager DR, Cohen IK. 1998. Physiology of the chronic wound. *Clin Plast Surg* 25: 341-356
153. Lazarus G, Cooper DM, Knighton DR, David JM, Roger EP, George R. 1994. Definitions and guidelines for assessment of wounds and evaluation of healing. *Archives of Dermatology* 130: 489-493

References

154. Loots MA, Kenter SB, Au FL, Van Galen W, Middelkoop E, Bos JD, Mekkes JR. 2002. Fibroblasts derived from chronic diabetic ulcers differ in their response to stimulation with EGF, IGF-I, bFGF and PDGF-AB compared to controls. *European Journal of Cell Biology* 81: 153-160
155. Bowler PG. 2002. Wound pathophysiology, infection and therapeutic options. *Ann Med* 34: 419-427
156. Diegelmann RF. 2003. Excessive neutrophils characterize chronic pressure ulcers. *Wound Repair Regen* 11: 490-495
157. Tarnuzzer RW, Schultz GS. 1996. Biochemical analysis of acute and chronic wound environments. *Wound Repair and Regeneration* 4: 321-325
158. Wallace H, Stacey M. 1998. Levels of tumor necrosis factor-alpha (TNF-alpha) and soluble TNF receptors in chronic venous leg ulcers—correlations to healing status. *Journal of Investigative Dermatology* 110: 292-296
159. Wetzler C, Kämpfer H, Stallmeyer B, Pfeilschifter J, Frank S. 2000. Large and sustained induction of chemokines during impaired wound healing in the genetically diabetic mouse: prolonged persistence of neutrophils and macrophages during the late phase of repair. *Journal of Investigative Dermatology* 115: 245-253
160. Barrientos S, Stojadinovic O, Golinko MS, Brem H, Tomic-Canic M. 2008. Growth factors and cytokines in wound healing. *Wound Repair Regen* 16: 585-601
161. Baumgartner I, Pieczek A, Manor O, Blair R, Kearney M, Walsh K, Isner JM. 1998. Constitutive expression of phVEGF165 after intramuscular gene transfer promotes collateral vessel development in patients with critical limb ischemia. *Circulation* 97: 1114-1123
162. Falanga V. 2005. Wound healing and its impairment in the diabetic foot. *Lancet* 366: 1736-1743
163. Renner R, Sticherling M, Ruger R, Simon J. 2012. Persistence of bacteria like *Pseudomonas aeruginosa* in non-healing venous ulcers. *European Journal of Dermatology* 22: 751-757
164. Sibbald RG, Coutts P, Woo KY. 2011. Reduction of bacterial burden and pain in chronic wounds using a new polyhexamethylene biguanide antimicrobial foam dressing—clinical trial results. *Advances in Skin and Wound Care* 24: 78-84
165. Emmert S, Brehmer F, Hänßle H, Helmke A, Mertens N, Ahmed R, Simon D, Wandke D, Maus-Friedrichs W, Däschlein G. 2013. Atmospheric pressure plasma in dermatology: ulcer treatment and much more. *Clinical Plasma Medicine* 1: 24-29
166. Isbary G, Zimmermann J, Shimizu T, Li Y-F, Morfill G, Thomas H, Steffes B, Heinlin J, Karrer S, Stolz W. 2013. Non-thermal plasma—More than five years of clinical experience. *Clinical Plasma Medicine* 1: 19-23
167. Harvey L, Arnold B, Kaiser Chris A, Monty K. Molecular cell biology. WH Freeman; 2008.
168. Ozaki K, Leonard WJ. 2002. Cytokine and cytokine receptor pleiotropy and redundancy. *Journal of Biological Chemistry* 277: 29355-29358
169. Klotz L-O. 2002. Oxidant-induced signaling: effects of peroxynitrite and singlet oxygen. *Biological Chemistry* 383: 443-456
170. Davies KJ. 2000. An overview of oxidative stress. *IUBMB Life* 50: 241-244
171. Sen CK, Roy S. 2008. Redox signals in wound healing. *Biochim Biophys Acta* 1780: 1348-1361
172. Wlaschek M, Scharffetter-Kochanek K. 2005. Oxidative stress in chronic venous leg ulcers. *Wound Repair Regen* 13: 452-461
173. D'Autréaux B, Toledano MB. 2007. ROS as signalling molecules: mechanisms that generate specificity in ROS homeostasis. *Nature Reviews Molecular Cell Biology* 8: 813-824
174. Lisanti MP, Martinez-Outschoorn UE, Lin Z, Pavlides S, Whitaker-Menezes D, Pestell RG, Howell A, Sotgia F. 2011. Hydrogen peroxide fuels aging, inflammation, cancer metabolism and metastasis: the seed and soil also needs "fertilizer". *Cell Cycle* 10: 2440-2449
175. Toren F. 2003. Oxidant signals and oxidative stress. *Current Opinion in Cell Biology* 15: 247-254
176. Circu ML, Aw TY. 2010. Reactive oxygen species, cellular redox systems, and apoptosis. *Free Radic Biol Med* 48: 749-762
177. Schäfer M, Werner S. 2008. Oxidative stress in normal and impaired wound repair. *Pharmacological Research* 58: 165-171
178. Gupta A, Singh RL, Raghubir R. 2002. Antioxidant status during cutaneous wound healing in immunocompromised rats. *Mol Cell Biochem* 241: 1-7

179. Roy S, Khanna S, Nallu K, Hunt TK, Sen CK. 2006. Dermal wound healing is subject to redox control. *Molecular Therapy* 13: 211-220
180. Edinger AL, Thompson CB. 2004. Death by design: apoptosis, necrosis and autophagy. *Curr Opin Cell Biol* 16: 663-669
181. Galluzzi L, Vitale I, Abrams JM, Alnemri ES, Baehrecke EH, Blagosklonny MV, Dawson TM, Dawson VL, El-Deiry WS, Fulda S, Gottlieb E, Green DR, Hengartner MO, Kepp O, Knight RA, Kumar S, Lipton SA, Lu X, Madeo F, Malorni W, Mehlen P, Nunez G, Peter ME, Piacentini M, Rubinsztein DC, Shi Y, Simon HU, Vandenabeele P, White E, Yuan J, Zhivotovsky B, Melino G, Kroemer G. 2012. Molecular definitions of cell death subroutines: recommendations of the Nomenclature Committee on Cell Death 2012. *Cell Death Differ* 19: 107-120
182. Remijsen Q, Kuijpers TW, Wirawan E, Lippens S, Vandenabeele P, Vanden Berghe T. 2011. Dying for a cause: NETosis, mechanisms behind an antimicrobial cell death modality. *Cell Death and Differentiation* 18: 581-588
183. Mohanty J, Jaffe JS, Schulman ES, Raible DG. 1997. A highly sensitive fluorescent micro-assay of H₂O₂ release from activated human leukocytes using a dihydroxyphenoxazine derivative. *Journal of Immunological Methods* 202: 133-141
184. Miller RW, Massey V. 1965. Dihydroorotic Dehydrogenase. II. Oxidation and Reduction of Cytochrome C. *J Biol Chem* 240: 1466-1472
185. Bekeschus S, Kolata J, Winterbourn C, Kramer A, Turner R, Weltmann KD, Broker B, Masur K. 2014. Hydrogen peroxide: A central player in physical plasma-induced oxidative stress in human blood cells. *Free Radic Res* 48: 542-549
186. Shapiro HM. Practical flow cytometry. John Wiley & Sons; 2005.
187. Böyum A. 1968. Separation of leucocytes from blood and bone marrow. *Scandinavian Journal of Clinical and Laboratory Investigations* 97: 77-81
188. Koopman G, Reutelingsperger C, Kuijten G, Keehnen R, Pals S, Van Oers M. 1994. Annexin V for flow cytometric detection of phosphatidylserine expression on B cells undergoing apoptosis. *Blood* 84: 1415-1420
189. Setsukinai K, Urano Y, Kakinuma K, Majima HJ, Nagano T. 2003. Development of novel fluorescence probes that can reliably detect reactive oxygen species and distinguish specific species. *J Biol Chem* 278: 3170-3175
190. Zielonka J, Kalyanaraman B. 2010. Hydroethidine-and MitoSOX-derived red fluorescence is not a reliable indicator of intracellular superoxide formation: another inconvenient truth. *Free Radical Biology and Medicine* 48: 983-1001
191. Salvioi S, Ardizzoni A, Franceschi C, Cossarizza A. 1997. JC-1, but not DiOC₆ (3) or rhodamine 123, is a reliable fluorescent probe to assess $\Delta\Psi$ changes in intact cells: implications for studies on mitochondrial functionality during apoptosis. *FEBS Letters* 411: 77-82
192. Bekeschus S, von Woedtke T, Kramer A, Weltmann K-D, Masur K. 2013. Cold Physical Plasma Treatment Alters Redox Balance in Human Immune Cells. *Plasma Medicine* 3: 267-278
193. Bekeschus S, Kolata J, Muller A, Kramer A, Weltmann K-D, Broker B, Masur K. 2013. Differential Viability of Eight Human Blood Mononuclear Cell Subpopulations After Plasma Treatment. *Plasma Medicine* 3: 1-13
194. Bekeschus S, Masur K, Kolata J, Wende K, Schmidt A, Bundscherer L, Barton A, Kramer A, Broker B, Weltmann KD. 2013. Human Mononuclear Cell Survival and Proliferation is Modulated by Cold Atmospheric Plasma Jet. *Plasma Processes and Polymers* 10: 706-713
195. Bekeschus S, Iséni S, Reuter S, Weltmann K, Masur K. 2015. Nitrogen Shielding of an Argon Plasma Jet and its Effects on Human Immune Cells. *IEEE Transactions on Plasma Science* 43: 776-781
196. Hoentsch M, Bussiahn R, Rebl H, Bergemann C, Eggert M, Frank M, von Woedtke T, Nebe B. 2014. Persistent effectivity of gas plasma-treated, long time-stored liquid on epithelial cell adhesion capacity and membrane morphology. *PLoS One* 9: e104559
197. Winter J, Tresp H, Hammer MU, Iseni S, Kupsch S, Schmidt-Bleker A, Wende K, Dunnbier M, Masur K, Weltmann KD, Reuter S. 2014. Tracking plasma generated H₂O₂ from gas into liquid phase and revealing its dominant impact on human skin cells. *J Phys D Appl Phys* 47: 285401
198. Bruggeman P, Schram DC. 2010. On OH production in water containing atmospheric pressure plasmas. *Plasma Sources Science & Technology* 19: 045025
199. Stuehr D, Marletta M. 1987. Induction of nitrite/nitrate synthesis in murine macrophages by BCG infection, lymphokines, or interferon-gamma. *The Journal of Immunology* 139: 518-525
200. Lundberg JO, Weitzberg E, Gladwin MT. 2008. The nitrate–nitrite–nitric oxide pathway in physiology and therapeutics. *Nature Reviews Drug Discovery* 7: 156-167

References

201. Witte MB, Barbul A. 2002. Role of nitric oxide in wound repair. *The American Journal of Surgery* 183: 406-412
202. Davies MJ. 2011. Myeloperoxidase-derived oxidation: mechanisms of biological damage and its prevention. *J Clin Biochem Nutr* 48: 8-19
203. Palmer RM, Ferrige A, Moncada S. 1987. Nitric oxide release accounts for the biological activity of endothelium-derived relaxing factor. *Nature* 327: 524-526
204. Reuter S, Wende K, Winter J, Blackert S, Harms M, Masur K, Schulz-von der Gathen V, Woedtke Tv, Weltmann K. Formation of reactive oxygen species (ROS) and their effect on DNA. Presented at 20th International Conference on Plasma Chemistry, Philadelphia, USA 2011;27.
205. Pacher P, Beckman JS, Liaudet L. 2007. Nitric Oxide and Peroxynitrite in Health and Disease. *Physiological Reviews* 87: 315-424
206. Beckman JS, Beckman TW, Chen J, Marshall PA, Freeman BA. 1990. Apparent hydroxyl radical production by peroxynitrite: implications for endothelial injury from nitric oxide and superoxide. *Proc Natl Acad Sci U S A* 87: 1620-1624
207. Tresp H, Hammer MU, Weltmann K-D, Reuter S. 2014. Effects of atmosphere composition and liquid type on plasma generated reactive species in biologically relevant solutions. *Plasma Med* 3: 45-55
208. Tian W, Kushner MJ. 2014. Atmospheric pressure dielectric barrier discharges interacting with liquid covered tissue. *Journal of Physics D: Applied Physics* 47: 165201
209. Starke P, Farber J. 1985. Ferric iron and superoxide ions are required for the killing of cultured hepatocytes by hydrogen peroxide. Evidence for the participation of hydroxyl radicals formed by an iron-catalyzed Haber-Weiss reaction. *Journal of Biological Chemistry* 260: 10099-10104
210. Nauser T, Koppenol W, Gebicki J. 2005. The kinetics of oxidation of GSH by protein radicals. *Biochemical Journal* 392: 693-701
211. Ciriolo MR, Palamara AT, Incerpi S, Lafavia E, Bue MC, DeVito P, Garaci E, Rotilio G. 1997. Loss of GSH, oxidative stress, and decrease of intracellular pH as sequential steps in viral infection. *Journal of Biological Chemistry* 272: 2700-2708
212. Hampton MB, Orrenius S. 1998. Redox regulation of apoptotic cell death in the immune system. *Toxicol Lett* 102-103: 355-358
213. Mandavilli BS, Janes MS. Detection of Intracellular Glutathione Using ThiolTracker Violet Stain and Fluorescence Microscopy. *Current Protocols in Cytometry*: John Wiley & Sons, Inc.; 2001.
214. Thorén FB, Betten Å, Romero AI, Hellstrand K. 2007. Cutting Edge: Antioxidative Properties of Myeloid Dendritic Cells: Protection of T Cells and NK Cells from Oxygen Radical-Induced Inactivation and Apoptosis. *The Journal of Immunology* 179: 21-25
215. Hyde H, Borthwick NJ, Janossy G, Salmon M, Akbar AN. 1997. Upregulation of intracellular glutathione by fibroblast-derived factor(s): enhanced survival of activated T cells in the presence of low Bcl-2. *Blood* 89: 2453-2460
216. Townsend DM, Tew KD, Tapiero H. 2003. The importance of glutathione in human disease. *Biomedicine & Pharmacotherapy* 57: 145-155
217. Suthanthiran M, Anderson ME, Sharma VK, Meister A. 1990. Glutathione regulates activation-dependent DNA synthesis in highly purified normal human T lymphocytes stimulated via the CD2 and CD3 antigens. *Proceedings of the National Academy of Sciences* 87: 3343-3347
218. Drummen GPC, van Liebergen LCM, Op den Kamp JAF, Post JA. 2002. C11-BODIPY581/591, an oxidation-sensitive fluorescent lipid peroxidation probe: (micro)spectroscopic characterization and validation of methodology. *Free Radical Biology and Medicine* 33: 473-490
219. Halliwell B, Chirico S. 1993. Lipid peroxidation: its mechanism, measurement and significance. *American Journal of Clinical Nutrition* 57: 715-725
220. Azenabor AA, Hoffman-Goetz L. 1999. Intrathymic and intrasplenic oxidative stress mediates thymocyte and splenocyte damage in acutely exercised mice. *J Appl Physiol* (1985) 86: 1823-1827
221. Dix TA, Aikens J. 1993. Mechanisms and biological relevance of lipid peroxidation initiation. *Chem Res Toxicol* 6: 2-18
222. Boulton S, Anderson A, Swalwell H, Henderson JR, Manning P, Birch-Machin MA. 2011. Implications of using the fluorescent probes, dihydrorhodamine 123 and 2',7'-dichlorodihydrofluorescein diacetate, for the detection of UVA-induced reactive oxygen species. *Free Radic Res* 45: 139-146

223. Leduc M, Guay D, Leask R, Coulombe S. 2009. Cell permeabilization using a non-thermal plasma. *New Journal of Physics* 11: 115021-115034
224. Franco R, Cidlowski JA. 2009. Apoptosis and glutathione: beyond an antioxidant. *Cell Death Differ* 16: 1303-1314
225. Lu M, Gong X. 2009. Upstream reactive oxidative species (ROS) signals in exogenous oxidative stress-induced mitochondrial dysfunction. *Cell Biology International* 33: 658-664
226. Leist M, Single B, Castoldi AF, Kühnle S, Nicotera P. 1997. Intracellular adenosine triphosphate (ATP) concentration: a switch in the decision between apoptosis and necrosis. *The Journal of Experimental Medicine* 185: 1481-1486
227. Porter AG, Jänicke RU. 1999. Emerging roles of caspase-3 in apoptosis. *Cell Death and Differentiation* 6: 99-104
228. Hampton MB, Orrenius S. 1997. Dual regulation of caspase activity by hydrogen peroxide: implications for apoptosis. *FEBS Lett* 414: 552-556
229. Rimon G, Bazenet CE, Philpott KL, Rubin LL. 1997. Increased surface phosphatidylserine is an early marker of neuronal apoptosis. *Journal of Neuroscience Research* 48: 563-570
230. Agaiby AD, Dyson M. 1999. Immuno-inflammatory cell dynamics during cutaneous wound healing. *J Anat* 195 (Pt 4): 531-542
231. Loots MA, Lamme EN, Zeegelaar J, Mekkes JR, Bos JD, Middelkoop E. 1998. Differences in cellular infiltrate and extracellular matrix of chronic diabetic and venous ulcers versus acute wounds. *J Invest Dermatol* 111: 850-857
232. Jameson J, Ugarte K, Chen N, Yachi P, Fuchs E, Boismenu R, Havran WL. 2002. A role for skin $\gamma\delta$ T cells in wound repair. *Science* 296: 747-749
233. Mahdavian Delavary B, van der Veer WM, van Egmond M, Niessen FB, Beelen RH. 2011. Macrophages in skin injury and repair. *Immunobiology* 216: 753-762
234. Gertner J, Wiedemann A, Poupot M, Fournie JJ. 2007. Human gamma delta T lymphocytes strip and kill tumor cells simultaneously. *Immunology Letters* 110: 42-53
235. Assimakopoulos SF, Vagianos CE, Patsoukis N, Georgiou C, Nikolopoulou V, Scopa CD. 2004. Evidence for intestinal oxidative stress in obstructive jaundice-induced gut barrier dysfunction in rats. *Acta Physiol Scand* 180: 177-185
236. Bickers DR, Athar M. 2006. Oxidative stress in the pathogenesis of skin disease. *J Invest Dermatol* 126: 2565-2575
237. Komori HK, Witherden DA, Kelly R, Sendaydiego K, Jameson JM, Teyton L, Havran WL. 2012. Cutting edge: dendritic epidermal $\gamma\delta$ T cell ligands are rapidly and locally expressed by keratinocytes following cutaneous wounding. *The Journal of Immunology* 188: 2972-2976
238. Havran WL, Jameson JM. 2010. Epidermal T cells and wound healing. *J Immunol* 184: 5423-5428
239. Janossy G, Greaves M. 1971. Lymphocyte activation: I. Response of T and B lymphocytes to phyto mitogens. *Clinical and Experimental Immunology* 9: 483
240. Holtfreter S, Broker BM. 2005. Staphylococcal superantigens: do they play a role in sepsis? *Arch Immunol Ther Exp (Warsz)* 53: 13-27
241. Remans P, Van Oosterhout M, Smeets T, Sanders M, Frederiks W, Reedquist K, Tak P, Breedveld F, Van Laar J. 2005. Intracellular free radical production in synovial T lymphocytes from patients with rheumatoid arthritis. *Arthritis & Rheumatism* 52: 2003-2009
242. Akbar AN, Borthwick NJ, Wickremasinghe RG, Panayiotidis P, Pilling D, Bofill M, Krajewski S, Reed JC, Salmon M. 1996. Interleukin-2 receptor common γ -chain signaling cytokines regulate activated T cell apoptosis in response to growth factor withdrawal: Selective induction of anti-apoptotic (bcl-2, bcl-xL) but not pro-apoptotic (bax, bcl-xS) gene expression. *European Journal of Immunology* 26: 294-299
243. Reddy M, Eirikis E, Davis C, Davis HM, Prabhakar U. 2004. Comparative analysis of lymphocyte activation marker expression and cytokine secretion profile in stimulated human peripheral blood mononuclear cell cultures: an in vitro model to monitor cellular immune function. *Journal of Immunological Methods* 293: 127-142
244. Mosmann TR, Coffman RL. 1989. TH1 and TH2 Cells: Different Patterns of Lymphokine Secretion Lead to Different Functional Properties. *Annual Review of Immunology* 7: 145-173
245. Fonseca AM, Porto G, Uchida K, Arosa FA. 2001. Red blood cells inhibit activation-induced cell death and oxidative stress in human peripheral blood T lymphocytes. *Blood* 97: 3152-3160

References

246. Bundscherer L, Wende K, Ottmuller K, Barton A, Schmidt A, Bekeschus S, Hasse S, Weltmann KD, Masur K, Lindequist U. 2013. Impact of non-thermal plasma treatment on MAPK signaling pathways of human immune cell lines. *Immunobiology* 218: 1248-1255
247. Davis PA, Corless DJ, Aspinall R, Wastell C. 2001. Effect of CD4(+) and CD8(+) cell depletion on wound healing. *Br J Surg* 88: 298-304
248. Bos J, Hagensaars C, Das P, Krieg S, Voorn W, Kapsenberg M. 1989. Predominance of "memory" T cells (CD4+, CDw29+) over "naive" T cells (CD4+, CD45R+) in both normal and diseased human skin. *Archives of Dermatological Research* 281: 24-30
249. Zhang D-s, Wang F, Wang G, Yang Y-p, Zhang L. 2009. Studying on Expression of CD45RA and CD45RO in the Psoriasis Vulgaris Skin Lesion. *Journal of Shenyang Medical College* 3: 018
250. Funatake CJ, Ao K, Suzuki T, Murai H, Yamamoto M, Fujii-Kuriyama Y, Kerkvliet NI, Nohara K. 2009. Expression of constitutively-active aryl hydrocarbon receptor in T-cells enhances the down-regulation of CD62L, but does not alter expression of CD25 or suppress the allogeneic CTL response. *Journal of Immunotoxicology* 6: 194-203
251. Egawa G, Kabashima K. 2011. Skin as a Peripheral Lymphoid Organ: Revisiting the Concept of Skin-Associated Lymphoid Tissues. *Journal of Investigative Dermatology* 131: 2178-2185
252. Malmberg K-J, Arulampalam V, Ichihara F, Petersson M, Seki K, Andersson T, Lenkei R, Masucci G, Pettersson S, Kiessling R. 2001. Inhibition of activated/memory (CD45RO+) T cells by oxidative stress associated with block of NF- κ B activation. *The Journal of Immunology* 167: 2595-2601
253. Gringhuis SI, Leow A, Papendrecht-van der Voort EAM, Remans PHJ, Breedveld FC, Verweij CL. 2000. Displacement of linker for activation of T cells from the plasma membrane due to redox balance alterations results in hyporesponsiveness of synovial fluid T lymphocytes in rheumatoid arthritis. *Journal of Immunology* 164: 2170-2179
254. Finnerty CC, Herndon DN, Przkora R, Pereira CT, Oliveira HM, Queiroz DM, Rocha AM, Jeschke MG. 2006. Cytokine expression profile over time in severely burned pediatric patients. *Shock* 26: 13-19
255. Mast BA, Schultz GS. 1996. Interactions of cytokines, growth factors, and proteases in acute and chronic wounds. *Wound Repair Regen* 4: 411-420
256. Hantash BM, Zhao L, Knowles JA, Lorenz HP. 2007. Adult and fetal wound healing. *Frontiers in bioscience: a journal and virtual library* 13: 51-61
257. Trengove NJ, Stacey MC, MacAuley S, Bennett N, Gibson J, Burslem F, Murphy G, Schultz G. 1999. Analysis of the acute and chronic wound environments: the role of proteases and their inhibitors. *Wound Repair and Regeneration* 7: 442-452
258. Barton A, Wende K, Bundscherer L, Hasse S, Schmidt A, Bekeschus S, Weltmann K, Lindequist U, Masur K. 2013. Non-thermal plasma increases expression of wound healing related genes in a keratinocyte cell line. *Plasma Med* 3: 125-136
259. Verhasselt V, Goldman M, Willems F. 1998. Oxidative stress up-regulates IL-8 and TNF- α synthesis by human dendritic cells. *European Journal of Immunology* 28: 3886-3890
260. Jozkowicz A, Was H, Taha H, Kotlinowski J, Mleczko K, Cisowski J, Weigel G, Dulak J. 2008. 15d-PGJ2 upregulates synthesis of IL-8 in endothelial cells through induction of oxidative stress. *Antioxidants & Redox Signaling* 10: 2035-2046
261. Müller I, Munder M, Kropf P, Hänsch GM. 2009. Polymorphonuclear neutrophils and T lymphocytes: strange bedfellows or brothers in arms? *Trends in Immunology* 30: 522-530
262. Taguchi M, Sampath D, Koga T, Castro M, Look DC, Nakajima S, Holtzman MJ. 1998. Patterns for RANTES secretion and intercellular adhesion molecule 1 expression mediate transepithelial T cell traffic based on analyses in vitro and in vivo. *The Journal of Experimental Medicine* 187: 1927-1940
263. Fiorentino DF, Zlotnik A, Mosmann TR, Howard M, O'Garra A. 1991. IL-10 inhibits cytokine production by activated macrophages. *J Immunol* 147: 3815-3822
264. Sánchez-Elsner T, Botella LM, Velasco B, Corbí A, Attisano L, Bernabéu C. 2001. Synergistic cooperation between hypoxia and transforming growth factor- β pathways on human vascular endothelial growth factor gene expression. *Journal of Biological Chemistry* 276: 38527-38535
265. Ishida Y, Gao J-L, Murphy PM. 2008. Chemokine receptor CX3CR1 mediates skin wound healing by promoting macrophage and fibroblast accumulation and function. *The Journal of Immunology* 180: 569-579
266. Cai H. 2005. Hydrogen peroxide regulation of endothelial function: origins, mechanisms, and consequences. *Cardiovasc Res* 68: 26-36

267. Tresp H, Bussiahn R, Bundscherer L, Monden A, Hammer M, Masur K, Weltmann K-D, Reuter S. 2014. Plasma Jet (V) UV-Radiation Impact on Biologically Relevant Liquids and Cell Suspension. *Bulletin of the American Physical Society* 59:
268. Bienert GP, Moller AL, Kristiansen KA, Schulz A, Moller IM, Schjoerring JK, Jahn TP. 2007. Specific aquaporins facilitate the diffusion of hydrogen peroxide across membranes. *J Biol Chem* 282: 1183-1192
269. Darr D, Fridovich I. 1994. Free radicals in cutaneous biology. *J Invest Dermatol* 102: 671-675
270. Neyens E, Baeyens J. 2003. A review of classic Fenton's peroxidation as an advanced oxidation technique. *Journal of Hazardous Materials* 98: 33-50
271. Dobrynin D, Fridman G, Friedman G, Fridman A. 2009. Physical and biological mechanisms of direct plasma interaction with living tissue. *New Journal of Physics* 11: 115020
272. Halliwell B, Gutteridge JM. 1992. Biologically relevant metal ion-dependent hydroxyl radical generation. An update. *FEBS Lett* 307: 108-112
273. Halliwell B. 1989. Free radicals, reactive oxygen species and human disease: a critical evaluation with special reference to atherosclerosis. *Br J Exp Pathol* 70: 737-757
274. Apel K, Hirt H. 2004. Reactive oxygen species: metabolism, oxidative stress, and signal transduction. *Annu Rev Plant Biol* 55: 373-399
275. Weiss S, Slivka A. 1982. Monocyte and granulocyte-mediated tumor cell destruction. A role for the hydrogen peroxide-myeloperoxidase-chloride system. *Journal of Clinical Investigation* 69: 255
276. Yoshida Y, Shimakawa S, Itoh N, Niki E. 2003. Action of DCFH and BODIPY as a probe for radical oxidation in hydrophilic and lipophilic domain. *Free Radical Research* 37: 861-872
277. Winterbourn CC, Kettle AJ. 2013. Redox Reactions and Microbial Killing in the Neutrophil Phagosome. *Antioxidants & Redox Signaling* 18: 642-660
278. Kim MH, Liu W, Borjesson DL, Curry FR, Miller LS, Cheung AL, Liu FT, Isseroff RR, Simon SI. 2008. Dynamics of neutrophil infiltration during cutaneous wound healing and infection using fluorescence imaging. *J Invest Dermatol* 128: 1812-1820
279. Brubaker AL, Schneider DF, Kovacs EJ. 2011. Neutrophils and natural killer T cells as negative regulators of wound healing. *Expert Rev Dermatol* 6: 5-8
280. DeLeo FR, Allen LA, Apicella M, Nauseef WM. 1999. NADPH oxidase activation and assembly during phagocytosis. *J Immunol* 163: 6732-6740
281. Frank DN, Wysocki A, Specht-Glick DD, Rooney A, Feldman RA, St Amand AL, Pace NR, Trent JD. 2009. Microbial diversity in chronic open wounds. *Wound Repair Regen* 17: 163-172
282. Schäffer M, Barbul A. 1998. Lymphocyte function in wound healing and following injury. *British Journal of Surgery* 85: 444-460
283. Dovi JV, Szpaderska AM, DiPietro LA. 2004. Neutrophil function in the healing wound: adding insult to injury? *Thromb Haemost* 92: 275-280
284. Drent M, Cobben NAM, Henderson RF, Wouters EFM, vanDiejenVisser M. 1996. Usefulness of lactate dehydrogenase and its isoenzymes as indicators of lung damage or inflammation. *European Respiratory Journal* 9: 1736-1742
285. Yamamoto A, Taniuchi S, Tsuji S, Hasui M, Kobayashi Y. 2002. Role of reactive oxygen species in neutrophil apoptosis following ingestion of heat-killed *Staphylococcus aureus*. *Clin Exp Immunol* 129: 479-484
286. Aoshiba K, Nakajima Y, Yasui S, Tamaoki J, Nagai A. 1999. Red blood cells inhibit apoptosis of human neutrophils. *Blood* 93: 4006-4010
287. Neeli I, Dwivedi N, Khan S, Radic M. 2009. Regulation of extracellular chromatin release from neutrophils. *J Innate Immun* 1: 194-201
288. Gupta AK, Hasler P, Holzgreve W, Gebhardt S, Hahn S. 2005. Induction of neutrophil extracellular DNA lattices by placental microparticles and IL-8 and their presence in preeclampsia. *Hum Immunol* 66: 1146-1154
289. Parker H, Albrett AM, Kettle AJ, Winterbourn CC. 2012. Myeloperoxidase associated with neutrophil extracellular traps is active and mediates bacterial killing in the presence of hydrogen peroxide. *J Leukoc Biol* 91: 369-376
290. Pryzwansky KB, Rausch PG, Spitznagel JK, Herion JC. 1979. Immunocytochemical Distinction between Primary and Secondary Granule Formation in Developing Human Neutrophils - Correlations with Romanowsky Stains. *Blood* 53: 179-185

References

291. Betz P. 1994. Histological and enzyme histochemical parameters for the age estimation of human skin wounds. *Int J Legal Med* 107: 60-68
292. Gold R, Zielasek J, Kiefer R, Toyka KV, Hartung HP. 1996. Secretion of nitrite by Schwann cells and its effect on T-cell activation in vitro. *Cell Immunol* 168: 69-77
293. Barbul A, Breslin RJ, Woodyard JP, Wasserkrug HL, Efron G. 1989. The effect of in vivo T helper and T suppressor lymphocyte depletion on wound healing. *Ann Surg* 209: 479-483
294. Barbul A, Sisto D, Rettura G, Levenson SM, Seifter E, Efron G. 1982. Thymic inhibition of wound healing: abrogation by adult thymectomy. *J Surg Res* 32: 338-342
295. Jameson J, Havran WL. 2007. Skin $\gamma\delta$ T-cell functions in homeostasis and wound healing. *Immunological Reviews* 215: 114-122
296. Norling L, Serhan C. 2010. Profiling in resolving inflammatory exudates identifies novel anti-inflammatory and pro-resolving mediators and signals for termination. *Journal of Internal Medicine* 268: 15-24
297. Trengove NJ, Langton SR, Stacey MC. 1996. Biochemical analysis of wound fluid from nonhealing and healing chronic leg ulcers. *Wound Repair and Regeneration* 4: 234-239
298. Eming SA, Krieg T, Davidson JM. 2007. Inflammation in wound repair: molecular and cellular mechanisms. *J Invest Dermatol* 127: 514-525
299. Mustoe TA, Pierce GF, Thomason A, Gramates P, Sporn MB, Deuel TF. 1987. Accelerated healing of incisional wounds in rats induced by transforming growth factor-beta. *Science* 237: 1333-1336
300. Duncan M, Berman B. 1985. Gamma interferon is the lymphokine and beta interferon the monokine responsible for inhibition of fibroblast collagen production and late but not early fibroblast proliferation. *The Journal of Experimental Medicine* 162: 516-527

Acknowledgements

This dissertation would not have been possible without the guidance of many individuals.

First and foremost, I would like to thank my supervisor Prof. Barbara Bröker (Institute of Immunology and Transfusion Medicine, Department of Immunology, University of Greifswald, Germany) for her trust and support of my PhD project. My deepest gratitude also goes to Dr. Julia Kolata who was always helpful in experimental planning, discussion of results, and critical review of manuscripts.

I further would like to thank colleagues at the Leibniz-Institute of Plasma Science and Technology (INP Greifswald, Germany) involved in this work, especially Prof. Klaus-Dieter Weltmann for providing funding, Dr. Kai Masur for his sustained support of my research, and Dr. Kristian Wende whose scientific judgment was always greatly appreciated. Fruitful discussions with Dr. Anke Schmidt, Dr. Sybille Hasse, Dr. Malte Hammer, Dr. Jörn Winter, and Helena Tresp were very helpful in this work, too. I also wish to cherish the mutual work and inspiring conversations with Sylvain Iséni. Further, I highly esteem the strong commitment of Anne Müller to this project and her assistance in the preparation of many thousands of samples for flow cytometry. Moreover, the image quantification of *neutrophil extracellular traps* would not have been possible without the skillful programming of Philipp Sodmann.

I am cordially grateful to Prof. Axel Kramer (Institute of Hygiene and Environment Medicine, University of Greifswald, Germany) for his confidence in my research project as well as his constant guidance in the preparation of manuscripts.

A valuable contribution to the experimental technique of flow cytometric and cell sorting was made by Vasilis Toxavidis (MD) and John Tigges at the Flow Cytometry Core Facility (Harvard Stem Cell Institute) under supervision of Dr. Peter Weller (MD) at the *Beth Israel Deaconess Medical Center* (Boston, USA).

I would also like to acknowledge my former colleagues at the *Centre for Free Radical Research* (Department of Pathology, University of Otago, Christchurch, New Zealand) and in particular Prof. Christine Winterbourn: her precise thinking, vast knowledge in redox biology, and unconditional support were indispensable for significant parts of this thesis. In addition, I thank Prof. Tony Kettle and Dr. Louisa Forbes for compelling scientific discussions and Dr. Rufus Turner for carrying out LC/MS experiments. Finally, I wish to express my sincerest appreciation to the work of Dr. Heather Parker and her amazing expertise in neutrophil biology which made investigations of plasma treatment on human neutrophils a great success.

I dedicate this thesis to my loving family.

Appendix

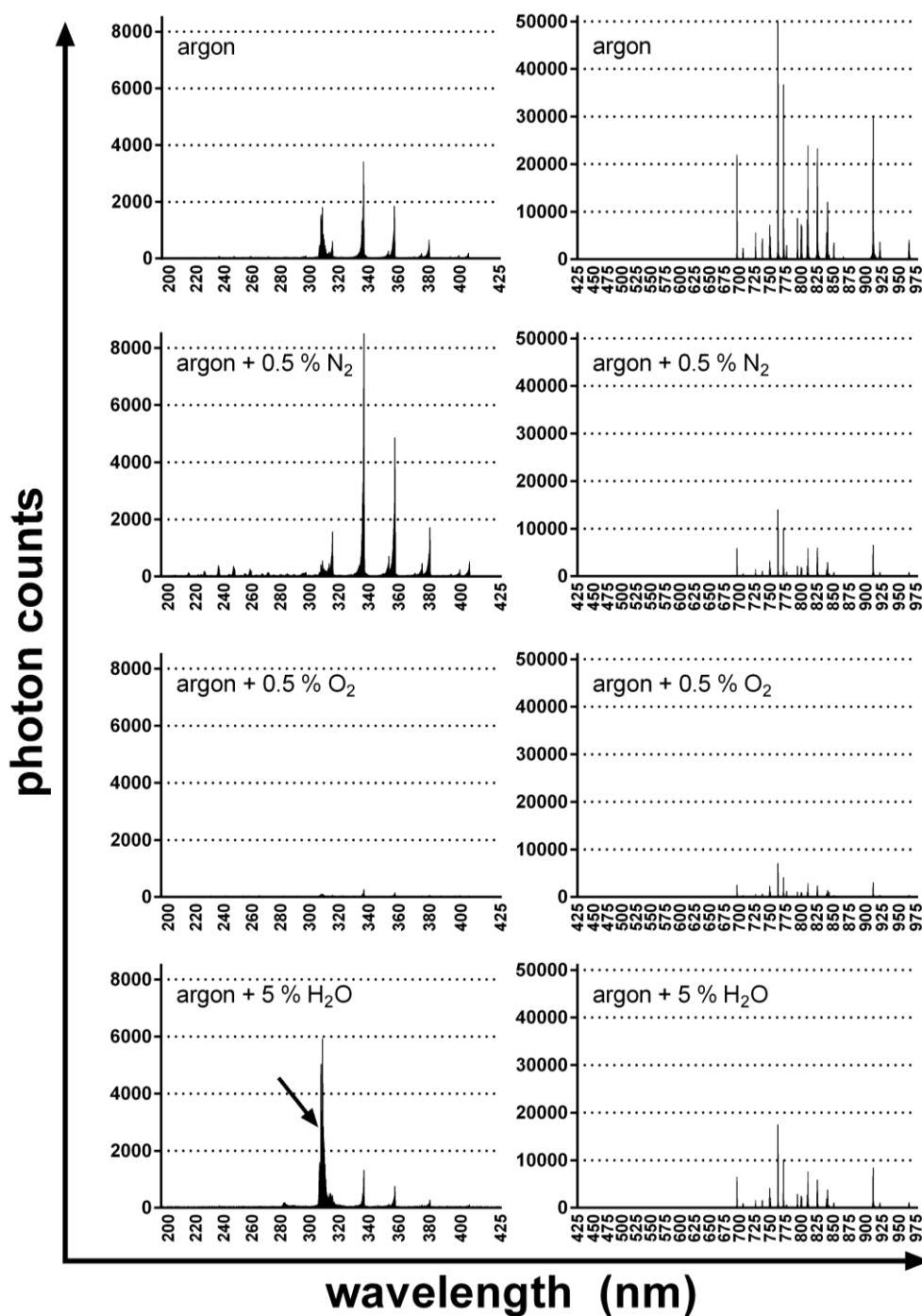


Fig. i: Feed gas composition modulated the optical spectrum of plasma.

Compared to argon alone (top row), addition of nitrogen to feed gas increased UV emission bands (left graphics), while oxygen reduced it. Humidified argon resulted in dramatically increased HO emission (arrow). In the visible/NIR spectrum (right graphics), any admixture of molecules other than argon to feed gas led to decreased intensities. Shown is one representative of three independent experiments.

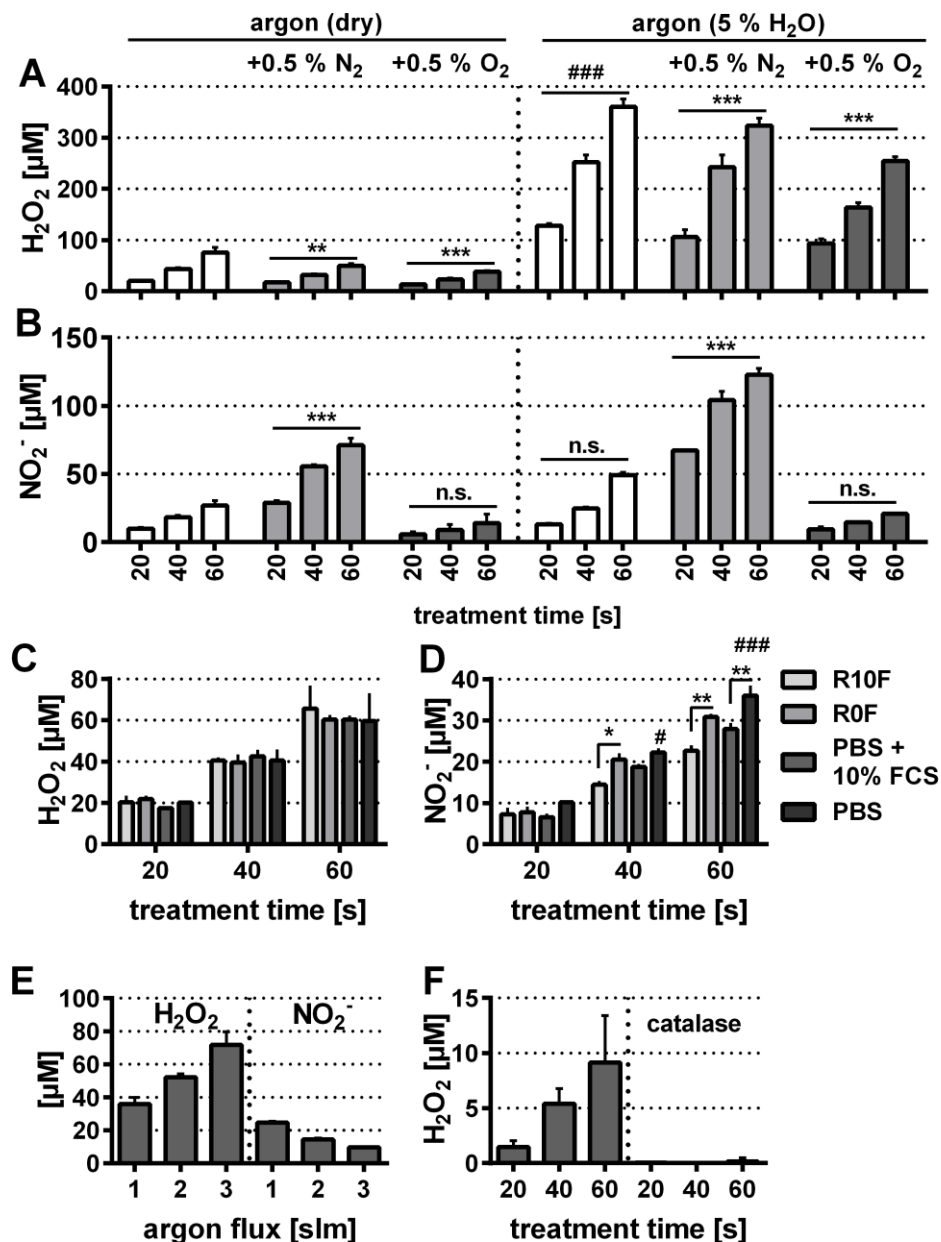


Fig. ii: H₂O₂- and NO₂⁻ concentrations were dependent on plasma parameters and medium properties.

Medium was plasma-treated for the indicated length of time and feed gas condition, and H₂O₂ (A) or NO₂⁻ (B) was immediately quantified. Humidified argon led to significantly higher H₂O₂ deposition in medium compared to dry gas conditions, while admixture of N₂ or O₂ decreased H₂O₂ levels compared to argon alone (A). Levels of NO₂⁻ were enhanced when N₂ was added to argon and further increased if humidified argon was used. Addition of O₂ decreased NO₂⁻ in dry or humid argon plasma-treated medium (B). H₂O₂ deposition was similar regardless of type of liquid treated (C). Nitrite production was modestly but significantly influenced by presence of FCS in medium or PBS, respectively (D). H₂O₂ and NO₂⁻ production in medium also inversely correlated to the argon feed gas flux (E). Medium was plasma-treated, incubated for 24 h at 37 °C, and H₂O₂ still detectable (F). Addition of catalase diminished H₂O₂ concentrations. Data are presented as mean + SD of two to six (A, B), two (C, D, E), and three (F) independent experiments. For statistical analysis (A, B), repeated measures two-way ANOVA was applied comparing group means between all groups (*Tukey* post test); ***/### p<0.001, ** p<0.01. For statistical analysis (C, D), repeated measures two-way ANOVA was applied comparing row (treatment time) means between groups (*Sidak* post test); ***/### p<0.001, ** p<0.01, */# p<0.05.

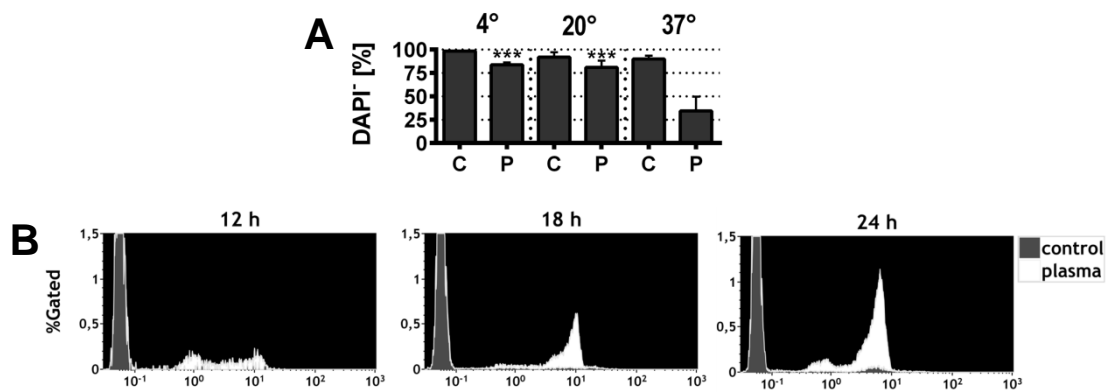


Fig. iii: Cell death was an active process and involved caspase 3 activation.

Cell death was an active process as cold, non-physiological incubation temperatures (4 °C, 20 °C) significantly decreased cytotoxicity in CD4⁺ T cells 24 h after plasma (60 s) treatment (A*). PBMCs were plasma-treated (60 s), stained for caspase 3/7-activity after different time points, and fluorescence in CD4⁺ T_H cells was measured by flow cytometry. Cells displayed active caspases 12 h onwards after treatment (B*). Data are presented as mean + SD (A*) or one representative (B*) of three independent experiments. Statistical analysis was performed using two-way ANOVA (Tukey post test).

*adapted from (192) with permission from Begell House

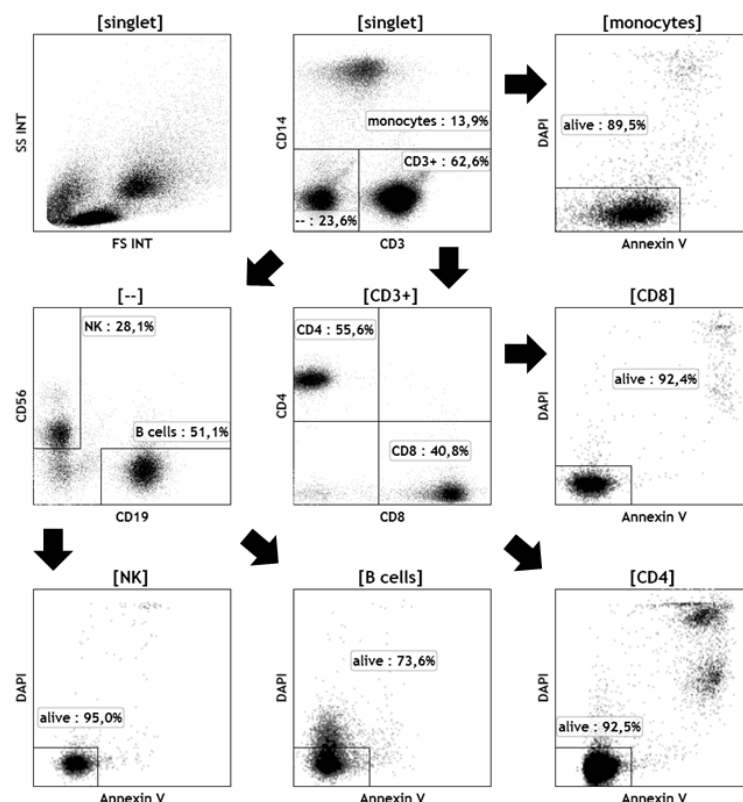


Fig. iv*: Gating strategy to detect survival of different PBMCs populations.

PBMCs were collected 24 h after plasma treatment and stained with antibodies directed against various cell surface antigens. After doublet discrimination, monocytes, T cells, and remaining lymphocytes were gated. Viability was determined assessing Annexin V and DAPI fluorescence for each cell type. Here, unstimulated control cells are shown. Shown is one representative of at least six independent experiments.

*adapted from (192) with permission from Wiley

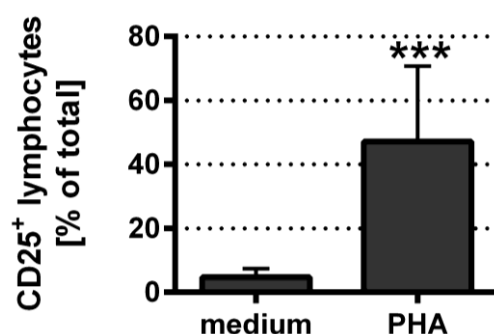


Fig. v: PHA activation induced CD25 expression in lymphocytes.

PBMCs were stimulated or left unstimulated O/N prior to plasma exposure. After 24 h, cells were harvested and stained for CD25 which was significantly increased in activated cells. Data are presented as mean + SD of 10 independent experiments. Statistical comparison was done using paired student's T test.

Tab. i*: Statistical comparison of survival of cell populations in the non-activated and activated regime.

Group means were calculated for each cell type and stimulation condition and compared against each other using two way ANOVA and *Sidak* post test.

**adapted from (193) with permission from Begell House*

comparison	non-activated		activated	
	<i>CI</i>	<i>significance</i>	<i>CI</i>	<i>significance</i>
monocytes vs. CD4 ⁺ T cells	12 to 34	***	4.3 to 25	***
monocytes vs. CD8 ⁺ T cells	12 to 34	***	5.5 to 26	***
monocytes vs. NK cells	3.1 to 27	**	9.8 to 31	***
monocytes vs. B cells	13 to 36	***	1.2 to 22	*
monocytes vs. $\gamma\delta$ T cells	9.3 to 40	***	3.3 to 31	**
CD4 ⁺ T cells vs. CD8 ⁺ T cells	-11 to 11	n.s.	-9.0 to 11	n.s.
CD4 ⁺ T cells vs. NK cells	-20 to 4.0	n.s.	-4.6 to 17	n.s.
CD4 ⁺ T cells vs. B cells	-9.8 to 13	n.s.	-13 to 7.5	n.s.
CD4 ⁺ T cells vs. $\gamma\delta$ T cells	-14 to 17	n.s.	-11 to 17	n.s.
CD8 ⁺ T cells vs. NK cells	-20 to 3.8	n.s.	-5.8 to 16	n.s.
CD8 ⁺ T cells vs. B cells	-10 to 13	n.s.	-14 to 6.4	n.s.
CD8 ⁺ T cells vs. $\gamma\delta$ T cells	-14 to 17	n.s.	-12 to 15	n.s.
NK cells vs. B cells	-2.8 to 22	n.s.	-20 to 2.0	n.s.
NK cells vs. $\gamma\delta$ T cells	-6.3 to 26	n.s.	-18 to 11	n.s.
B cells vs. $\gamma\delta$ T cells	-16 to 16	n.s.	-8.5 to 20	n.s.

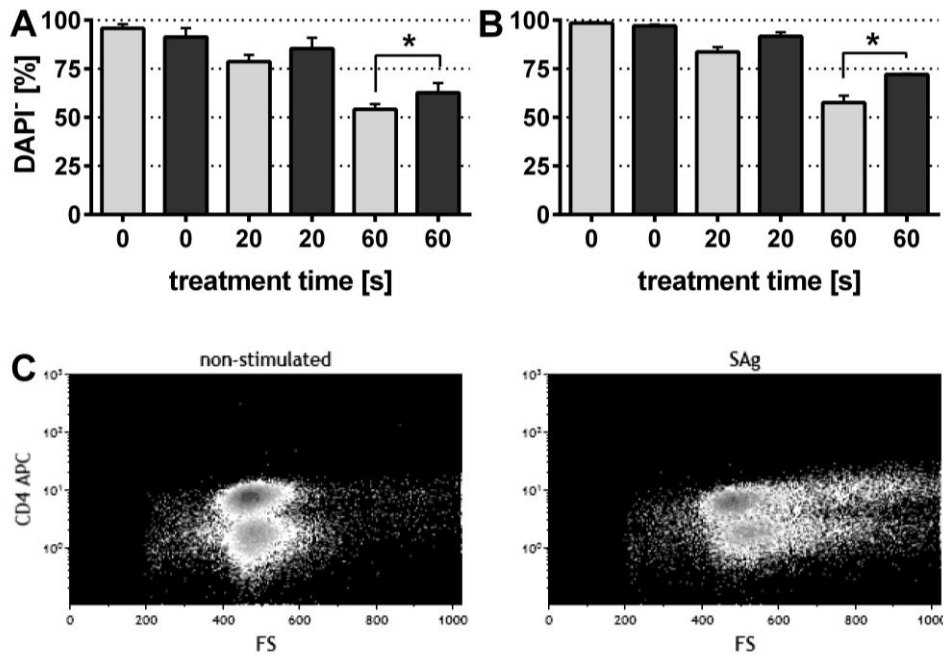


Fig. vi: Superantigen stimulation improved T cell survival in plasma-treated PBMCs.

PBMCs were isolated and cultured in medium with or without an equal mixture of staphylococcal superantigens (SEB, SEI, TSST, SEO, SEQ, final concentration 1 $\mu\text{g/ml}$) O/N. Cells were plasma-treated and afterwards incubated again for 24 h. Then, cells were stained for CD3, CD4, and CD8 expression and DAPI uptake before analysis by flow cytometry. Significantly less dead CD4^+ (A) and CD8^+ cells (B) were measured in PBMCs incubated with SAg compared to non-stimulated cells. Activation of CD4^+ T cells was confirmed by their increased forward scatter signal in SAg-incubated cells (C, right plot) compared to non-stimulated cells (C, left plot). T lymphocytes enlarge upon activation by various stimuli. Data are presented as mean + SD (A, B) and one representative (C) of three independent experiments. For statistical comparison, paired student's t test was used.

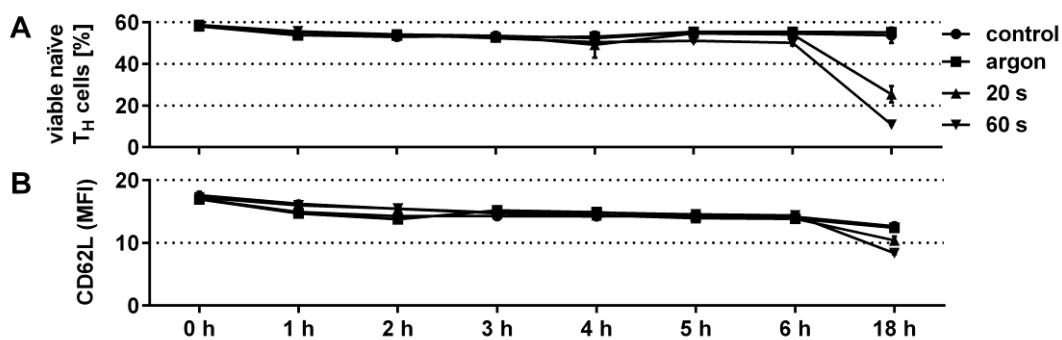


Fig. vii: Plasma treatment did not induce down-regulation of CD62L in CD45RA^+ T cells.

$\text{CD3}^+/\text{CD4}^+$ T_H cells (10^6 per ml in R10F) were fluorescence-activated cell sorted from PBMCs and subsequently plasma-treated. Percentages of CD62L^+ cells among CD45RA^+ and DAPI (viable) T cells were assessed at different time points following exposure to plasma. CD62L was not actively down-regulated within 6 h after plasma (A). Median fluorescence intensity of CD62L in $\text{CD4}^+/\text{CD45RA}^+/\text{CD62L}^+/\text{DAPI}$ cells was also similar within 6 h after exposure to plasma compared to non-treated controls (B). Shown are means \pm SD of duplicates of one representative of three independent experiments.

Tab. ii: Cytokine profile in supernatants of PBMCs.

PBMCs were incubated with or without PHA (500 ng/ml) O/N prior to plasma treatment. Cells were incubated for 24-72 h and cytokine concentrations determined in supernatants in a quantitative or semi-quantitative manner. Results are summarized from experiments of 3-6 donors.

Cytokine/ Chemokine	-PHA -Plasma	-PHA +Plasma	+PHA -Plasma	+PHA +Plasma
CCL2 (MCP1)	+	↓	n.d.	n.d.
CCL3 (MIP-1 α)	++	↓	n.d.	n.d.
CCL4 (MIP-1 β)	++	↓	n.d.	n.d.
CCL17 (TARC)	+	-	n.d.	n.d.
CCL22 (MCD)	-	-	n.d.	n.d.
CXCL1 (GRO α)	+	↑	n.d.	n.d.
CXCL9 (MIG)	-	-	n.d.	n.d.
CXCL10 (IP-10)	-	-	n.d.	n.d.
CXCL11 (I-TAC)	-	-	n.d.	n.d.
Eotaxin	-	-	n.d.	n.d.
G-CSF	-	-	-	-
GM-CSF	+	-	++	↓
IFN γ	+	-	+++	↓
IL-1 α	+	-	+++	↓
IL-1 β	-	-	+++	↓
IL-2	-	-	+++	-
IL-4	-	-	+	-
IL-5	-	-	+++	↓
IL-6	-	-	+++	↓
IL-8	+	↑	+++	↑
IL-12	-	-	+	-
IL-13	-	-	++	-
IL-17 α	-	-	+	↓
RANTES	++	-	n.d.	n.d.
TGF β	+	↑	++	↑
TNF α	-	-	+++	↓
VEGF	+	-	++	↑

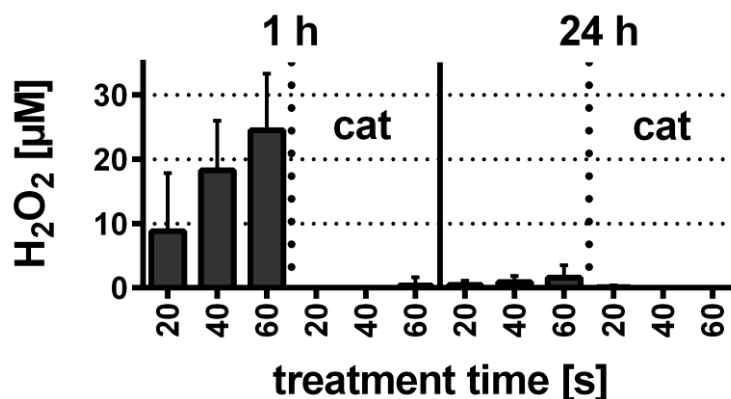


Fig. viii*: H_2O_2 concentrations in supernatants of PBMCs 1 h and 24 h after plasma treatment.

PBMCs were plasma-treated in R10F with or without catalase present (5 U/ml), and incubated for 1 h or 24 h at 37 °C. Supernatants were taken off and H_2O_2 was quantified using Amplex ultra red assay. One hour after treatment, H_2O_2 levels were lower than in medium alone (25 μM compared to 60 μM in treated medium alone, Fig. 8A). This indicated a reaction or detoxification of H_2O_2 in presence of cells. After 24 h, only background levels of H_2O_2 were measured. In presence of catalase, no H_2O_2 was detectable. Data are presented as mean + SD of seven independent experiments.

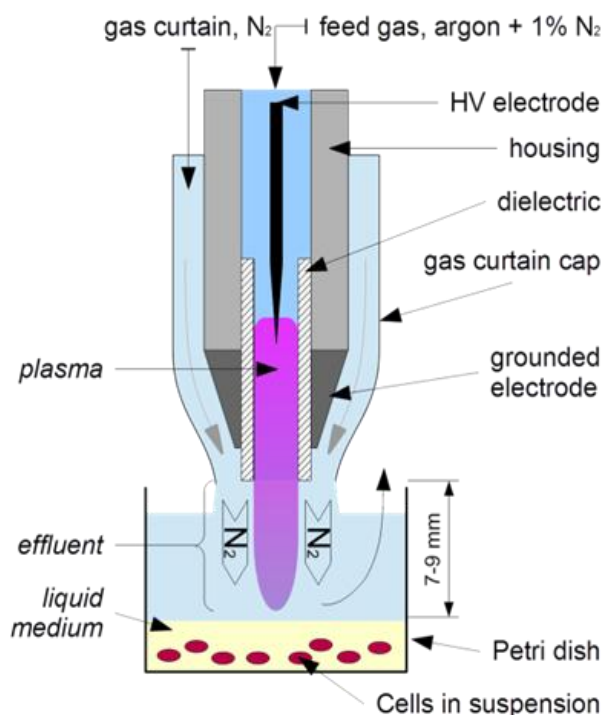


Fig. ix*: Schematics of the shielding (gas curtain) setup.

When plasma left the nozzle it was shielded by nitrogen (2 slm) running in a gas curtain cap in order to control ambient species influx to the plasma effluent. The feed gas used was argon with 1 % N_2 . The distance between the nozzle and plasma-treated cell suspension was 7-9 mm.

**adapted from (195) with permission from IEEE*

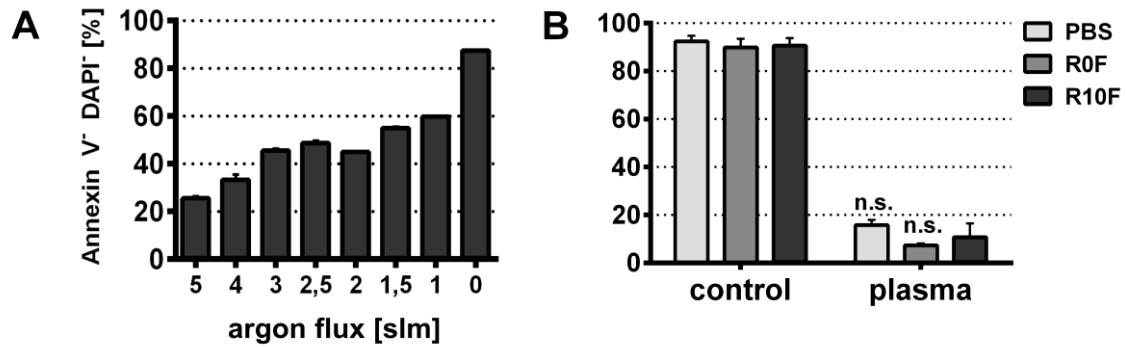


Fig. x: Plasma cytotoxicity positively correlated with increasing argon gas fluxes, but was not dependent on protein present in medium.

PBMCs (10^6 per ml in R10F) were seeded in 24 well plates and plasma-treated (20 s) using different gas fluxes from 1 to 5 slm (**A**). Cells were incubated for 24 h at 37 °C, harvested, and stained with Annexin V and DAPI. Percentage of viably lymphocytes increased with decreasing gas fluxes. Similarly, PBMCs were plasma-treated (60 s) in three different liquids (medium with FCS, medium without FCS, PBS) and lymphocyte viability was determined 24 h after exposure (**B**). No difference in cytotoxicity of plasma treatment was measured between different liquids used. Data are presented as mean + SD of duplicates (**A**) and of three independent experiments (**B**).

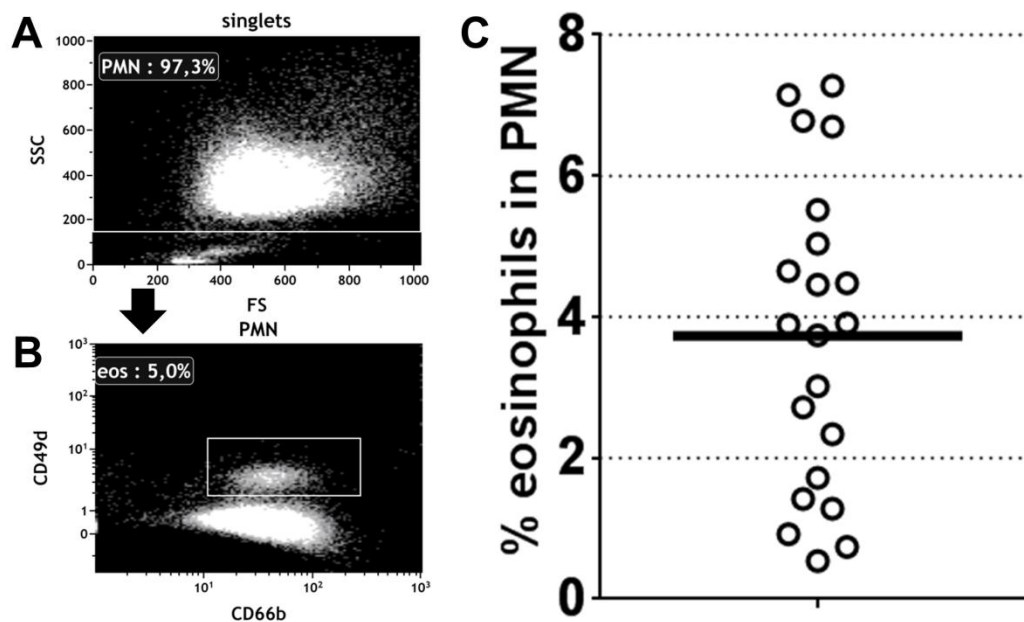


Fig. xi: Gating and verification of neutrophils and eosinophils.

Isolated PMNs were always verified to purity and eosinophil content. PMNs were gated from non-PMNs (**A**) and cells discriminated between CD49d^{dim} eosinophils and CD49d^{low} neutrophils (**B**). Alternatively, autofluorescence of eosinophils was used. Numbers of eosinophils were compared for 21 donors (**C**), horizontal line represents median. Eosinophil content was within expected range and usually below 5 %.

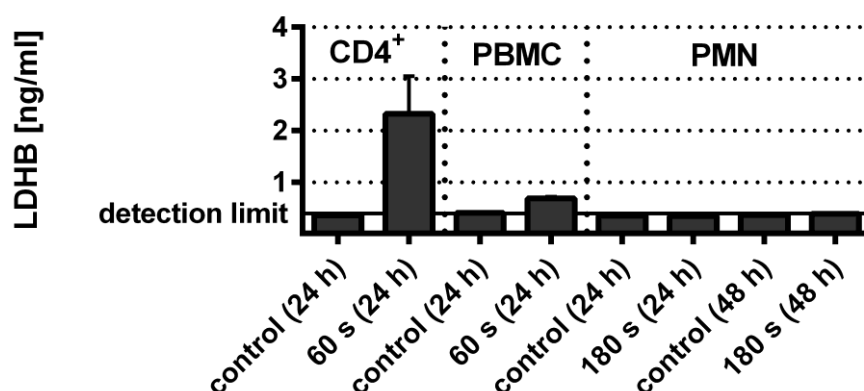


Fig. xii: LDHB was measured in supernatants of plasma-treated T_H cells and PBMCs but not PMNs.

Purified CD4⁺ T_H cells, PBMCs, or PMNs (10⁶ per ml in R10F) were seeded into 24 well, plasma-treated, and subsequently incubated for 24 h or 48 h at 37 °C. Suspension was harvested, centrifuged, and supernatants stored at -80 °C until analysis. Lactate dehydrogenase B (LDHB) ELISA was performed and LDHB content in supernatants quantitated using a LDHB-standard curve (0.15 to 4.80 ng/ml). No LDHB was found in supernatant of controls of any cell type investigated. In supernatants of plasma-treated CD4⁺ T_H cells substantial amounts of LDHB were measured, possibly due to lack of apoptotic clearance by monocytes/macrophages as present in PBMCs. Supernatants of plasma-treated PBMCs contained only little LDHB. No LDHB was measured in supernatants of plasma-treated (180 s) PMNs. Data are presented as mean + SD of three independent experiments.

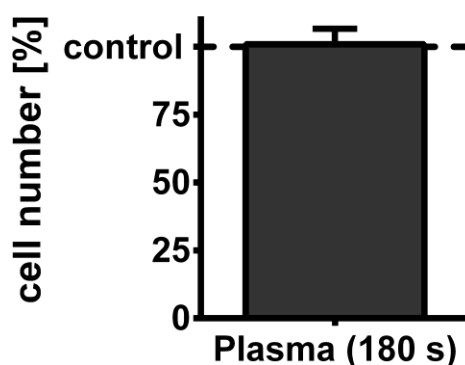


Fig. xiii: Plasma treatment did not lead to immediate adherence of neutrophils to cell culture plastic.

Immediately before plasma treatment (3 min) PMNs (10⁶ per ml in Hank's) were seeded into a well of a 24 well plate. Immediately after plasma treatment, cells were aliquoted (four times 200 µl each) in 96 well plates and quantitatively compared to control neutrophils. Control cells also spent 3 min in the 24 well plate. No difference was found between plasma-treated and control cells. This validated that results in superoxide production cytochrome C assay did not derived from different cell numbers in cuvettes but less actual activity per cell. Data are presented as mean + SD of four independent experiments.

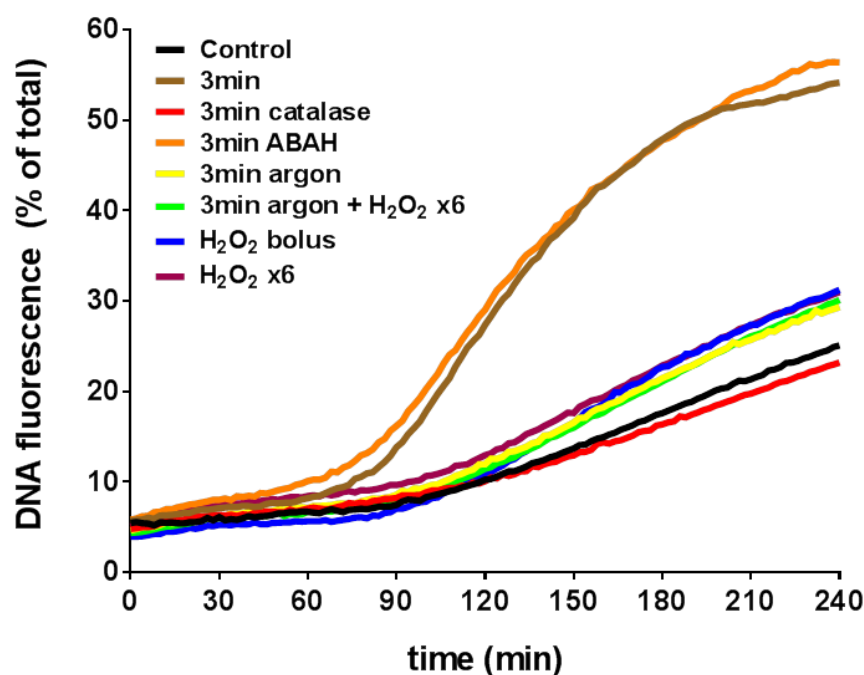


Fig. xiv: Catalase prevented extracellular DNA formation but H₂O₂ or argon did not replicate it.

Neutrophils were exposed to various conditions and DNA release was monitored over 4 h. Total fluorescence was normalized against Triton X-100 treated cells (100 %). Plasma treatment resulted in strong DNA fluorescence. Catalase abrogated this but H₂O₂ (180 μ M) did not replicate it. This was similar for argon or argon and addition of H₂O₂ added in six times 30 μ M portions. Moreover, MPO inhibition with 4-ABAH of plasma-treated neutrophils did not give different results as plasma-treated cells alone. One representative of three experiments is shown.

Tab. iii: Cytokine profile in supernatants of PMNs.

After exposure to plasma, neutrophils were incubated for 24 h and cytokine levels were determined in supernatants in a quantitative or semi-quantitative manner. Results are summarized from experiments of 3-4 different donors.

Cytokine/ Chemokine	non-treated	plasma-treated
CCL2 (MCP1)	+	↓
CCL3 (MIP-1 α)	+++	↓
CCL4 (MIP-1 β)	+++	↓
CCL17 (TARC)	++	-
CCL22 (MCD)	+++	-
CXCL1 (GRO α)	+++	-
CXCL9 (MIG)	+++	↓
CXCL10 (IP-10)	+++	-
CXCL11 (I-TAC)	+++	↑
Elastase	-	-
Eotaxin	-	-
GM-CSF	-	-
IFN γ	-	-
IL-1 α	-	-
IL-1 β	+	↓
IL-2	-	-
IL-4	-	-
IL-5	-	-
IL-6	+	↓
IL-8	+	↑
IL-10	-	-
IL-12	-	-
IL-13	-	-
IL-17 α	-	-
IL-33	-	-
RANTES	+++	↓
TGF β	+	↑
TNF α	+	↓
TSLP	-	-